NAVAL POSTGRADUATE SCHOOL
Monterey, California
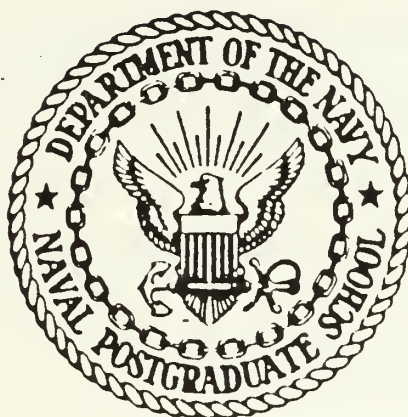
THESIS

A CONCEPTUAL DESIGN OF AN INERTIAL
NAVIGATION SYSTEM
FOR AN AUTONOMOUS SUBMERSIBLE TESTBED
VEHICLE

by

Rex G. Putnam Jr.

September 1987

Thesis Advisor   Roberto Cristi

T234366

REPORT DOCUMENTATION PAGE

REPORT SECURITY CLASSIFICATION UNCLASSIFIED		1b RESTRICTIVE MARKINGS			
SECURITY CLASSIFICATION AUTHORITY		3 DISTRIBUTION/AVAILABILITY OF REPORT Approved for public release; distribution is unlimited.			
DECLASSIFICATION/DOWNGRADING SCHEDULE					
PERFORMING ORGANIZATION REPORT NUMBER(S)		5 MONITORING ORGANIZATION REPORT NUMBER(S)			
NAME OF PERFORMING ORGANIZATION Naval Postgraduate School	6b OFFICE SYMBOL (If applicable) 62	7a NAME OF MONITORING ORGANIZATION Naval Postgraduate School			
ADDRESS (City, State and ZIP Code) Monterey, California 93943-5000		7b ADDRESS (City, State, and ZIP Code) Monterey, California 93943-5000			
NAME OF FUNDING/SPONSORING ORGANIZATION	8b OFFICE SYMBOL (If applicable)	9 PROCUREMENT INSTRUMENT IDENTIFICATION NUMBER			
ADDRESS (City State and ZIP Code) -		10 SOURCE OF FUNDING NUMBERS			
		PROGRAM ELEMENT NO	PROJECT NO	TASK NO	WORK UNIT ACCESSION NO

TITLE (Include Security Classification)
A CONCEPTUAL DESIGN OF AN INERTIAL NAVIGATION SYSTEM FOR AN AUTONOMOUS SUBMERSIBLE TESTBED VEHICLE / UNCLASSIFIED

PERSONAL AUTHOR(S)
Putnam, Rex, G. Jr.

TYPE OF REPORT Master's Thesis	13b TIME COVERED FROM _____ TO _____	14 DATE OF REPORT (Year Month Day) 1987 September	15 PAGE COUNT 131

SUPPLEMENTARY NOTATION

COSATI CODES			18 SUBJECT TERMS (Continue on reverse if necessary and identify by block number)
FIELD	GROUP	SUB GROUP	Inertial navigation, Autonomous Vehicle, Small submarine, Fiber optic gyro, Ring laser gyro

ABSTRACT (Continue on reverse if necessary and identify by block number)

The autonomous submersible testbed vehicle is arguablely the single most useful tool available to the submarine designer for designing modern technologically advanced submarines. The submarine's need for advancement and breakthrough capabilities has never been more critical than the present. The autonomous submersible testbed vehicle is designed to provide those advancements and breakthroughs to the United States Navy. A likely envisionment of the autonomous submersible vehicle is derived.

The design of the autonomous submarine depends heavily on the inertial navigation system that is used to control it. Indeed, it can be considered as the brain that forms the basis for operating the entire vehicle. Recent advancements in gyro technology and computer hardware

20 DISTRIBUTION/AVAILABILITY OF ABSTRACT ☑ UNCLASSIFIED/UNLIMITED ☐ SAME AS RPT ☐ DTIC USERS	21 ABSTRACT SECURITY CLASSIFICATION UNCLASSIFIED	
NAME OF RESPONSIBLE INDIVIDUAL Professor Roberto Cristi	22b TELEPHONE (Include Area Code) (408) 646-2223	22c OFFICE SYMBOL 62

DD FORM 1473, 84 MAR
83 APR edition may be used until exhausted
All other editions are obsolete

SECURITY CLASSIFICATION OF THIS PAGE
UNCLASSIFIED

have made a small, reliable, and inexpensive inertial navigation system possible. These new technologies are examined and an evaluation made as to their application to this type of vehicle. Industry's ability to manufacture these new gyros is surveyed, and actual data from manufactures are examined.

Finally, a conceptual design of an inertial navigation system for the autonomous submersible is presented along with conclusions and recommendations as to the current effects of gyro technology on the inertial navigation design. The conclusions and recommendations are considered to have importance in other applications as well as the autonomous submersible vehicle design.

S N 0102- LF- 014- 6601

A Conceptual Design of an Inertial Navigation System
for an Autonomous Submersible Testbed Vehicle

by

Rex G. Putnam Jr.
Lieutenant, United States Navy
B.S., United States Naval Academy, 1981

Submitted in partial fulfillment of the
requirements for the degree of

MASTER OF SCIENCE IN ELECTRICAL ENGINEERING

from the

NAVAL POSTGRADUATE SCHOOL
September 1987

THESIS DISCLAIMER

The reader is cautioned that computer programs developed in this research may not have been exercised for all cases of interest. While every effort has been made, within the time available, to ensure that the programs are free of computational and logic errors, they cannot be considered validated. Any application of these programs without additional verification is at the risk of the user.

ABSTRACT

The autonomous submersible testbed vehicle is arguablely the single most useful tool available to the submarine designer for designing modern technologically advanced submarines. The submarine's need for advancement and breakthrough capabilities has never been more critical than the present. The autonomous submersible testbed vehicle is designed to provide those advancements and breakthroughs to the United States Navy. A likely envisionment of the autonomous submersible vehicle is derived.

The design of the autonomous submarine depends heavily on the inertial navigation system that is used to control it. Indeed, it can be considered as the brain that forms the basis for operating the entire vehicle. Recent advancements in gyro technology and computer hardware have made a small, reliable, and inexpensive inertial navigation system possible. These new technologies are examined and an evaluation made as to their application to this type of vehicle. Industry's ability to manufacture these new gyros is surveyed, and actual data from manufactures are examined.

Finally, a conceptual design of an inertial navigation system for the autonomous submersible is presented along with conclusions and recommendations as to the current effects of gyro technology on the inertial navigation design. The conclusions and recommendations are considered to have importance in other applications as well as the autonomous submersible vehicle design.

TABLE OF CONTENTS

LIST OF TABLES

9

LIST OF FIGURES

I. AN INTRODUCTION TO THE AUTONOMOUS SUBMERSIBLE VEHICLE

A. WHY AN AUTONOMOUS SUBMERSIBLE TESTBED VEHICLE ?

The idea that an unmanned craft can be used in areas where a manned craft would be either impractical, unsafe, or vastly more expensive, is not a new idea. Unmanned space probes have been used for many years, providing an economical and practical vehicle for use in space. Unmanned subs are often employed in offshore oil rig applications, where the safety hazards of continued rig operation make a manned vehicle undesirable. Indeed, unmanned vehicles have proven through years of use to be practical, economical, and indispensable. [Ref. 30: pp. 465-471]

That an unmanned Autonomous Submersible Vehicle would be considered as an useful platform in a modern Navy, is then simply a natural extension of these same ideas. An autonomous submersible testbed vehicle is the logical first step in the development and evaluation of this type craft for use in the Navy. Additionally, the autonomous submersible testbed vehicle will provide a testing platform from which state of the art techniques and equipment can be safely evaluated without unnecessarily risking the lives of submariners. The implication of modern technology arriving in the fleet sooner and better tested is obvious.

1. What does "Autonomous" mean ?

The Webster Dictionary defines autonomous as something that is "undertaken or carried on without outside control : self-contained ". When examined in the context of an autonomous submersible testbed vehicle, the term implies an unmanned submersible vehicle that is capable of operating and performing assigned tasks independently, without any external control being required. Thus, unlike other unmanned vehicles that rely on a tethered command line to direct the vehicle from afar, this vehicle would have no umbilical cord. Accordingly, the vehicle would not suffer from the limitations that such a command link imposes. [Ref. 2: pp. 571-575]

2. Inherent Design Advantages of the Autonomous Submersible

An unmanned submersible vehicle does not require huge design margins and safety factors to operate safely. The cost should some design failure result is measured in dollars, not in the lives of perhaps hundreds of people. Thus design margins can be reduced and safety factors eliminated. Extensive backup and safety systems are not

required nor desired. Life support systems are not needed. In effect, the only required systems are those that are actually needed to operate the submersible. [Ref. 30: pp. 465-471] Also, these individual systems are less costly as they are designed to function throughout a much smaller design range, a design range closer to the expected range. Significant space savings should result enabling a much smaller submarine hull. [Ref. 28: p. 15-16] Overall, extensive monetary savings are to be expected.

3. Operational Advantages of the Autonomous Submersible

The major advantage associated with a submarine is that the submerged submarine is invisible to the above water world. Thus, the submarine offers an operational advantage to the Navy that no other naval vessel shares, an inherent stealth capability. The smaller unmanned submarine would be even harder to detect. It has a much smaller sonar cross-section, and can be made to be virtually silent quite easily. The shallow unmanned submarine is harder to see visually as well, and even if seen may be taken for a large fish.

A much smaller hull shape would lead to a much lower draft, hence the unmanned submarine would be able to travel safely in waters far too shallow for larger vessels. Potentially, this may enable a much closer approach to the desired objectives. Additionally, since the craft is unmanned, the submarine is far more easily put to use in water that is too dangerous or too sensitive for a manned submarine. The implications given by the operational advantages are not trivial.

4. Advantages in Research and Development

The need for an autonomous submersible testbed vehicle in evaluating potential autonomous submersible vehicle applications and testing new equipment and operational concepts is critical to maintaining a modern and technologically advanced submarine force. The rival super powers have long recognized the significance of the submarine in naval strategy, and the threat their submarines pose is increasing at an alarming rate. Their numbers are staggering and their quality is good and getting better rapidly. [Ref. 9: pp. 95-98] The unmanned autonomous submersible testbed vehicle will provide an excellent platform to conduct testing and evaluation of the revolutionary technology becoming available with modern advances. The result is that modern technology should arrive for use in the fleet sooner, should be better tested, and should be better understood.

One advantage the unmanned submersible has is in the risk category. The captain of a manned submarine is primarily concerned with the safety of the ship and

13

crew. Thus new or poorly understood procedures and equipment are often met with skepticism by the men who operate the submarine. Indeed, a captain may well be unwilling to perform a specified test because of his greater concerns for safety of his crew. An unmanned sub has no such limitations. If the unmanned sub is lost, the result is not the catastrophe that the captain of a larger manned submarine worries about. The unmanned sub is relatively cheap, and risks no lives. Thus, it clearly makes sense to test state of the art technology equipment and the accompanying operational procedures in an unmanned submersible.

Another unmanned submersible advantage in the testing environment is that the unmanned submersible will perform the programmed task exactly as instructed. Thus a means of performing the test repeatedly with little or no difference between the execution of the individual tests is afforded. A manned submarine has men driving the sub, and thus is less likely to perform the tests exactly the same way each time and is much more expensive to keep occupied in testing operations. The unmanned submarine is much more predictable and much cheaper to use. Tests can be iterated, more tests can be performed, and all the data compiled and analyzed throughout the process. With a dedicated testbed, a full manned submarine is not left waiting for the scientists and engineers to analyze the data and iterate experiments. The resulting repeatability yields vital field data on actual equipment performance that is far more precise and accurate. Hence, subsequent analysis and revisions will be based on better data and thus be much more effective than the revisions might otherwise have been.

A final advantage that the autonomous submersible testbed vehicle would have over a manned submarine is that the unmanned sub would be designed as a testbed vehicle, the manned submarine is designed as a warship. The testbed vehicle is designed such that new equipment can be easily installed and tested. Modular design of all the equipment is likely. The manned submarine is not so easily modified. It may not be inconceivable to perform daily modifications and testing on the unmanned submarine, whereas the same would be impossible on the manned version. Ship alterations and modifications are a major undertaking on the manned submarine warship.

B. UNIQUE ASPECTS OF THE AUTONOMOUS SUBMERSIBLE TESTBED VEHICLE

The most fundamental condition levied on the design of a submarine is that the submarine must be at or near neutral buoyancy when submerged. Thus submarines

are difficult to design because of the direct relationship between weight and buoyancy. Weight and space are also interconnected, so that any change, even a minor one, effects the design of the submarine and must be considered.

The fundamental design quantity for a submarine is volume rather than weight. Submarine designs often begin with estimates of the required internal space and dimensions. The pressure hull is fixed by these values. [Ref. 9: pp. 18-19]

Aside from the pressure hull, the power plant is the major dense component of the submarine. Batteries are relatively heavy and consume a great volume, especially when endurance is critical. Thus, propulsion space can occupy a large majority of the small submarine. [Ref. 9: p. 24]

1. Desired Capabilities of the Testbed Vehicle

The autonomous submersible testbed vehicle would ideally function as a prototype as well as a testing platform. Accordingly, the testbed vehicle should have many of the same design goals. Thus, it becomes clear that the testbed vehicle should be designed with the operational requirements that an autonomous submarine would require as well as the design goals that are unique to the testbed function. The desired capabilities of this vehicle are as follows:

1. Optical Capability - The ability to take underwater and above water pictures and to make video recordings.
2. Sonar Search Capability - The ability to execute a search of an assigned area using either active or passive sonar.
3. Intelligence Gathering Capability - The ability to record sonar information and visual information for later analysis.
4. Stealth Capability - The ability to execute its assigned mission without being detected.
5. Open Ocean Navigating Capability - The ability to safely navigate in the open ocean environment.
6. Restricted Water Navigating Capability - The ability to safely operate in restricted or inland waters.
7. Component Replacement Capability - The ability to rapidly and easily replace both major and minor vehicle systems.

The optical equipment requirements demands that a camera be able to view the exterior surroundings about the submersible. This requires underwater lighting. Additionally, if the camera is located inside the vehicle, a transparent window is needed. If the camera is to be external to the hull, allowances must be made to deal with controlling the camera and for protecting the camera against external perils.

The sonar search capability requires that the submersible be able to faithfully conduct a search pattern over the geographic area to be searched. It also requires a high resolution medium range active sonar as well as a broadband passive sonar. On-board processing may not be required, except to the extent that the submersible avoid any obstacle in its path.

The intelligence gathering capability requires that some type of data recording be able to be made for later analysis. An alternate method of retrieving the gathered intelligence data would be to radio the information to some processing center. This would clearly sacrifice the stealth and may give away the submersible's position. It must be recognized that in some cases the unmanned submersible may be considered expendable and thus the sacrifice in probability of detection determined acceptable. The intelligence desired may include visual information obtained above or below the water as well as electromagnetic emissions obtainable via an antenna.

Stealth is the submarine's greatest asset. Its great value, indeed its mystique, lies in its invisibility. Much of submarine technology is intended to preserve that invisibility in the face of increasingly sophisticated means of submarine detection. The stealth capability requires that the submersible be able to operate without giving its presence or position away. Thus, it must be able to operate without any active sonar transmissions or radio emissions, and to control the exposure of any masts or antennas that are used. [Ref. 9: pp. 136-138]

The requirement to be able to easily remove and install major and minor vehicle systems leads to a modular system design concept. All systems and system components need to be scrutinized to include this modular concept wherever possible. A generally available power distribution system is required, as is some means of securely attaching and securing the various systems and their components.

The safe navigation of the ship requires that the ship be able to detect and avoid obstacles in its path. The obstacle could be a sea mountain, a buoy, another vessel, or any number of unforseen items. The submersible must be able to monitor the depth of water below its keel to preclude running into the bottom. This may require some form of a secure fathometer. Additionally, the submersible must be able to reliably monitor its own water depth to avoid exceeding its design parameters. The various navigational aspects will be greatly expanded throughout this writing.

2. Hull Construction and Diving Depth Considerations

The submarine hull shape is a real consideration to the design of the sub. In principle the ideal pressure hull shape is a sphere, the strongest shape, and the shape most often used in very deep-diving submersibles. However, usable volume is sacrificed and water drag is very high for spherical hull shapes.

Thus, submarine hulls are often built around a cylinder with hemispherical caps at the ends. This is the most practical compromise between weight, strength, and arrangement. Frames are often used to strengthen the hull structure. They act as integral parts of a ship's girder when the ship is exposed to longitudinal or transverse stresses. [Ref. 28: p. 18-19] They may be externally framed or internally framed. Despite its cost in volume, internal framing has important advantages. Water pressure tends to press the skin of the pressure hull into the internal frames, and away from external frames. Moreover, the welds in an external frame are more vulnerable to stress enhanced corrosion. [Ref. 9: p. 20]

For any cylindrical pressure hull, strength declines as the diameter increases; deeper diving requires either a narrower or thicker pressure hull or a new stronger hull material. A simple change in hull material can have a dramatic effect on diving performance. A stronger material directly relates to a deeper diving capability. However, new hull materials introduce their own new and often unknown problems, like welding problems and corrosion problems. The USS Thresher, which was lost on diving trials in 1963, introduced the new HY80 steel which was later found to have suffered from defective welds. Although the loss of an unmanned submarine cannot compare to this tragedy, it benefits the unmanned submarine design to be as small as possible to maximize its strength aspect. [Ref. 9: pp. 20-23] A final note is that a small unmanned submarine hull could itself be invaluable in the research efforts directed at new hull materials for new deeper diving manned submarines.

The other major limitation on diving depth is the strength of the hull penetrations to water pressure. Examples of hull penetrations include propeller shafts, periscopes, and cable runs from external equipment such as sonar transducers and external underwater cameras. As the submarine dives deeper, it becomes harder to maintain absolute watertightness in the hull penetrations. Thus significant engineering effort needs to be directed at the design of these hull penetrations. [Ref. 9: pp. 22-23] The unmanned submarine would clearly prove of use for research and development in this area, as no captain would want an unproven hull penetration design on their vessel.

The classic single-hull submarine carries all of its tankage inside the pressure hull. In consequence, it is the simplest to build, especially for small subs, and has the least hull surface area. However, the internal tankage detracts from the limited internal volume of the submarine. As the need for more reserve buoyancy increases, a larger internal tank capacity is required. Thus, it behooves the designer to minimize the reserve buoyancy to the least actually required. [Ref. 9: pp. 22-23] As the unmanned submarine does not require a great surface capability, the reserve buoyancy requirement can be kept quite small.

A final consideration of the hull shape is that when underwater, the drag is proportional to the surface area of the submarine. Also, for a fixed hull volume, appendages such as a fixed sail or the diving planes contribute heavily to hull drag. For a fixed speed, the power required to propel the craft is proportional to the hull drag. Thus, minimizing hull drag equates to a smaller power plant requirement and enables more room inside the submarine for other vital equipment. Drag resistant coatings such as those used by America II racing yacht, may prove to be another valuable research area.

3. **Buoyancy Control and Maneuverability Considerations**

How easily a submarine can dive depends upon how much buoyancy it must lose before it can sink below the water. The true density of sea water is influenced by its temperature, its salinity, and the pressure under which it exists. Furthermore, the increasing density of sea water which results from the pressure effects at a greater depth may be offset by the decrease in buoyancy of the submarine associated with the pressure hull compression. Since temperature and salinity gradients exist in the ocean, the ship must have a means of compensating for these density gradients as they occur. The buoyancy force must be controlled to near neutral buoyancy if the depth is to be controlled. [Ref. 33: pp. 3-5] This is accomplished by controlling the weight of the ship. The weight is adjusted by flooding water into a tank, by forcing water out of a tank, or by using a syntactic foam buoyancy system. Syntactic foam buoyancy systems are relatively complex, and expensive. The more common means of buoyancy control is through the tankage. The tanks commonly found on submarines include: an external main ballast tank, an external or internal ballast tank, and an external or internal variable ballast tank. [Ref. 35,23: pp. 1253-1259, pp. 1786-1793]

The external main ballast tank is usually formed by having a shell that covers the pressure hull. The space between the pressure hull and the external shell forms a

floodable volume that can be use as a gross control to buoyancy. This main ballast tank has the advantage that it does not need to be made to withstand deep depth water pressure, as when submerged, water pressure is allowed on both sides of the external shell. Additionally, since the water pressure does not tend to compress this external shell, acoustic absorbing tile can be advantageously placed on the shell and will not have a strong tendency to fall off as the pressure hull is compressed. Thus stealth can be improved. The main disadvantage is that the main ballast tank allows no variable water level to provide the fine buoyancy control desired. [Ref. 33: pp. 1-2]

The external and internal ballast tanks must be made to withstand deep depth submergence pressure. The internal ballast tanks may either function as a gross buoyancy control or function as a variable buoyancy control. The gross control internal ballast tank would function to either be completely empty or full. The variable ballast tank would be partially full and able to compensate for any change to submarine buoyancy as it occurs. In general, air pressure could be used to control the water flow into and out of these ballast tanks. Indeed, it is possible to provide depth control using only variable ballast tank operations to control the buoyancy force. [Ref. 23: pp. 1786-1793]

The other means of providing ship control is through the diving planes and the rudder. These appendages can greatly increase ship's drag, especially when the planes are placed at a large angle. These appendages are used to provide a continuous means of controlling the ship. The diving planes control the ship's depth, and the rudder controls the ship's heading. These planes can add significant flow noise, thus it is desired to match the size of these control surfaces to the size of the submarine. The optimal match will result in a more controllable submarine, with the least amount of controlled surface motion and the least amount of added drag. [Ref. 9: pp. 20-24]

When a submarine moves through the water, forces arise which act on the hull with some vertical components. These components may become quite large when near the sea surface, especially when involved in a heavy sea state. These forces may overbalance or overcome the more static buoyancy forces discussed above. The controlling surface planes provide a means of controlling the submarine motion as a response to these forces. The forces may be categorized as follows: [Ref. 33: p. 51]

1. Planing forces due to the hull form.
2. A vertical component of the propulsive force determined by the angle of the hull.
3. Planing forces due to the angle of the diving planes.

Well placed diving planes enable the control of the angle of the submarine. This can provide some measure of ship control of each of the three types of forces. The diving planes directly control the lift force exerted by them through the angle at which they are applied. They also tend to control the angle of the hull, in that the diving planes form a moment arm with respect to the hull's center of gravity. The speed of the ship is controlled by the ship's propulsion system, and helps determine the magnitude of these three types of forces. The diving plane's angle, hull angle, and ship's speed combine to give the ship depth control as a response to the vertical forces the submarine may encounter. [Ref. 33: pp. 51-54]

4. Power Plant Considerations

Their are several options available as to the type of power plant. The types of propulsion includes closed-cycle engine power, fuel cell power, nuclear power, and electric power. Among these various types the battery supplied electric motor is ideally suited for this specific task. It provides the simplicity, low cost, and quiet operation required and it needs the least interior volume. The usual lead-acid batteries are very heavy, but cheap. Alternatives include silver-zinc and silver-cadmium, both of which are lighter and more compact but more costly and intolerant to cycling. All present gas hazards that must be addressed. A typical lead-acid battery can deliver about 0.013 hph/lb at the 1-hour discharge rate or about 0.033 hph/lb at a 100-hour discharge rate. Other types of batteries can deliver as much as 0.07 hph/lb at the high discharge rate and slightly more at lower rates. [Ref. 9: pp. 133-134]

Regardless of the type, any power plant must provide for the propulsive and distributive power requirements of the submarine. Typically, the propulsive power requirements account for the large majority of power plant capacity needs. As the power plant may occupy the large majority of a small submarine's volume, assessing the propulsion requirement is critical to the submarine design.

This submarine must be able to travel at a minimum rate of 10 knots. This is the minimum speed believed necessary so as to be able to overcome any expected current and still execute the assigned mission. It is possible that stronger than 10 knot currents may exist in inland waters, but usually slack times exist in these strong currents within which the submarine may be able to safely navigate. Thus, such a speed capability should not severely limit the submersible's operational capability. A higher speed would limit the submarine's endurance and is therefore not desired. To further enhance the submersible's range and endurance, a slower 6 knot speed may be desired. This would enable significantly longer missions to be executed.

The final and perhaps most important aspect of the propulsion machinery is the noise. Most submarine noise is propulsion related. There are three major sources of propulsion related noise. These include:

1. Flow noise along the hull and from excited sea life.
2. Propeller related noise and cavitation.
3. Machine related noise passed through the hull.

Flow noise as the submarine passes through the water is generally broadband noise. It may be reduced by a smoother hull surface with less drag, hull coatings, and covered hull openings. Hull openings and holes may resonate at a specific speed and flow condition, resulting in a loud tone. Propeller noise is characterized by a continuous hiss modulated by the beats of the blade rate. Cavitation is a loud broadband noise that results when low pressure zones at the propeller tips form vapor bubbles which later collapse causing noise. Proper propeller design trys to avoid cavitation. Recent submarines may employ pump-jets instead of propellers to further reduce cavitation effects. The primary machine related noise of most electric submarines is associated with gearing. Modern electric motors are designed to rotate at the propeller rate, thereby avoiding the gear noise. Such submarines may be virtually silent. [Ref. 9: pp. 95-96,136-138]

5. **Navigation and Operating Considerations**

a. *The Underwater Environment from the Submarine*

From the perspective of the submarine, the surface is a horrible place to be. The submarine is vulnerable there and easily detected. The submarine is not very sea worthy when surfaced. The round bottom of the submarine makes the submarine roll very badly even in calm seas. Submerged, the submarine is as steady as a rock, safe, and a potent adversary.

But the submarine is blind when underwater. There are no windows to enable the submarine to see where it is going. Even if a window existed, the visibility would be far too bad to be useful in navigating the ship. The modern submarine is forced to steer blindly with few if any navigational fixes for months at a time. The sea bottom is rocky and full of mountains and caverns that are far larger those on land. The submarine therefore relies on its sonar and its inertial navigation system to keep it safe.

b. Submerged Operating Considerations

When the submarine is submerged it must still avoid collisions with any contacts. Since these contacts cannot be seen, the sound the contact makes is used to determine the contact's location, heading, and speed. Deep draft vessels and other submerged contacts must be avoided to prevent collisions. Additionally, other obstacles may present themselves such as sea mountains and shallow zones that must also be navigated around. The submarine must steer clear of these contacts, as no contact will know where the submarine is located. How will an unmanned submarine evaluate and evade these contacts ? In a multiple contact environment the submarine may have to steer to avoid several contacts simultaneously. An algorithm to effect these skills is mandatory for the unmanned submarine to function safely.

If the contact is not making noise, the submarine may not hear it. A ship with its engines not running, or a small vessel in a rain storm may not be detected. A fishing vessel towing its nets present another hazard. Thus, navigating the submarine requires constant vigilance and care. The simplest operation must be executed with full cognizance of these hazards.

Strong underwater currents and large density gradients may confront the submarine at any time. Entering or leaving the Gulf Stream is a prime example of when a large current and density gradient could be expected. A sudden change in the buoyancy of the submarine could cause the sub to suddenly surface or to fall below its rated maximum depth. A means of adjusting for the maximum expected change in water density is required. The maximum density change expected in the ocean is about 3.8%, thus the variable ballast capacity should be designed to hold 3.8% of the submarine's displacement. [Ref. 33: pp. 3-11]

Despite all the hazards facing the submarine, the submarine must still be able to maintain a course, establish its position, and determine a course to steer in order to accomplish its objective.

c. Surfacing Operating Considerations

When a submarine wishes to come shallow or surface, the uncertainties with regards to other contacts in the area becomes the major concern. A contact that is on a collision course, but has too small a draft to present a problem to the deep submarine is now a threat that must be dealt with. As the distance to the contact is not known, the submarine may actually come up underneath the contact. Furthermore, it is quite possible that a strong thermal gradient layer may be hiding the

22

surface contacts from the submarine's sonar. Thus, the surfacing submarine's hazard is that of a collision at sea. Accordingly, the submarine must be ready to quickly dive and return to the deep sea should anything unexpected occurs. Once deep, the submarine can always re-evaluate and try to surface again.

d. The Inertial Navigation Solution

Navigation from a submarine is not a simple task. None of the modern navigation systems such as Omega, Loran, Satellite Navigation, or the future NAVSTAR Global Positioning System can adequately provide a navigational position, or fix, to the submerged submarine. To obtain such a fix from these systems, the submarine is forced to come to the surface and raise an antenna. This exposes the submarine to detection, and as a result the submarine is most vulnerable at these times. The submarine must therefore rely on some other means of navigation for normal submerged operations.

The inertial navigation system senses the submarine's acceleration and integrates once to determine the submarine's velocity and again to determine its position. Since the accelerations are sensed relative to the Earth, the submarine's navigational position relative to the earth is obtained. Thus, the inertial navigation system can provide a continuous navigational track independent of any outside information. [Ref. 29,9: pp. 17-12 to 17-17, p. 154] In fact however, since the calculations are performed with finite accuracy and with some errors involved, errors accumulate with time. The need for external navigation fixes when using an inertial navigation system is markedly curtailed despite their errors. [Ref. 9: p. 154]

In this unmanned autonomous submersible testbed vehicle the inertial navigation system must provide attitude control, navigation track control, and submarine ship control functions. The attitude control function maintains the submarine in the desired attitude by controlling the submarine in pitch, roll, and yaw. [Ref. 29: p. 17-1 to 17-2] The navigation track control functions as an autopilot, and must dampen out fluctuations that would tend to deflect the submarine from its intended track. The submarine ship control functions to place the submarine at the desired depth and to avoid any obstacles or hazards to safe navigation. This implies that the inertial navigation system must provide control signals to the diving plane, rudder, buoyancy, and propulsion controllers.

As a depth gauge pressure reading offers a more reliable and accurate depth indication, a depth gauge sensor should be incorporated into the inertial navigation

system. This could easily be handled through the Kalman filter implementation that is detailed in later chapters. Ultimately, this will lead to a more accurate inertial navigation system and provide more accurate positioning data.

C. A PRELIMINARY CONCEPT OF THE AUTONOMOUS SUBMERSIBLE VEHICLE

One possible design concept of the autonomous submersible testbed vehicle is presented here to provide some means of establishing some common reference from which detailed analysis of the inertial navigation system can proceed. Although many other variations of such a vehicle are conceivable, this is perhaps the most likely concept of such a vehicle.

The submersible is based on a cylindrical pressure hull, about 20 feet in length and 8 feet in diameter. An external shell covers the pressure hull and forms a small main ballast tank, to which acoustic absorbing tiles are attached. The submersible has a small rudder that protrudes far enough down to enter the propeller wash. The propeller is a multi-blade propeller or a pump-jet propulsor. There is no sail plane area. Diving planes are near the aft end of the hull. The sonar transducers are hull mounted. Two small camera extendable pressure proof housings are located in the forward part of the external shell; one holds a video camera and the other a 35mm SLR camera.

Internally, about 50% of the volume is dedicated to propulsion space. The propulsion is a silver-cadmium battery powered electric motor. No reduction gears are used. The remaining usable interior space has a securing lattice network composed of standard connectors. A power distribution grid is incorporated within the securing network. A single variable ballast tank is located amidships and provides the variable buoyancy control desired. A small electric pump determines the water level in the tank, and an air connection provides a more rapid means of tank level control.

An inertial navigation system, comprised of small gyros and a dedicated microprocessor, is based on a Kalman filter implementation to reduce gyroscope errors. The Kalman filter receives inputs from an electronic depth gauge sensor, which provides the primary depth indication and is used to reduce inertial errors. The NAVSTAR Global Positioning System, which should be fully deployed by 1990, provides the navigation fixes required to reset the inertial navigation system. The GPS system is a satellite-based system comprised of eighteen satellites in six orbital planes, from which a receiver can triangulate its position with a very high degree of accuracy.

[Ref. 3: pp. 1177-1186] The inertial navigation system will provide control signals to the several device controllers to effect submarine control.

II. A STUDY OF PREVIOUSLY EXISTING SUBMERSIBLE INERTIAL NAVIGATION GUIDANCE SYSTEMS

A.   FUNDAMENTALS OF INERTIAL NAVIGATION

Inertial navigation is a system of navigating a vehicle without referring to any navigational aids that are external to the vehicle. A pure inertial navigation system relies on Newton's laws of motion, primarily that a body at rest will remain at rest unless some external force is applied to it and that a body in motion will continue to move in a straight line unless some force acts on it. This type of navigation involves measuring time, gravitation, acceleration, and angular velocity, and performing the necessary calculations and data processing to determine an estimate of the vehicle's navigational position. [Ref. 36: p. 2]

Inertial navigation depends upon several key physical laws. Depending upon the exact mechanization approach used to effect the inertial navigation system, these may include the constancy of momentum, the constancy of the speed of light, the existance of gravity, and the accurate measurement of time or its equivalent. [Ref. 15: p. 1156] Although an inertial navigation estimated position cannot be considered a true navigational fix in the fullest sense of the word, the inertially determined position is often far more accurate than standard navigational fixes.

Essentially, an inertial navigation system measures all the accelerations which a vehicle encounters, translates these accelerations to the equivalent accelerations in the stored reference system, integrates these translated accelerations with respect to time to get velocity, and integrates again to obtain position. Equation 2.1 describes this operation. The velocity initial conditions and position initial conditions are required in these integrations. The velocity initial conditions must be as accurate as possible to prevent a large error in the estimated position from developing.

$$\int \int a(t)\, dt \;=\; \Delta x \qquad\qquad\qquad \text{(eqn 2.1)}$$

Regardless of the type of engineering implementation used, all inertial navigation systems must perform the following functions: [Ref. 4: p. 1-2]

1.   Establish and maintain a reference frame of coordinates.
2.   Measure specific forces applied.
3.   Have knowledge of the gravitational field.

4. Time integrate the specific force data to obtain velocity and position information.

The reference frame is maintained using the gyroscope. A mechanical gyroscope has a very large angular momentum. Since the inertially referred time rate of change of angular momentum is proportional to the applied torque, and the torque is directly related to the applied force or acceleration, then the torque applied can be measured and compensated for, resulting in an ability to maintain the gyroscope oriented along a known axis. Thus, a mechanical gyroscope can maintain a known spatial reference direction. Hence, three appropriately located gyroscopes can define a reference coordinate system. This forms the basis for establishing and maintaining a reference frame of coordinates for the inertial navigation system.

The inertial navigator must also measure the specific forces or accelerations applied. The forces applied are typically measured using accelerometers. Many designs are presently in use, but most work on a simple variation of the pendulum. The pendulum is mounted such that the motion of the vehicle is related to the motion of the platform to which the pendulum is attached. The motion of the pendulum strictly follows Newton's laws of motion, and thus can be directly related to acceleration.

Unfortunately, Einstein's principle of equivalence states that it is impossible for an accelerometer to distinguish between inertial accelerations and gravitational accelerations. Thus, in order for the measurements from the accelerometer to correlate to the inertial acceleration, detailed knowledge of the local gravitational field is necessary. [Ref. 4: p. 2] The local gravitational field accelerations must be accounted for if an inertial position is to be found with sufficient accuracy.

Once the coordinate reference frame has been established, and the inertial accelerations determined, a double integration with respect to time produces the change in position with respect to the stored reference position. A means of establishing initial velocity conditions and initial position conditions completes the inertial navigating solution. Additional refinements would include some means of resetting the navigational position periodically to correspond with externally derived or navigationally fixed positional inputs.

The gyroscope type that is discussed first is the single degree of freedom mechanical spinning wheel gyroscope, the simplest type. Other types of gyroscopes will be introduced, but in all cases these other gyroscopes will be identified by their type. Unless specifically stated, the gyro should be assumed to be the single degree of freedom mechanical gyro.

Finally, it must be realized that several other means of establishing a stable fixed reference frame exists and are presently being developed. The mechanical gyroscope is by far the most common in use in inertial navigation systems and will therefore be discussed in length. However, modern technology offers significant opportunities for future inertial navigation systems. Therefore, a section is devoted to these other reference frame techniques.

1. Simple Mathematical Concepts

The properties of generalized inertial frames can be deduced from the framework of classical mechanics. Newton's first law states that a body at rest will remain at rest unless some external force is applied to it and that a body in motion will continue to move in a straight line unless some force acts on it. The uniformity of motion can be verified using an inertial coordinate system. An inertial reference frame would be one in which each of the three noncoplanar axes used to define the coordinate system could be defined by the trajectories of bodies in motion which have no forces acting on them (straight line trajectories). Any reference inertial frame can be expressed through a simple translation from any other inertial reference frame. Equation 2.2 describes a simple linear translation.

$$r = r' + v * t \qquad \text{(eqn 2.2)}$$

Given the concept of an inertial reference frame, any arbitrarily moving frame can be expressed as a simple translation from the inertial frame of reference. Thus, the inertial navigation problem involves a translation of sensed motion to an equivalent in the reference frame. This involves acceleration vector and velocity vector transformations. These transformations have been solved for arbitrary rotations and translations, and solutions are readily available in published references. [Ref. 5,20: pp. 21-34, pp. 57-75] In a frame of arbitrary rotation and translation, Newton's second law takes the form of Equation 2.3 [Ref. 5: p. 3]

$$\sum F_i + \sum F = m\,\frac{d^2r}{dt^2} \qquad \text{(eqn 2.3)}$$

The F_i's, called apparent forces, are proportional to the mass of the body acted upon and are functions of the relative motion of the selected reference system

and the arbitrary frame. The F's, represents the sum of all the real forces applied to the mass, m. The second derivative of the position vector, r, which is normally viewed as the acceleration, completes the expression of Newton's second law of motion. The apparent forces are classified according to Table 1. [Ref. 5: p. 4] A functional block diagram of a single axis position indication system based on an Earth frame of reference, is presented in Figure 2.1. In this Figure, the output of the accelerometer is the total acceleration sensed by the accelerometer, a_{ip} . The acceleration component due to gravity, G, must be subtracted from this total to give the inertial acceleration. The reference direction is arbitrarily called X. Thus, the component of gravity in the x-direction, G_x, is the acceleration component of gravity that must be subtracted from the total acceleration to get the inertial acceleration. The procedure to determine this component of gravity involves establishing the relationship between the x-direction and the true vertical direction (sensed by Schuler's oscillations) and determining the local gravitational field strength, which is solved in the gravitational field intensity computer. Additional corrections included involve corrections for the apparent forces, in this case chiefly the Coriolis and centripetal forces.

TABLE 1

APPARENT FORCES

Apparent Force	Relative Motion of Frame
Einstein	Linear Acceleration
Euler	Angular Acceleration
Centrifugal	Angular Velocity
Coriolis	Angular Velocity

The concept of an inertial frame can be extended to include any frame within which Newton's laws of motion apply within some limited region or bound. This allows a local reference frame relative to the Earth to be used. However, the gravitational field of the Earth must be considered to be superimposed on this reference frame for the analysis to be accurate.

An excellent development of the rigorous mathematics involved describing the gyroscopic phenomena is presented in McClure. [Ref. 20: pp. 75-115] This development concludes with Euler's dynamical equations, which form the fundamental mathematical equations describing gyroscopic phenomena. The mathematical
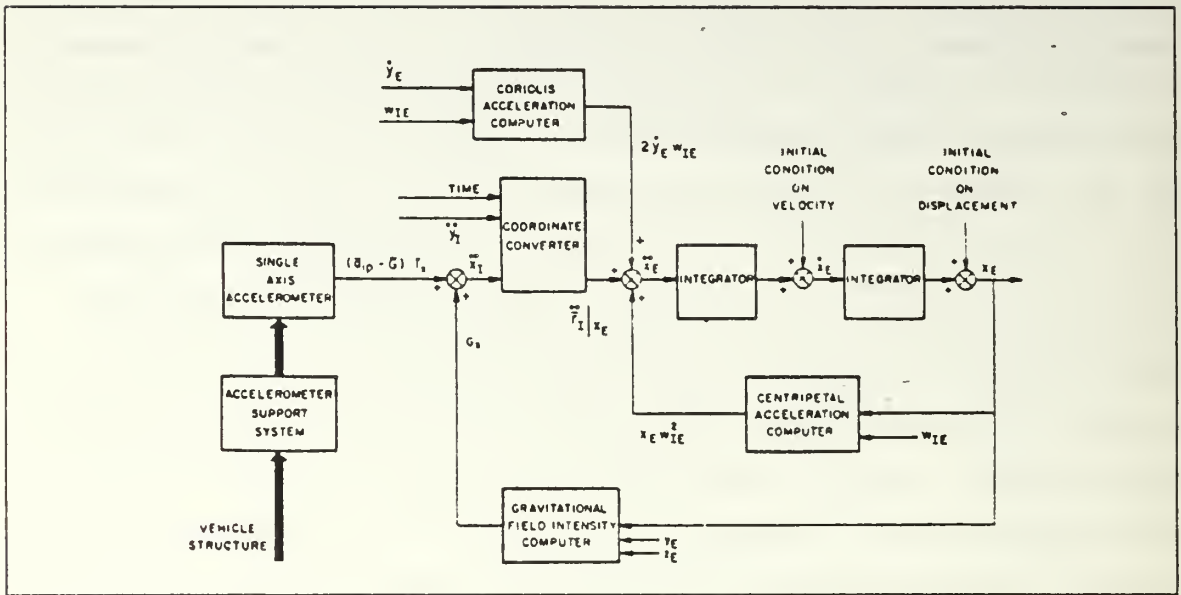
Figure 2.1 The Mechanics of Inertial Positioning [Ref. 18: p. 76].

foundations of the gyroscope are well documented, and need not be repeated, although concepts derived from this analysis will follow in the next section.

2. **The Mechanical Gyroscope**

   a. *Properties of a Simple Mechanical Gyroscope*

The first phenomenon noticed on examining a mechanical gyro is stability. As a toy, children are fascinated by the spinning top that manages to stand at a single point. As long as the top spins, it is able to stand. The mere fact that the top is rotating gives it stability, despite its having an inherently unstable shape. The spinning gives the top angular momentum and as a result stability. Similarly a gyro shows this same stability. Because a gyro's angular momentum is likely to be many magnitudes larger, the stability exhibited is much greater. Thus, the gyro trys to keep a stable position in space. Or more specifically, the gyro tends to keep its spin axis fixed in space. [Ref. 11: pp. 13-14]

The second phenomenon a gyro exhibits is precession. If a spinning gyro is imagined that is standing upright with its axle pointing up, as in Figure 2.2, and if a force is directed on the spin axis such that it would appear that the force should push the gyro to the right, then the gyro resists the applied force. In fact, the gyro will tilt in a direction that is orthogonal (forms a 90° angle, in this case) to the applied force. The exact direction of the tilt depends on the direction of the spin. A nonspinning

30
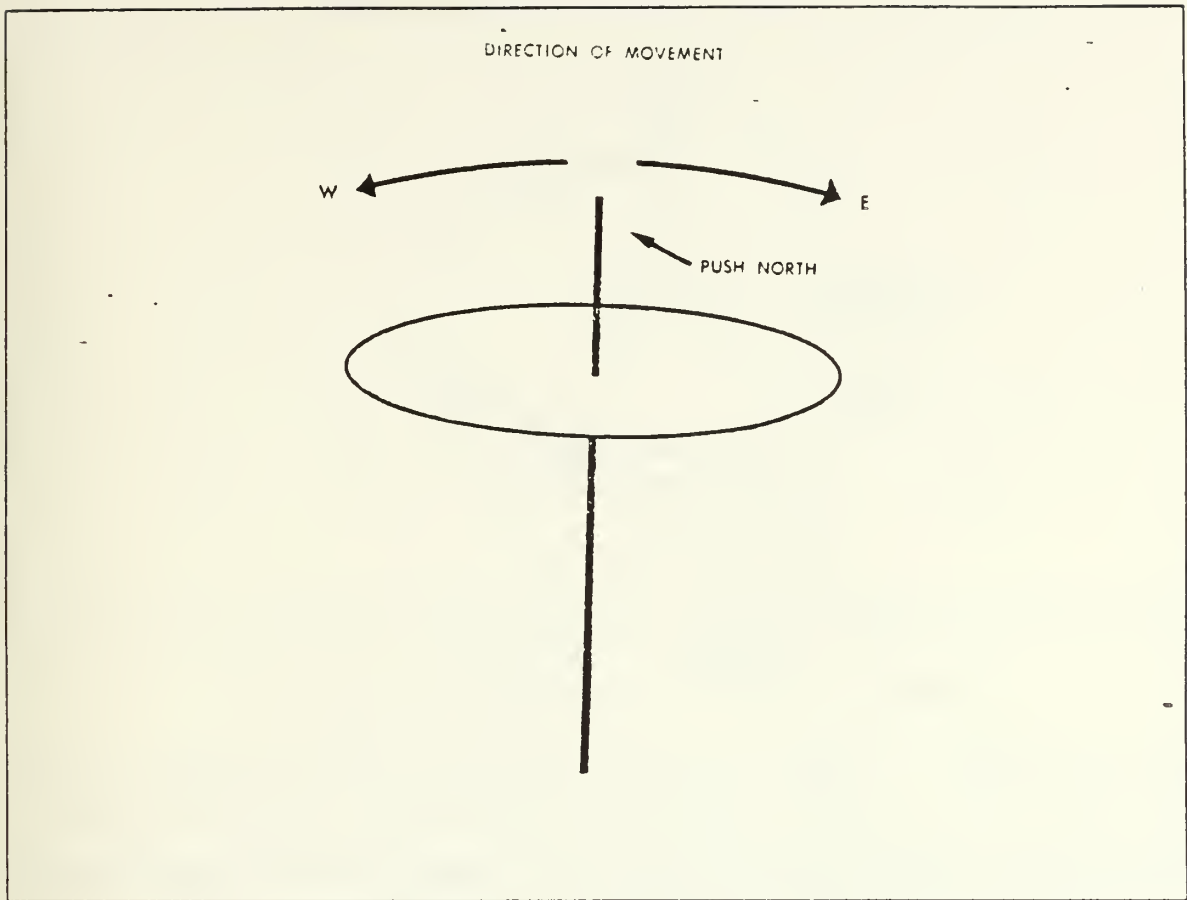
Figure 2.2   Precession Example 1 [Ref. 11: p. 2].

gyro would tilt in the direction pushed by the force, but a spinning gyro tilts in a direction 90° to the force in the direction of the spin, see Figure 2.3. The resultant rotation, about an axis perpendicular to the prior angular momentum and the disturbing angular velocity, is called precession and is a phenomenon which is a fundamental property of the dynamics of the compound rotation of all physical bodies. Precession of a rotating body under the application of a torque or moment of force which is not measured about the axis of the prior angular momentum is commonly called gyroscopic reaction. [Ref. 20: p. 97]

The last phenomenon of interest with gyros, is that a mechanical gyro is able to precess at a rate that is proportional to the magnitude of the force causing the precession and that the rate of precession does not accelerate as the force is continued. Specifically, if a spinning gyro is pushed as before, with the force being perpendicular to the spin axis, then the gyro will tilt in the direction 90° to the pushing force in the
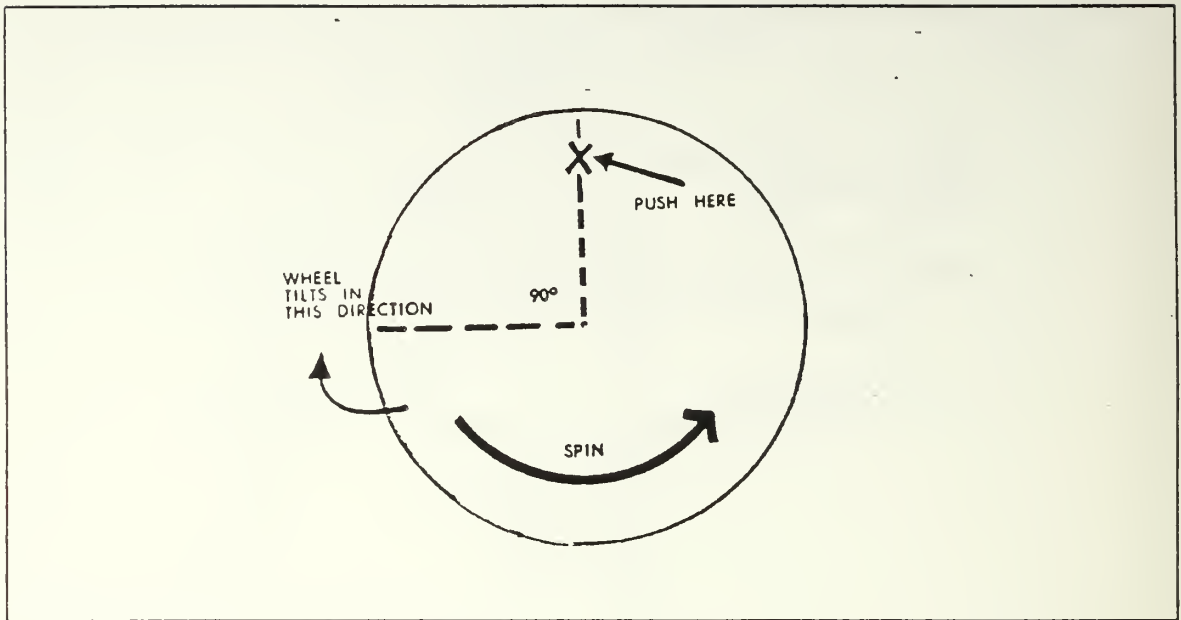
Figure 2.3   Precession Example 2 [Ref. 11: p. 3].

direction of the spin.   It might be expected that should the force continue to be applied, that the rate of motion of the tilt would tend to increase. This is not the case. In fact, the rate of motion of the tilt is constant as long as the force is applied, and ceases when the force is removed.   Figures 2.4 and 2.5 detail this result.

These phenomena are completely expressed in the Euler dynamical equations that were referred to in the prior section, and are as a consequence of the gyro's angular momentum and angular acceleration.   In discussing these phenomena the effects of friction has been ignored.   In any real system, friction exists and must be compensated for.

b.   *The Gimbal as a Gyroscopic Mount*

(1)   *The Single Degree of Freedom Gyro*.   To convert a spinning gyroscopic element into a useful device, it is mounted into a movable gimbal.   The gimbal is simply the frame or supporting structure which supports the gyroscopic element.   The gimbal is in turn mounted in a gyro case.   The gimbal is left free to move about the output axis relative to the case, and the output axis is perpendicular to the spin axis of the gyroscopic element.   This describes the single degree of freedom gyro.   The axis which is perpendicular to both the output and spin axes is the input or sensitive axis. The input axis is the axis for which a turning rate or angle is measured and is the stable reference axis that the gyroscopic element provides for the inertial navigation system.   [Ref. 21: pp. 90-92] See Figure 2.6 and Figure 2.7 for details.

32
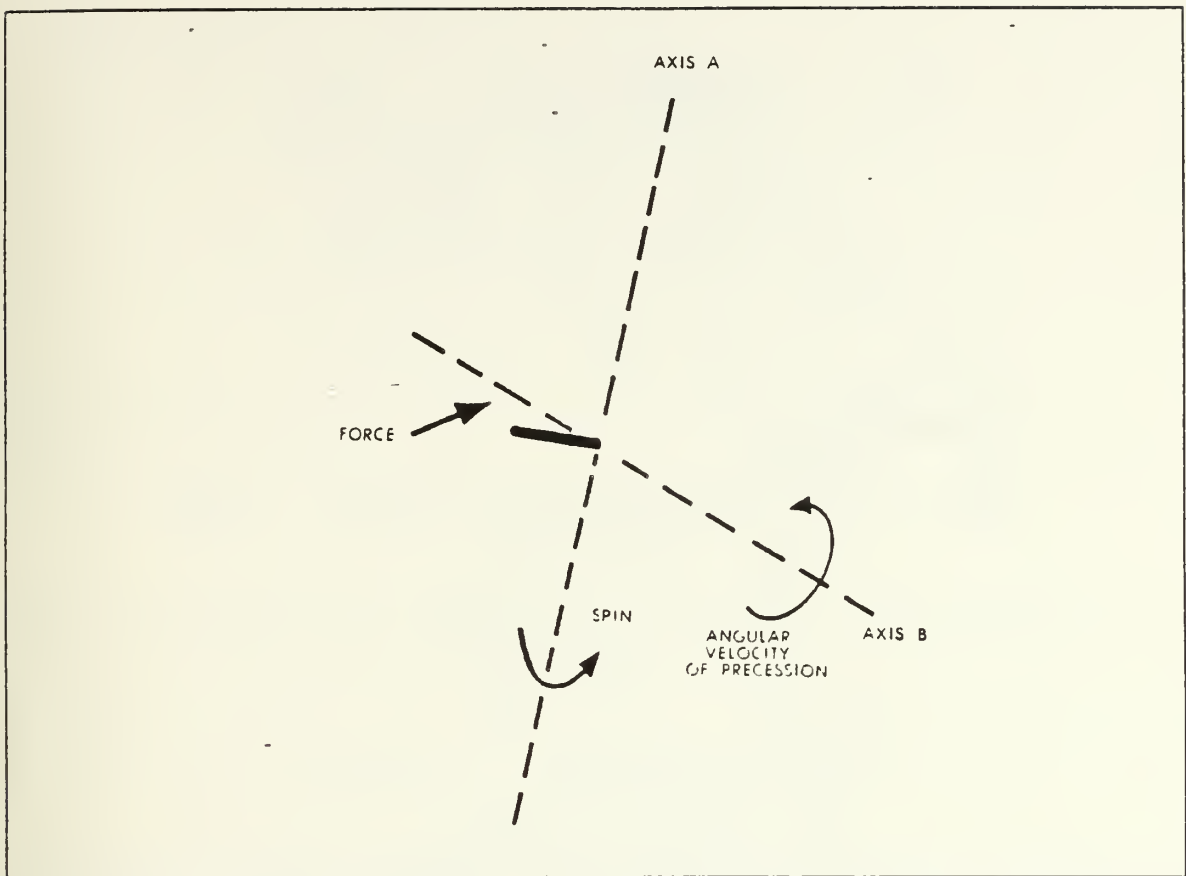
Figure 2.4   Precession Acceleration Example 1 [Ref. 11: p. 4].

The one degree of freedom gyro uses the precession phenomenon to maintain its reference axis. Accordingly, there is an input and an output axis on the single degree of freedom gyro. The single degree of freedom gyro has the following characteristics: [Ref. 4: pp. 69-70]

1. The float element can only rotate relative to the case about the output axis.
2. The gyro rotor gimbal is rigid.
3. All motions take place along the principal float axes such that products of inertia can be ignored.
4. The gyro rotor is maintained at a constant speed relative to the float.

(2) *The Two Degrees of Freedom Gyro.*   If the single degree of freedom rotor-gimbal assembly is mounted inside another gimbal so that it can turn on a second set of pivots which are at right angles to the inner gimbal pivots, then a two degree of freedom gyro results. See Figure 2.8 for details. This gyro is effectively isolated from any external motion in the horizontal plane. This gyro uses the

33
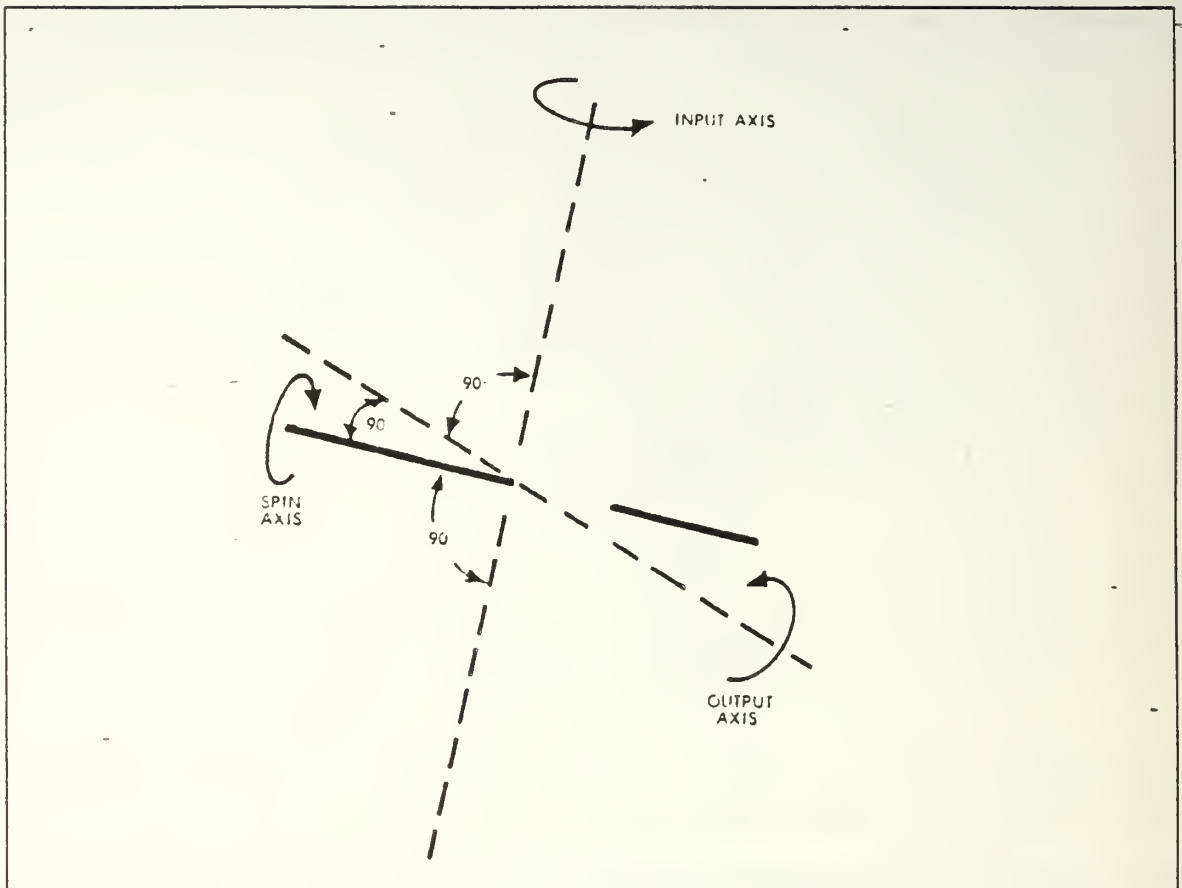
Figure 2.5   Precession Acceleration Example 2 [Ref. 11: p. 4].
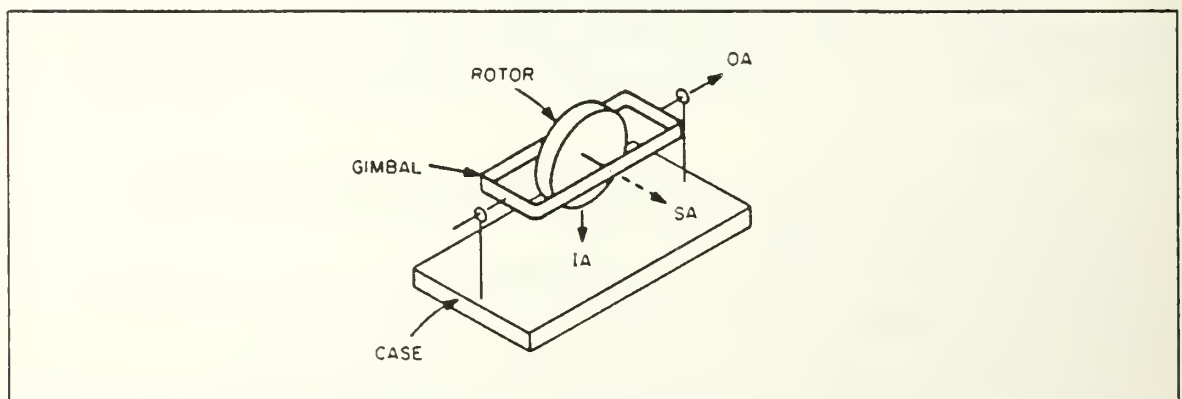
Figure 2.6   The Basic Single Degree of Freedom Gyro [Ref. 36: p. 13].

phenomenon of gyroscopic stability to maintain its reference axis, thus there is no input or output axis as in the one degree of freedom case. The spin axis provides a fixed line of reference. [Ref. 11: pp. 6-7]

34
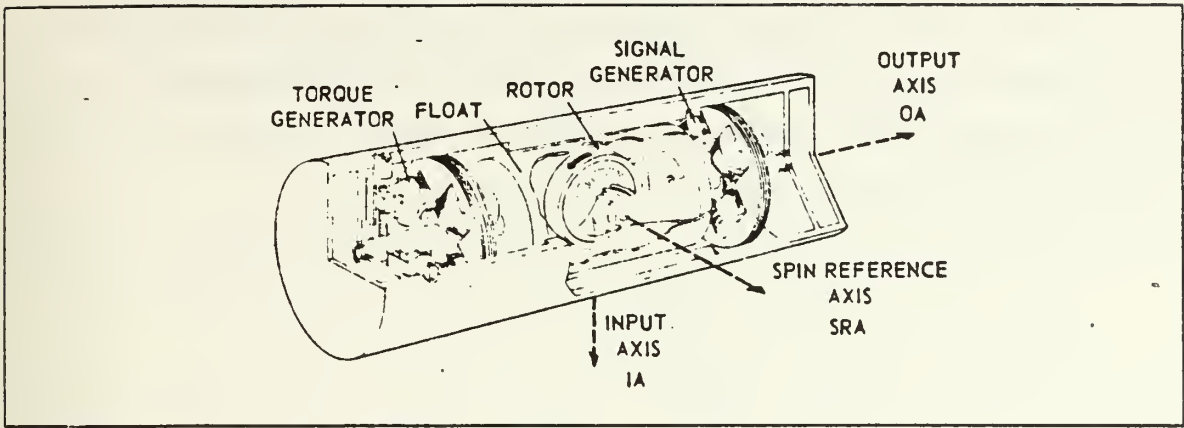
Figure 2.7   The Single Degree of Freedom Gyro [Ref. 36: p. 14].
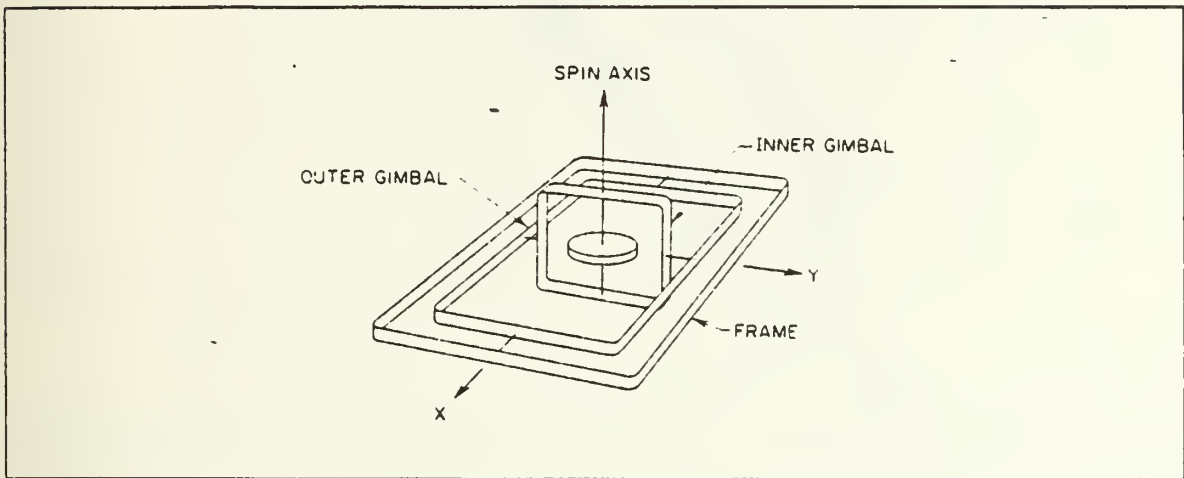
Figure 2.8   The Two Degrees of Freedom Gyro [Ref. 36: p. 18].

One problem that can occur is when the inner gyro gimbal rotates around the full 90° and aligns with the outer gimbal. This is called gimbal lock, and the result of it is that the gyro assembly suddenly acts like a single degree of freedom gyro. Should this occur, the spin axis will no longer be stable, but rather precess, causing the outer gimbal to rotate. To prevent this from occuring, mechanical stops are installed.

c.   The Integrating Gyroscope

In the rate gyro, a spring is attached to the movable arms of the gimbal such that the spring opposes any movement of the gyro about its free axis. The

greater the displacement of the gyro about its free axis, the larger the spring resistance that results. The rate gyro precession is opposed by the spring, and the displacement of the rate gyro from neutral is proportional to the rate or velocity component of the vehicle in the free axis direction. Such a gyro is called a rate gyro. See Figure 2.9 for a simple illustration of the rate gyro. [Ref. 11: pp. 7-9]
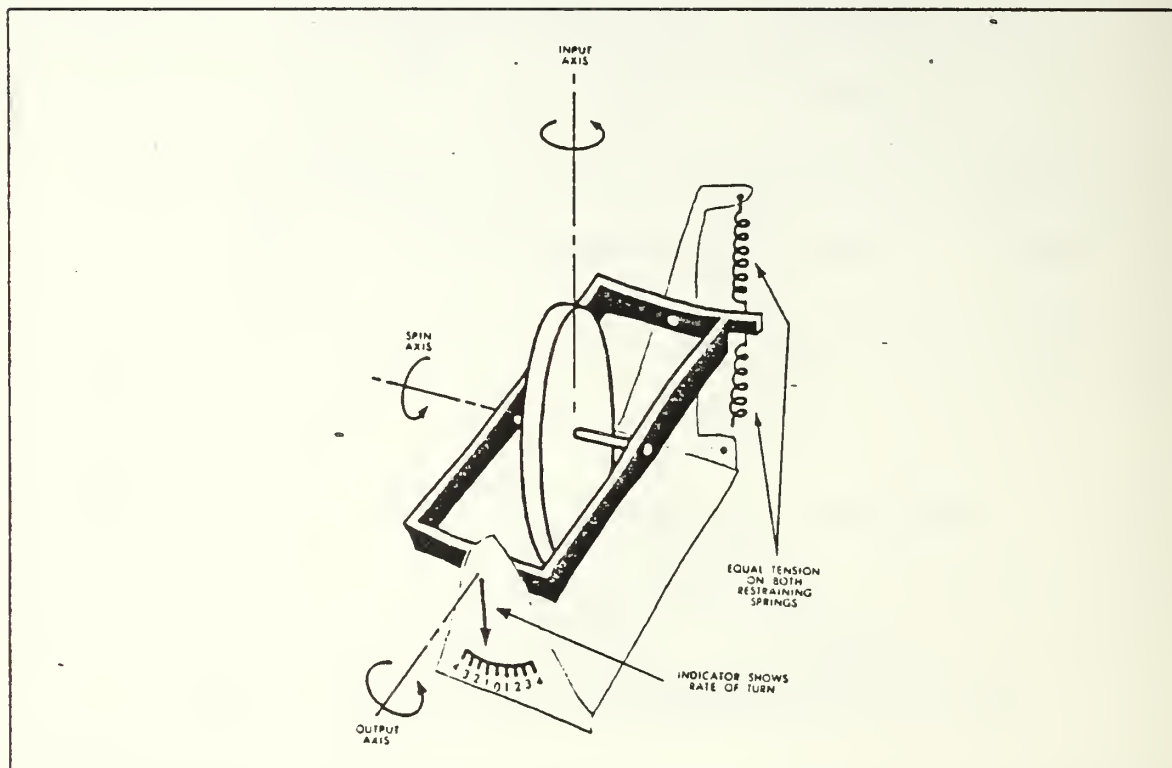
Figure 2.9   The Rate Gyro [Ref. 11: p. 7].

If the spring is replaced with a viscous dampening, an integrating gyro is produced. In such a gyro, the restraining force exerted by the viscous damper is proportional to the gyro precession rate, instead of being proportional to the precession displacement as in the rate gyro. This is desirable because the angular position data is then given directly, without the need for a separate electronic integrator. Additionally, the integrating gyro offers several significant advantages. These include a lower drift rate, more sensitivity, and a wider dynamic range.

The lower drift rate results from the fact that the gyro is floating in a dense fluid which relieves much of the load that was on the gimbal bearings. The result is less friction, and thus lower drift rates. [Ref. 11: pp. 7-9]

A small signal generator is used to measure the total displacement angle through which the gimbal moves. This angle can be measured very accurately, and as only a single integration is involved to get angular position, the instabilities and error growth involved in a second integration are avoided. Additionally, the angular accelerations·on an object can change very abruptly, while an object's mass tends to dampen the changes in angular velocity. The overall result is that the integrating gyro is more sensitive and able to cover a wider range of velocities. [Ref. 11: pp. 7-9]

Most gyros in use today, for control of stable platforms, are of the integrating gyro type. The main problem associated with such a gyro is that it is extremely sensitive to any disturbance of its spin axis. In such a gyro, even the small errors can build to a large error in position over sufficient time.

d. The Torquer

The torquer in an integrating gyro is usually a small synchronous motor which has an output proportional to the voltage input. The torquer functions to measure the precession without permitting too much gimbal movement. This prevents the unlimited precessional freedom of the gimbal, which could radically change the rotor's input axis. A second function of the torquer is to provide a means of positioning and applying torque to the gimbal in order to provide a means of positioning and stabilizing the gyro on gyro startup or reset. [Ref. 11: p. 11]

e. The Accelerometer

An accelerometer is a device that measures the rate of change of the velocity of the component to which it is attached. Examples of accelerometers include: a seismic mass type, a pendulous type, a quartz crystal type, and an optical type. Seismic mass accelerometers are spring and mass setups which are dampened to prevent excessive oscillation. The pendulous accelerometers were discussed previously. Quartz crystal accelerometers are proving very accurate. One such example, the vibrating beam accelerometer, uses a flexure-mode resonator in a beam configuration which restrains the crystal mass. A change in tension results from any accelerations which causes the crystal's frequency of oscillation to change. Optical accelerometers based on the Sagnac effect are coming to fruition. Optical accelerometer devices are being built now that pose a serious challenge to the earlier accelerometer designs. [Ref. 15: p. 1166]

f. The Strapped Down Gyroscopic Platform

The strapped down inertial navigation system is also known as an analytic inertial navigation system. The strapped down system does not physically maintain a reference frame, unlike the other inertial navigation systems. The strapped down gyro system uses the gyro outputs to calculate the relative orientation between the system's initial or stored state and its present state. Essentially, the reference frame is stored in memory instead of being physically maintained.

The strapped down inertial navigation systems are a subject of intense interest because they do not require a gimbal structure and thus offer a marked reduction in mechanical complexity, system size, and cost. Until recently, however, the strapped down systems were impractical due to computer limitations. The only computers able to handle the computational capacity required were far too large and expensive for most inertial navigation systems. However, newer technologies have come about, which offer inexpensive computers with sufficient capacity for this task. Transformation theory must be used extensively in the strapped down inertial navigation system, and must be applied to both the gyro and the accelerometer outputs. The physical indications of north, south, east, or west are available only after the computer transformations have been performed.

The rapid motion of a vehicle in roll, pitch, and yaw subject the strapped down inertial devices to a much greater range of motion than the inertial components that are mounted on a "stable table" and are therefore isolated from such motion. Although a strapped down inertial navigation system imposes a larger dynamic range requirement on inertial instruments, recent designs in these components have overcome these shortcomings.

The problem of alignment in a strapped down inertial navigation system is basically that of determining the initial transformation matrix which relates the instrumented body frame to the reference computational frame. In an operational vehicle, the problem is even more difficult because a suitable determination of the initialization matrix must be made within a reasonably short period of time, without including effects from deleterious motions of the vehicle. A two-stage alignment scheme offers one solution to the problem. A Kalman filter implementation may also be of benefit. [Ref. 4: pp. 2-6]

3. The Non-Mechanical Rotating Wheel Gyro

a. *The Electrostatically Supported Gyro*

In this instrument the reference gyroscopic element is a spherical conducting body of beryllium or aluminum. The reference element spins at a very high speed in a vacuum, and is supported by an electric field. Since the tangential electric field at the surface of a good conductor essentially vanishes, the field will not exert a torque on a perfectly spherical element.

The rotor is given a higher moment of inertia about its polar axis than about its equatorial plane, so that the alignment of the element can be monitored. In the electrostatic gyro, a three axis feedback system is required to keep the rotor centered between supporting field electrodes. The strength of the applied field is controlled by varying the current in the electrodes with changes in the electrode capacitance corresponding to the gyro element motion.

This system has been shown to be more accurate and more reliable than the mechanical spinning wheel gyros. However, the increased computational demands and higher system costs have restricted its use. The electrostatic supported gyroscope is used primarily in critical defense department tasks, such as in the inertial navigation system of the SSBN strategic ballistic missile submarine. [Ref. 15: pp. 1172-1173]

b. *The Nuclear Magnetic Resonant Gyro*

Atomic particles such as protons, neutrons, and electrons have intrinsic angular momentum. The use of this angular momentum for gyroscopic measurements is the idea behind the nuclear magnetic resonance gyroscope. The nuclear magnetic resonance gyroscope uses the intrinsic angular momentum of the nucleus as a whole. A net nuclear magnetization is established, in most cases by optical pumping, and the exchange of angular momentum between the nuclei of various atoms is measured by measuring the net circularly polarized resonant radiation. The basic rotational and precessional information can be obtained from observations of the net nuclear angular momentum, and hence a gyroscope formed. Recent laboratory tests have demonstrated performance in the range of a few hundredths of a degree per hour. However, the system is rather complex and expensive, and is thus unsuitable for most applications. [Ref. 15: pp. 1174-1175]

c. *The Optical Gyro*

There are two types of optical gyros of interest. They are the Ring Laser Gyro and the Fiber Optic Gyro. Both depend on the constancy of the speed of light

through a medium to sense changes in velocities. The Sagnac effect describes this phenomenon. The ring laser gyro uses a laser which is directed in a ring by precisely positioned high quality optical mirrors, and senses velocity changes as a change in the frequency of the laser light. The fiber optic gyro use lasers directed through a fiber optic cable that is spun around a spool to sense these change in velocity using the exact same Sagnac principle.

The major advantages that these devices offer are extremely high reliability, significantly lower costs, and a much smaller size. These advantages are extremely important in the design of an inertial navigation system for an autonomous submersible testbed vehicle. Thus, these devices will be examined in detail in the next chapter.

B. EXPANDING THE THEORY OF INERTIAL NAVIGATION

1. Frames of Reference

There are three general types of inertial navigation systems: geometrical, semi-analytical and analytical. The geometrical system uses two reference frames: an inertially mounted reference frame and a local navigational frame. The inertially mounted frame maintains the initial frame of reference. The local navigational frame follows the motion of the vehicle. Any difference between the two frames provides information on actual vehicle motion. The semi-analytical system uses only one reference frame, which may either be an inertially nonrotating frame or a local navigating one. If the individual gyros are untorqued, then the inertially nonrotating reference frame must be instrumented within some memory device. The inertial navigation system that physically instruments the inertially nonrotating coordinate system is commonally referred to as a space stabilized inertial navigation system or SSINS. Analytical systems do not physically implement a reference frame, but rather use the gyro outputs to calculate analytically the relative orientation between the system's initial and present state. This type of system is most commonly referred to as a strapped-down inertial navigation system. [Ref. 4: pp. 3-5]

The geometric system is the most mechanically complex and largest of these three types of systems. Reliability tends to be poor. At least 5 gimbals are required to provide latitude, longitude, roll, pitch, and yaw information. It has the advantage of requiring less data processing, but with the advances of modern computing this system has limited use for the small submersible vehicle. [Ref. 4: p. 4] The expense and space requirements make this system unacceptable.

40

The semi-analytical inertial navigation system is by far the most common. Only one reference frame is required, thus enabling a smaller and less expensive system. At least 3 gimbals are required to provide the navigational quantities of latitude, longitude, roll, pitch, and yaw. [Ref. 4: p. 4] This system is still expensive, mechanically complex, and occupies too much space for a small submarine.

The analytical inertial navigation system is the least mechanically complex. No gimbal structure is required. This provides a reduction in the system size, weight, mechanical complexity, and cost. The disadvantage of such a system is the computational capacity required. Until the recent introduction of small and cheap modern microprocessors came about, this was the limiting facter affecting its implementation. [Ref. 4: p. 4] The smaller size, cheaper price, and better reliability makes the strapped-down system the best choice for the small submarine.

The choice of which reference frame to implement is another matter, and depends on the exact use of the vehicle as to which is best. Typical reference frames considered include: inertial frame, geographic frame, Earth frame, geocentric frame, body frame, and tangent frame.

The inertial frame is centered at the center of the Earth and is nonrotating with respect to the stars. The geographic frame which recognizes the ellipticity of the Earth, is centered at the guidance location point, and has one axis pointing downward along the normal of the ellipsoid with the other axis free depending upon the guidance grid. The Earth frame is centered at the center of the Earth and is nonrotating with respect to the Earth. This frame rotates about the Earth's polar axis relative to the inertial frame at the Earth's sidereal rate. The geocentric frame has one axis coincident to the geocentric radius to the guidance location point, and the other two axes dependent on the guidance grid. [Ref. 36: pp. 19-30] The body frame is centered about the vehicle's center of mass, and its axis positions are dependent upon the guidance grid. The tangent frame is an Earth fixed frame which is aligned with a geographic frame at a fixed location on the Earth. Typically, the fixed location would be a landing site, guidance radar, or some other convenient point of reference. [Ref. 4: pp. 34-35]

2. Schuler Oscillations

Unless the accelerometer is exactly horizontal to the surface of the Earth, a component of the measured acceleration will be due to gravity. As the accelerometer departs from this exact horizontal surface, say because of some misalignment error or stable platform error, then the accelerometer has a false acceleration imparted on it due

to gravity. If the accelerometers are reporting accelerations due to gravity as well as the inertial accelerations, then the feedback system that controls the stable platform includes an error which exacerbates the problem. These errors would multiply with the square of the elapsed time, and the resulting distance data would be useless. [Ref. 11: pp. 18-19]

The Schuler principle is used to solve this problem. Schuler reasoned that a true local vertical, with respect to the center of the Earth, could be found using an undamped accelerometer with a natural period equal to that of a pendulum's period having a string length equal to the radius of the Earth. Such a pendulum would have its plumb bob at the Earth's center of gravity, and would not move regardless of how one moved the point of suspension around the surface. Schuler then reasoned that if any undamped physical system oscillated naturally at the Schuler period, then it would oscillate uniformly about the true vertical. The Schuler principle therefore provides a means for identifying the exact local vertical with respect to the Earth's center of gravity. [Ref. 11: pp. 18-19]

The Schuler period has been found to be 84.4 minutes. Thus, an accelerometer and gimbal system with a natural frequency of 84.4 minutes will oscillate uniformly about the true vertical. Once the true vertical is located, the reference frame can be precisely positioned and maintained.

Additionally, Schuler tuning effectively holds all system related errors within a maximum bound. This is because pseudo-accelerations manifest themselves as a response to system errors because of the Schuler tuning, which result in a stable platform oscillation that opposes the error buildup. For example, if an acceleration that is too small for the accelerometer to register occurs, then the system will not respond to the acceleration. Thus, the stable platform will not be compensated and eventually depart from its established reference position. The resulting gravity input will then be seen as an acceleration in the direction that the vehicle is actually moving, and the system will be able to catch up to where it should be to within a very minor error factor. [Ref. 11: p. 20]

Terrestrial inertial navigation need not involve explicit computation of the gravitational field components. If spherical coordinates are instrumented, and the true vertical is determined, then position can be given in terms of longitude and latitude where the deflection of the vertical is neglected. Inaccuracies resulting from such a system will be small and bounded. [Ref. 18: pp. 17-45]

The three axis Schuler tuned gyro system exhibits the following characteristics. It developes a large 24-hour component arising from the Earth's rotation. It develops uniform beats which occur at the 84-minute vertical oscillations. The latitude errors resulting from constant gyro drift remains bounded. The longitude error contains a periodic bounded error component and a small nonperiodic error component that grows without bound.

3. Error Characteristics of an Inertial Platform

The analysis of the inertial navigation system errors has been intensive and has led to several effective techniques to reduce the magnitude of the errors. The major sources of inertial navigation errors are as follows. [Ref. 21: pp. 209-225]

1. Gyro drift rate errors.
2. Accelerometer measurement errors.
3. Accelerometer alignment errors.
4. Gyro system alignment errors.
5. Gravity anomalies and deflections in the vertical.

Linear analysis conducted on these error sources has determined the behavior of these errors with time, and derived sets of simultaneous, linear, first order differential equations for all the system errors and for certain linear combinations of these errors. These differential equations have been solved, and their solutions correspond to the physical behavior of inertial navigation systems. The characteristic equation of the inertial system has been expressed and has been shown to have imaginary roots with two predominant periods of oscillation, one at 84 minutes and another at 24 hours. The 84 minute oscillations are composed of two components of neighboring frequencies which produce beats. The beats results from the coupling between the north and east vertical loops that results because of the Coriolis force compensation terms. [Ref. 5: pp. 139-169]

The longitude error has an oscillatory component which depends on the bounded azimuth error as well as an unbounded error component equal to the time integral of the gyro drift rate component that is parallel to the Earth's polar axis. The latitude error depends only on the azimuth component, and is bounded. [Ref. 5: p. 169]

Finally, the different inertial navigation system types, geometric, semi-analytical, and analytical, have slightly different error responses. The geometric and semi-analytic gyros have constant gyro drift forcing terms provided that the drift of the

individual gyros is constant. The constant drift results in settled latitude and azimuth errors, or latitude and azimuth errors that vary sinusoidally about a bias value, depending upon the initial conditions. The analytical system has constant gyro drift components that are modulated and will excite the system at a resonant frequency, thereby causing slowly growing oscillations. However, the effect is small for operating times less than 12 hours. [Ref. 4: pp. 139-169] In general, the error of most concern is the gyro random rate error as this error tends to result in a build up of position error with time that is more significant than the other error sources.

4. Characterizing Inertial Navigation Performance

The last decade has seen a marked increase in the technical efforts placed on inertial navigation system design. Applications for modern inertial navigation systems have come about that saw inertial navigation as an expensive curiosity just a few years ago. Acute competition in terms of product performance, reliability, and cost has fostered emerging technologies at an ever increasing rate. An effort to define the performance required in the inertial navigation system for the autonomous submersible is therefore in order, as this is directly related to system cost.

One of the design goals of the inertial navigation system is to enable the submersible to operate for periods of the order of 10 hours and still have enough navigational accuracy to adequately return to a mother ship. There are several means of directing the submersible to the mother ship once the submersible has closed within a maximum range. These could include the use of a sonar beacon to guide the submersible to the mother ship, having the submersible obtain a reset navigational fix and then proceed to the mother ship, or simply having the submersible surface and signal the mother ship and have the mother ship go to the submersible.

Each of these submersible retrieval methods would have a corresponding effect on the maximum permissible error. In general, the operating procedures and guidelines are the largest factors in deciding what error can be accepted. The classification of the acceptable performance ratings of an inertial navigation system are an appropriate first step in guiding the navigating system design process. [Ref. 15: p. 1166] The following classifications are the author's, relative to the proposed autonomous submersible vehicle, and are given in Table 2.

TABLE 2
CLASSIFICATION OF INERTIAL NAVIGATION SYSTEMS

Accuracy	*Position and Velocity Errors*
low accuracy	position error 0.75 nmi/hr velocity error 2.5 ft/sec
medium accuracy	position error 0.25 nmi/hr velocity error 1.5 ft/sec
high accuracy	position error 0.10 nmi/hr velocity error 0.5 ft/sec

III. ADVANCED TECHNOLOGY GYROSCOPES

The conventional mechanical gyroscope that was described in the previous chapter has several major disadvantages. Since the reliability of a system is related to the number of moving parts, designing a reliable mechanical gyroscope has been extremely difficult. To further complicate the matter, modern mechanical gyros must have some form of an isolation table if they are to be used in a high accuracy inertial navigation system, to protect the gyro from external forces. The result is that either a large gimbal support structure must be used with the mechanical gyro, or a lower accuracy inertial navigation system must be accepted. As a large gimbal structure implies higher costs, and the lower accuracy gyro implies poorer performance, a large effort has been made to find other alternatives.

The economical benefit to the company which provides an accurate low cost inertial navigation and guidance system will be tremendous. Virtually any moving vehicle could potentially realize advantageous applications from such a system. With every moving vehicle becoming a potential customer, the gyroscope industry has realized this economic opportunity, and is very aggressively attempting to develop such a system.

The civilian need for a cheap and accurate inertial navigation system is immense. Uses such as airplane navigation, satellite control, oil well logging, and submersible navigation, are just a few of the present needs. [Ref. 14: p. 54] General Motors has continually shown off inertial guidance and mapping systems in their futuristic prototype automobiles. Should a cheap and reliable inertial navigation and guidance system become available, then the economies of scale should reduce the cost even more.

For the Navy, the over the horizon targeting problem would become trivial, as the target's coordinates could easily be given in latitude and longitude from any inertially equipped vehicle. Since essentially every naval vehicle could have an inertial system, a universal coordinate system would naturally follow. A helicopter could easily detail its exact position without having to reference any other object. Position updates could be made with virtually no error nor any time lag. The significance to logistics would be great. With the entire military universally adopting a global reference frame,

from which all strategic and tactical information could be based, command and control functions would be greatly simplified. All the individual military actions could be conducted using the same standard global reference frame. The faster and more accurate flow of information that would result, would enable commanders at all levels to perform more efficiently and to be better able to accomplish the tasks assigned. The end result would be a more responsive and capable military force.

This chapter addresses the development of the two gyroscopes that hold the most promise of enabling this cheap, reliable, and versatile inertial navigation system. The ring laser gyro has already been deployed in naval ships and aircraft, and is widely available today. The fiber optic gyro is largely still in the development phase, but promises all the accuracy required at a small fraction of the cost of any other gyro system. Both gyros work on the same physical principle, the constancy of the speed of light within a medium, and both will be discussed at length in the sections that follow.

A.   OPTICAL GYROSCOPES IN GENERAL

1. An Introduction into the Optical Gyroscope

Fiber optic sensors offer a number of unique features which make them attractive for a variety of applications. Among these are that a fiber optic sensor can be made to be virtually immune to electromagnetic interference, is non-electrical, can be made to be very sensitive, small in size, and lightweight. Fiber sensors can be made to detect changes in light intensity, frequency, phase, and polarization.

In 1897, Oliver Lodge theorized that light could exhibit a gyroscopic behavior. Specifically, he noticed that the amount of time required by light to transverse a circular pathway depended upon whether the pathway was stationary or rotating. He further determined that the time difference varied with the rate of the rotation and the length of the optical path. In 1904, Michelson concurred with Lodge and hypothesized that it should be possible to measure the rotation of the Earth using beams of light traveling in opposite directions around the periphery of an area. Although an intriguing hypothesis, a practical use of the phenomenon was not put to use because of the inadequacies of the technologies available at that time. [Ref. 16: pp. 1-3]

Modern technology has brought the ability to accurately measure small differences in time, as well as small changes in light's frequency, phase, intensity, and polarization. Laser and fiber optic technology has made the optical gyroscope possible. Through this technology, two types of optical gyros have emerged, the ring laser gyro and the fiber optic gyro.

47

The ring laser gyroscope is the more developed optical gyro. Although extremely sensitive and accurate, the real advantage that the ring laser gyroscope has over the mechanical gyroscope is that the mechanical gyro has many complicated moving parts while the ring laser gyro has virtually none. Thus, the ring laser gyro is far easier to maintain, and therefore less costly, than the mechanical gyro. Ring laser gyroscopes also feature instant turn on, whereas mechanical gyroscopes require significant periods of time to attain rated speed and accuracy. However, the ring laser gyro requires extremely fine mirrors which must be mounted within very small tolerances. The result is that the ring laser gyroscope is still a moderately expensive product.

The fiber optic gyroscope is the more promising of the two optical gyroscopes in terms of cost. The fiber optic gyroscope does not require any mirrors and does not demand exact positioning of its components. The expectation of a very low cost continues to be anticipated. The fiber optic gyroscope also has the advantage of a smaller size and a more variable package shape. However, the fiber optic gyroscope is still being developed. Although prototypes are being made, the companies developing them are very secretive about any specifics of how certain problems are being addressed. However, the research and development effort continues to be very strong, and it is likely that full production of fiber optic gyroscopes will begin by 1990.

2. **The Sagnac Effect**

The fundamental cause of the doppler frequency shift has been described as the rate of change with respect to time of the path length that a sound wave travels. Extrapolating this principle to wave motion in general, and light waves in specific, gives a means of envisioning the optical gyroscopic effect. More specifically, it has been shown that light will exhibit a frequency shift that is somewhat similar to the doppler analogy.

Suppose an observer is inside a reflective circular ring, and that he emits a pulse of light in such a way that half of the light pulse transverses the ring in each direction. If the ring is stationary, then both halves of the light pulse will return to the observer at exactly the same time. However, if the ring is rotating then one of the light pulses would have to travel farther than the other, because the observation point has moved closer towards the pulse with the shorter distance to travel. As the speed of light is a constant, an arrival time difference would be observed. This difference in time would be directly attributable to the difference in path length. [Ref. 1: pp. 94-95]

48

Stated another way, the difference in the pulse arrival time would be proportional to the first derivative of the optical path length with respect to time. Additionally, since the ring continues to rotate in the same direction, the observer would see that the two light pulses are no longer at the exact same frequency. He would notice that the change in frequency is also proportional to the first derivative of the optical path length with respect to time. [Ref. 31: pp. 11-12] This appears to be directly analogous to the doppler effect presented above, in which the difference in sound pitch (or frequency) is proportional to the first derivative of the path length of the sound waves with respect to time. George Sagnac first demonstrated this rotation induced difference in path length, called the Sagnac effect, in 1913.

A definition of the Sagnac effect is that it is is the nonreciprocating phase difference experienced by light propagating along opposite directions in a rotating frame. [Ref. 8: p. 66] The Sagnac effect is a relativistic, rotation induced frequency shift due to a path length difference between optical waves which counterpropagate around a closed optical path. The rotation induced path length difference is given by Equation 3.1. [Ref. 24: p. 93]

$$\Delta L \ = \ 2 L R \Omega / c \qquad \text{(eqn 3.1)}$$

where:

ΔL = the rotation induced path length difference
L = the total path length of the closed optical path
R = the radius of the path
Ω = the angular velocity
c = the speed of light through the path medium

The Sagnac frequency shift, Φ, that occurs as a response to the rotation induced path length difference is given by the Equation 3.2. [Ref. 24: p. 94]

$$\Phi \ = \ 2 \pi L D \Omega / \lambda c \qquad \text{(eqn 3.2)}$$

where:

Φ = the Sagnac frequency shift
L = the total path length of the closed optical path
D = the diameter of the path
Ω = the angular velocity
λ = the optical wavelength through the medium

c = the speed of light through the path medium

In a ring laser gyro, the frame is a resonant cavity through which the light passes. The rotation is set up by directing the light path around the frame. The light is directed around the frame using highly refined mirrors. Figure 3.1 shows this basic configuration. [Ref. 19: pp. 48-49]
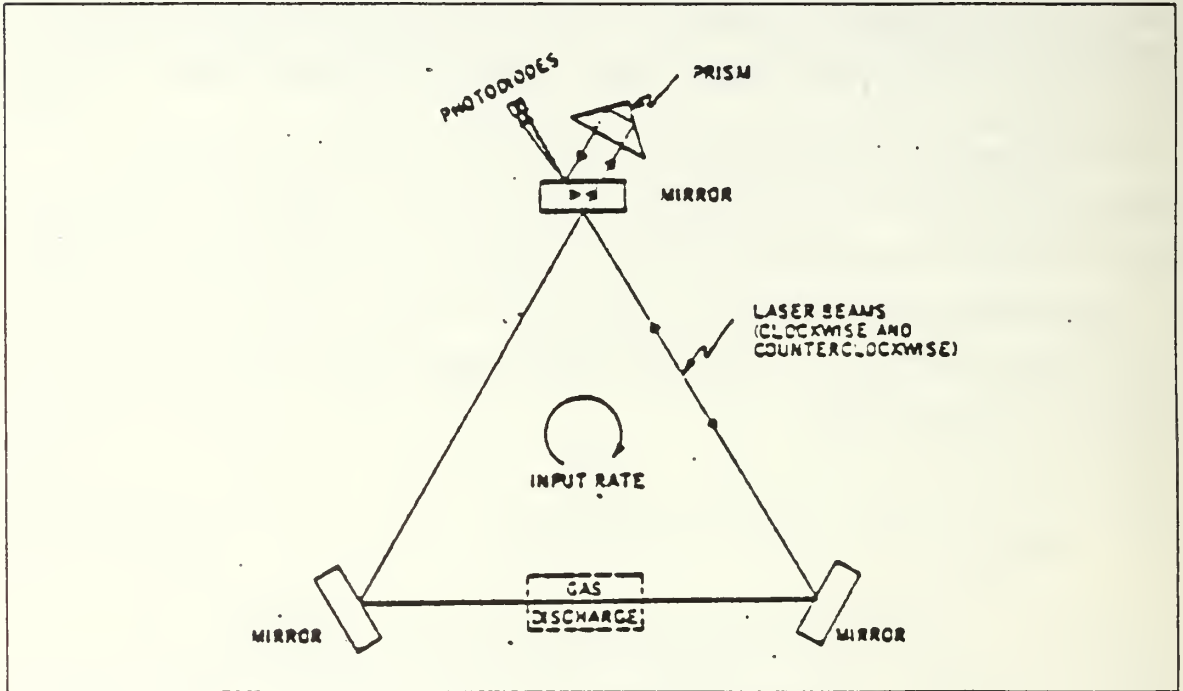
Figure 3.1   The Basic Configuration of a Ring Laser Gyro [Ref. 31: p. 11].

The fiber optic gyro uses a fiber optic cable to form the frame. The fiber optic cable is wrapped in a coil, usually around a spool. The rotation is set up by light traveling within the fiber cable and around the spool. Figure 3.2 shows this basic configuration. The semitransparent mirror functions to split the laser beam in two exact halves, which then travels in opposite directions around the fiber coil. The screen represents the detector, which would sense the Sagnac frequency shift. [Ref. 1: pp. 96-98]

In both optical gyros, the rotation of the light is established by directing the light beams around the frame. Any motion perpendicular to the axis of the frame, will result in a component of the angular velocity being sensed by the light propagating
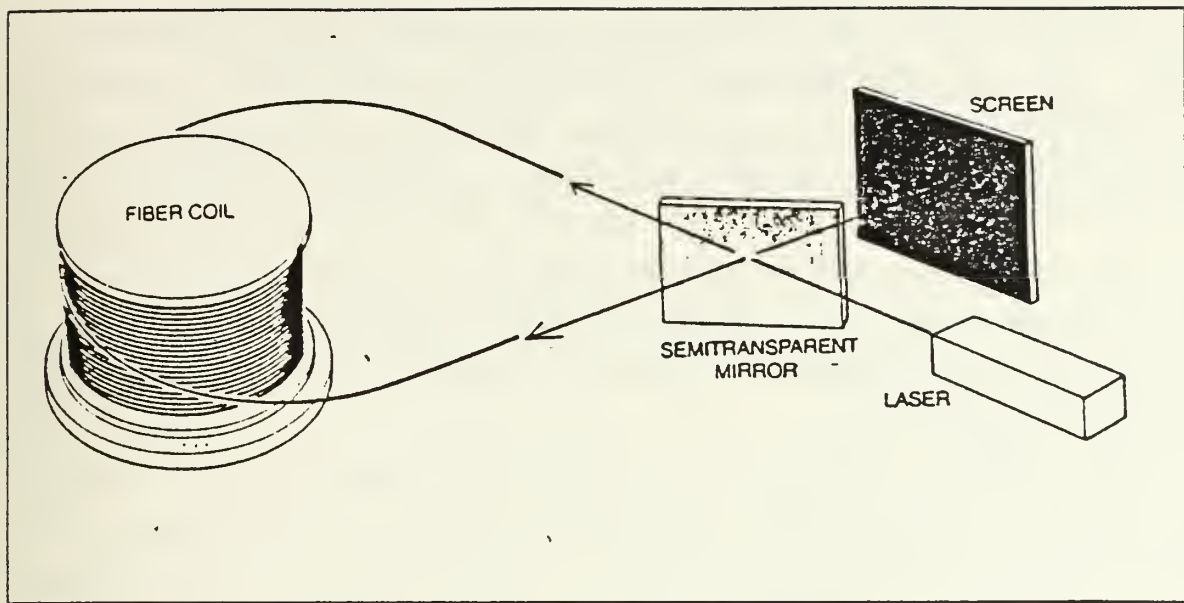
Figure 3.2 The Basic Configuration of a Fiber Optic Gyro [Ref. 1: p. 97].

around the frame. The light beams will be subjected to a change in the path length proportional to the angular velocity component experienced. Thus, the light will undergo a Sagnac phase shift that is proportional to this angular velocity component.

Since the light beams will be shifted in frequency proportional to the angular velocity component perpendicular to the axis of the optical frame, all that needs to be done to design a gyro is to sense this frequency shift and compute this angular velocity component. The angular velocity component then can be integrated with respect to time, to give the change in angular position perpendicular to the axis of the gyro. Three such gyros would define a reference coordinate system from which inertial navigation could be conducted.

A laser is used within these device frames because a laser's light is essentially composed of a single frequency. The more nearly the laser is to the ideal single frequency light source, the better. This is necessary because the frequency shift from the light source frequency gives the Sagnac shift. If a single frequency light source is used, then detection of the frequency shift is greatly simplified. [Ref. 7: pp. 68-71]

B. RING LASER GYROSCOPES

1. The Basic Ring Laser Gyro

When a DC voltage is applied across a laser cavity, an electrical discharge is established in a mixture of helium and neon gases. The discharge energy excites the

51

helium and neon atoms into several higher energy states. [Ref. 32: p. 3] Neon has a pseudo-stable high energy state in which some of the excited neon atoms become entrapped. These entrapped neon atoms will not be able to freely relax from this higher energy level and return to the lower ground energy state. This relatively stable high energy state is very near the same energy level as some of the excited helium atoms. Because these energy levels are so close, these neon atoms and helium atoms can easily exchange energies with one another. The end result is that many more neon atoms become entrapped in this pseudo-stable high energy state. This process is known as energy pumping, because the neon atoms are pumped into the pseudo-stable high energy state. [Ref. 32: p. 3]

Light amplification occurs when a photon strikes the excited neon atom in the pseudo-stable high energy state, giving it the additional energy it needs to escape out of its pseudo-stable high energy state and allowing it to relax to its low ground energy state. The atom relaxes to its low energy state by ejecting a photon of the proper quantum energy. Since the pumping process has pushed many neon atoms into the entrapped pseudo-stable energy state, a chain reaction occurs and a net gain of photons result, all of which are at about the same energy. This net gain of photons is called lasing. [Ref. 32: p. 3]

In a laser cavity, the photons are emitted in all directions. However, only the light that radiates in a straight line between the two or more mirrors is reinforced by repeated trips through the gain medium. The repeated amplification of the light reflecting between the mirrors soon attains saturation, and a steady state oscillation occurs. This light oscillating between the mirrors is the laser beam. A small percentage of this laser beam may be allowed to pass through one of the mirrors, providing a source of laser light. A laser gyro operates much like an ordinary laser, but rather than having just two mirrors it contains three or more. This allows the laser beam to travel around an enclosed area, forming the laser optical path. [Ref. 32: p. 3]

If the cavity is in motion, the laser will undergo a Sagnac frequency shift. However, in normal operating conditions, the frequency shift is very small. For example, when exposed to the Earth's rotational rate of 15 degrees per hour, the Sagnac frequency shift of the laser beam is on the order of 4.0 hertz. Given that the laser frequency is nominally 4.7×10^{14} hertz, this Sagnac frequency shift represents a very tiny change. Even at an angular change of 360 degrees per second, the resulting frequency change is only one part in 1.4 billion. Measuring this frequency change directly would be exceedingly difficult. [Ref. 32: p. 4]

The extreme accuracy required in measuring the small Sagnac frequency shift of the laser light presents an enormous problem even when using the latest modern technology. As of yet, there is simply no acceptable means of measuring the frequency shift of the laser beam with sufficient accuracy to make the single laser ring laser gyro viable. However, a solution has been found and it is critical to the construction of the ring laser gyro.

The ring laser gyro configuration described above will actually result in two distinct laser beams forming, with each laser beam traveling in exact opposite directions. If the two laser beams are combined, then the two light waveforms will destructively and constructively interfere with each other forming a composite lightwave that has a slowly varying intensity level of light which varies proportionally to the Sagnac frequency shift. The slow variations in the light intensity can be easily sensed, and an output that is proportional to the angular rate of the laser gyro produced. [Ref. 19: p. 48]

Several mechanizations exist for measuring the Sagnac frequency shift. These mechanizations can be grouped into the following categories. [Ref. 8: p. 66]

1. The resonant mechanization uses a resonant cavity in which the optical resonant frequencies are given by the path length. The resonant frequencies occur when the path length is an exact integer number of optical wavelengths around the cavity. Although changes in the path length are small, because the frequency of light is about 10^{14} hertz, the resulting change in the resonant frequency occuring from even small changes in the path length is substantial. This change is on the order of about 30 kilohertz. [Ref. 19: p. 49]

2. The interferometric mechanization measures the Sagnac effect directly by recombining counterrotating optical waves to form a single optical wave whose intensity varies sinusoidally with the frequency shift. The frequency and phase relationship between the two light beams are determined by examining the composite light wave.

3. The hybrid mechanization uses a combination of the other two mechanizations to measure the Sagnac effect.

The resonant mechanization is best visualized by examining an optical ring resonator, such as shown in Figure 3.3. The optical resonant frequencies of the cavities are controlled by the path length, and occur when there are an integral number of optical wavelengths around the cavity. When the resonator is at rest, the clockwise (CW) and counterclockwise (CCW) path lengths are identical. However, if the resonator is rotating the clockwise and counterclockwise path lengths are different. The path lengths are shifted proportionally to the rate of rotation. This difference in

53

the resonant frequencies between the clockwise and counterclockwise paths, ΔF, is given by Equation 3.3. [Ref. 24: p. 94]

$$\Delta F = 4 A \Omega /(n P \lambda) \qquad \text{(eqn 3.3)}$$

where:

A = the total area enclosed by the optical cavity

Ω = the angular velocity

n = the index of refraction of the medium in the optical path

P = the perimeter of the optical cavity

λ = the free space wavelength of the optical waves
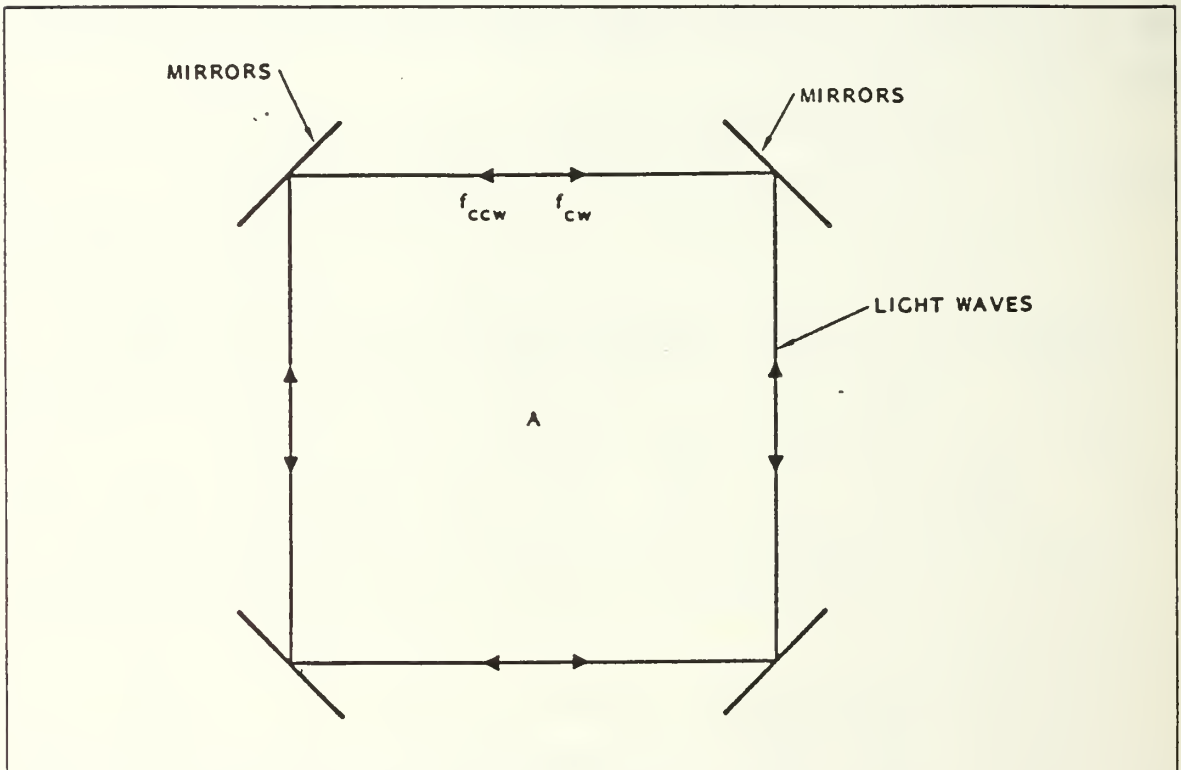
Figure 3.3   An Optical Ring Resonator [Ref. 17: p. 94].

The two resonant frequency light waves are amplified using a gain medium in the cavity, to cause bidirectional oscillations. As the cavity rotates, the frequencies of oscillation in the clockwise and counterclockwise directions change in accordance with changes in the path length, but related to the light wavelengths. The resulting

frequency light that is reinforced has a fairly large total frequency shift, as compared to the Sagnac frequency shift. A portion of the circulating optical waves are tapped off and combined, forming a single light beam whose intensity will oscillate relatively slowly in proportion to the frequency difference of the two component resonant light waves. The beat frequency of this oscillation in intensity is measured, and can be equated to angular velocity. The frequency of these oscillations is known as the ring laser gyro beat frequency. This is the method that is used more commonly in the ring laser gyro.

In the interferometric mechanization, light from the laser source is split into two parts and each part is directed in opposite directions around the closed optical path. At the detector at the end of the optical path, the two counterrotating light beams are recombined, forming a composite light beam whose intensity varies sinusoidally at the twice the Sagnac shift frequency. The total photocurrent, I, is thus proportional to the Sagnac frequency shift, Φ, in accordance with Equation 3.4. This is the method normally used with the fiber optic gyro. [Ref. 24: p. 94]

$$I = I_0 (1-\cos(\Phi)) / 2 \qquad \text{(eqn 3.4)}$$

where:

I = the total photocurrent of the composite light beam

I_0 = the maximum peak photocurrent

Φ = the Sagnac frequency shift

A simple photomultiplier tube is normally adequate to sense the relatively slowly varying intensity levels associated with these Sagnac frequency sensing mechanizations. The photodetectors can either be set up to measure the total photocurrent or to count the fringes in the resulting fringe pattern. By measuring the photocurrent and applying Equations 3.2 and 3.4 or 3.3 and 3.4, depending on the sensing mechanization used, the angular velocity can be determined.

If the light wave intensity is sensed, and if the total frequency shift is very near zero or some integer multiple of the source wavelength, then the detector will sense no measurable photocurrent. Even small errors caused by the imperfect photodetector sensitivity will tend to build up with time. Although, controlling the sensitivity of the detector will limit the error introduced by these low intensity conditions, and a phase modulation and synchronous demodulation scheme will

adequately allow the frequency shift information to be recovered, another possible method of detection is desired. This other method of detection would involve detection of the fringe pattern that is formed in the combined light wave. If the lasers are at the same frequency, then the fringe pattern formed in the composite light wave will be stationary. If the lasers have some frequency shift, then the fringe pattern will move at a rate proportional to the frequency shift. Thus, a photomultiplier tube that is setup to detect the fringes as they cross the detector, will output a series of pulses at a rate proportional to the frequency shift of the laser beams. [Ref. 32: p. 4]

This photodetector will produce a digital pulse code modulated signal which needs no further processing before it is supplied to a microprocessor. Assuming that the frequency shift is due only to the Sagnac effect, the slowly oscillating intensity light is a direct function of the angular velocity perpendicular to the gyro axis.

2. The Ring Laser Gyro Errors

a. Ring Laser Gyro Error Sources

If the ring laser gyro was a perfect device, then the fringes that developed at the detector would be directly proportional to the component of motion that occurred perpendicular to the plane formed by the optical path. If the ring was not moving, then the fringes should remain stationary. In practice, however, actual performance deviates from this ideal behavior. This deviation is known as the ring laser gyro error.

There are two major sources of ring laser gyro error. The first is a ring laser gyro bias effect and the second is frequency locking. The bias effect makes the fringes move even when the ring laser gyro is stationary. The frequency locking makes the fringe movement constant when the ring is moving. It is generally a problem only at low ring rotation rates.

The gyro bias effect arises when the gases (helium and neon) inside the optical ring flow. Gas flow is an unwanted consequence of the fact that power must be supplied to the ring in order to generate the lasers. This power is normally a large electric field, which ionizes some of the gas and creates a plasma which moves within the electric field. This stirs up the gases and results in a net gas flow along the path of the laser beam. Consequently, even when the ring is still, the standing light wave can rotate. [Ref. 1: p. 98]

The frequency locking is an error which occurs due to the backscatter of the laser light when it strikes the mirror. A perfect mirror would reflect all the incident

photons, and have no backscatter. A bathroom mirror backscatters about one in every twenty photons. A good ring laser gyro mirror backscatters only about one in every five thousand photons. Despite using such high quality mirrors, frequency locking continues to be a problem. [Ref. 1: pp. 98-99]

The backscatter of laser light interferes with the main laser beams, coupling with them and forming a standing or preferred light wave. It is the tendency to prefer a particular wave pattern that results in frequency locking. It is best visualized by considering the setup in Figure 3.4, in which a thin sheet of glass is fixed inside the optical path. The thin sheet of glass is used to represent the mirror imperfections, and the mirrors in the figure are assumed to be perfect. A very small amount of the laser beam that strikes the glass sheet will be reflected back in the opposite direction. The standing wave of light that is preferred is one in which a zero or null occurs exactly at the glass sheet, as this will result in no destructive scattering. Since the glass sheet is fixed to the ring, the standing wave will try to rotate with the ring. At low rotation rates the standing wave is able to rotate with the ring, but at higher rates it cannot. Thus, at low rotation rates the frequency locking phenomenon occurs. [Ref. 1: p. 99]
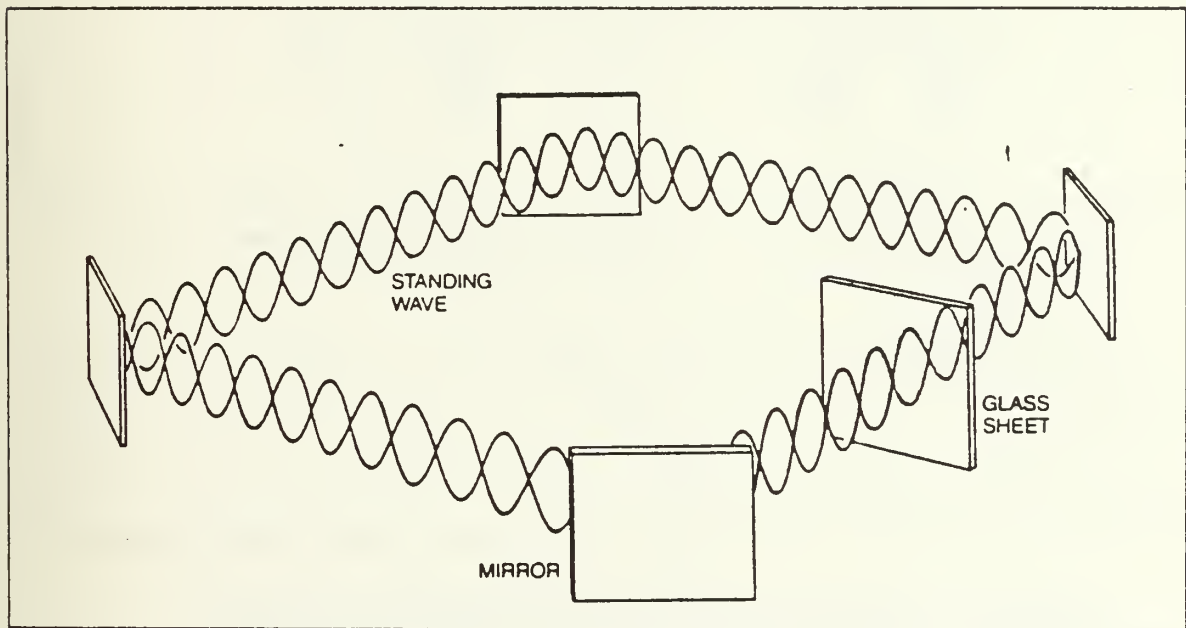
Figure 3.4   The Concept of Frequency Locking [Ref. 1: p. 98].

The phenomenon of frequency locking between coupled oscillators has been well documented using classical mechanics. In the ring laser gyro it was shown

that the backscatter from the mirrors was the source of the coupling problem. The degree of the coupling is directly dependent upon the amount of backscatter. Two solutions have presented themselves. The first is to use better mirror technology, and the second it to find a form of biasing that would circumvent the lock-in at low rotation rates. The most common way of implementing this biasing to circumvent the lock-in at low rotation rates, is to mechanically oscillate the entire ring cavity such that the motion sweeps through the region where lock-in occurs. This maintains an effective output for all rotation rates within the design band. [Ref. 19: pp. 49-50]

This is called mechanical dithering, and its effects can be analyzed using standard frequency modulation theory. Figure 3.5 details the effects of the mechanical dither. Without the mechanical dither, the gyro locks up when near zero input. Within this dead zone, the gyro produces no output. With mechanical dithering, the dead zone is broken up into several smaller pieces that occur at harmonics of the dither frequency. This is a known effect that can be compensated for. Figure 3.6 shows a simple four mirror implementation of the mechanically dithered ring laser gyro. [Ref. 19: pp. 49-50]
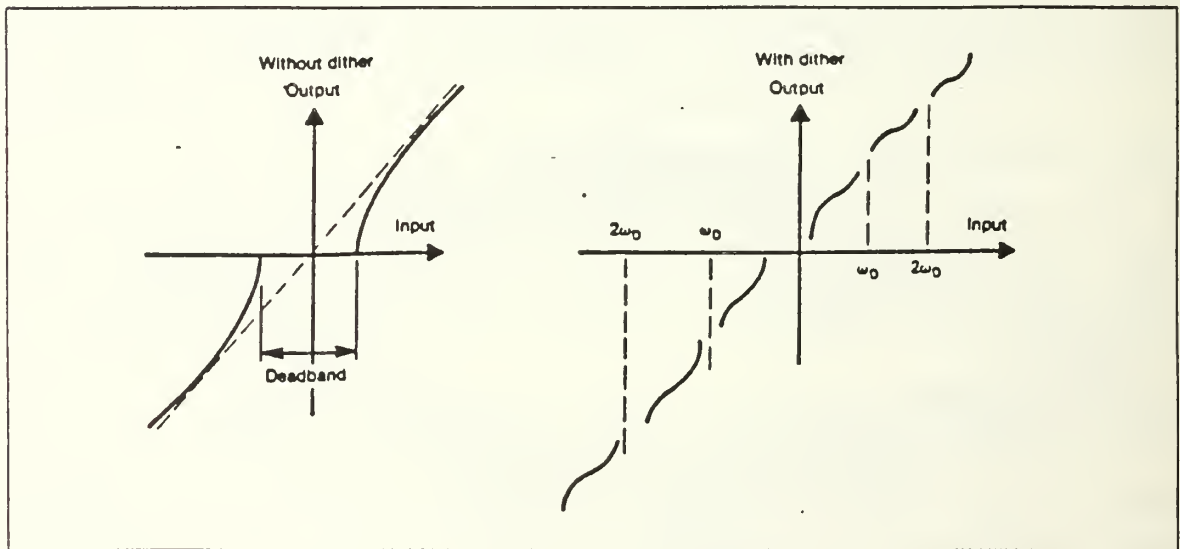
Figure 3.5   The Effects of a Mechanical Dither [Ref. 19: p. 51].

The frequency locking and bias problems are technical problems. In principle they can be completely eliminated. Ultimately, the accuracy of the ring laser gyro will only be subject to the dictates of the Heisenberg uncertainty principle which
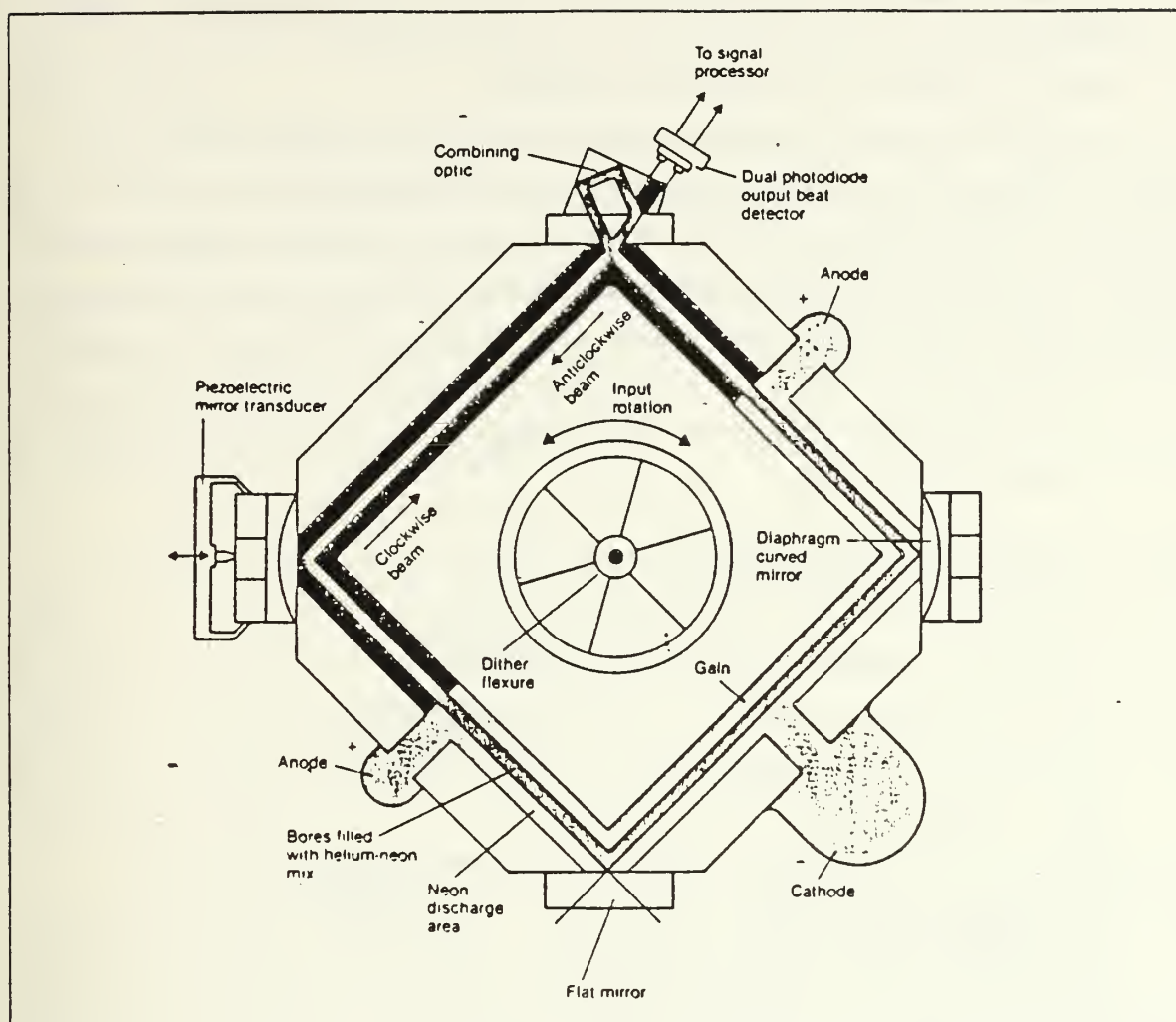
Figure 3.6   A Mechanically Dithered Ring Laser Gyro [Ref. 19: p. 50].

states that it is impossible to simultaneously know the exact position and velocity of a subatomic particle. When applied to the ring laser gyro this means that the standing wave light will move very slightly even when the ring is stationary. Remarkably, the technology has advanced to the point to where large ring laser gyros are closing in on these theoretical limits. [Ref. 1: p. 9]

b. Laser Accuracy Enhancement Techniques

Several techniques have come about which enable the ring laser gyro error to be minimized. These include some of the following techniques. [Ref. 19,16: pp. 51-52, p. 1]

1.   Limiting laser beam competition.

2.   Incorporating a three or four mirror single block design.

3..   Kalman filter implementation to reduce accumulated errors.

59

4. Appropriate material construction, and temperature compensation of inertial components.

5. Magnetic shielding of the sensor block assembly.

In general, the two counter rotating laser beams in a ring laser gyro have a tendency to compete with each other, and only one direction will lase at a time. The net effect is that the laser pulses at a very rapid rate. If however, roughly equal amounts of the neon-20 and neon-22 isotopes are used in the gain medium in the ring laser cavity, then a stable operation is obtained. The lasing gain curves for neon-20 and neon-22 are given in Figure 3.7. The favorable separation between these two curves is one of the primary reasons for using helium-neon gas mixtures in the ring laser design. [Ref. 19: pp. 50-52]
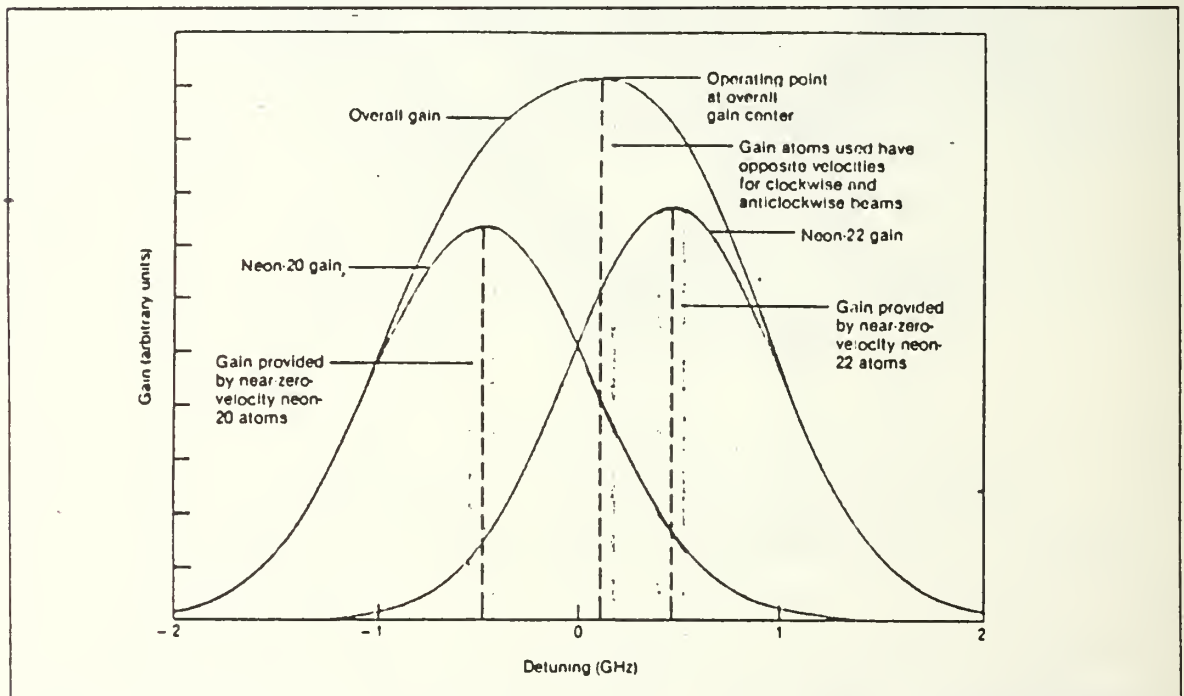
Figure 3.7   Lasing Gain Curves for Neon-20 and Neon-22 [Ref. 19: p. 52].

The three mirror design is used by most companies manufacturing ring laser gyros. The three mirror design proponents claim that their design offers fewer mirrors which means fewer losses with fewer faces to polish and lower production costs. The three mirrors inherently form a plane, further minimizing errors. The four mirror proponents argue that backscatter and absorption are less in their designs because of the less loss incurred when the angle of incidence is 45°. Additionally, the

square is inherently more sensitive, as the ratio of the configurational area to the perimeter is larger in the square design. However, neither design has emerged as clearly superior.

The current design trend is to build the entire three axis ring laser gyro inside a single monolithic block. This adds structural rigidity, and allows for a more automated production. The monolithic block material is of vital concern. Ideally, the material would be a hard, and electrically nonconducting material with a low thermal coefficient of expansion. The most popular materials used today are glass ceramic compounds. [Ref. 19,16: pp. 51-52, p. 1]

C. FIBER OPTIC GYROSCOPES

1. An Overview of the Fiber Optic Gyroscope

The free world market for fiber optic components was over a billion dollars in 1985, and has shown a consistent pattern of growth that has been forecasted to continue at least through the next decade. The fiber optic sensor systems portion is expected to exceed 841 million dollars in 1994. Of these amounts, the fiber optic gyroscope is expected to comprise about 51% of the sensor market through the 1990's. [Ref. 22: pp. 102-103]

The free world production of fiber optic gyroscopes in 1984 consisted only of a few prototypes for testing and evaluation. In 1985 the production of these gyroscopes was largely confined to about 100 units built by McDonnell Douglas and Standard Electrix Lorenz. In 1987 and 1988, production is expected to commence in several major corporations, including: Litton, Singer-Kearfott, Allied/Bendix, British Aerospace, Honeywell, Rockwell, Martin-Marietta, and Mitsubishi, just to name a few companies involved in this effort. [Ref. 22: pp. 105-108]

Many fiber optic devices depend on the same components. Devices such as birefringence fibers, coupler-based devices, polarizers, and beam splitters are shared among many different fiber applications. These devices are being rapidly improved, and are becoming much cheaper due to the enormous drive coming from the telecommunications industry. As mass production of the key elements and subassemblies for the fiber optic gyro occurs, it is anticipated that significant cost advantages for the fiber optic gyro will accrue. This situation will be further augmented by the ability to assemble the units under conventional manufacturing conditions as opposed to the more stringent clean room conditions required of other types of gyros. [Ref. 25: p. 210] Additionally, fiber optic gyros offer several advantages over other gyro systems, which include the following. [Ref. 25: p. 205]

1. An all solid state design which lends itself to extended operational life.
2. High reliability, low maintenance, and low life cycle costs.
3. A high degree of environmental ruggedness.
4. Instant turn on.
5. Small packaging with significant geometric flexibility.
6. Insensitivity to accelerations.
7. Low power requirements.
8. No critical alignments.
9. Potential low cost given continuing developments being driven by the telecommunications industry.
10. Potential for greater sensitivity than current gyro systems.

Applications of fiber optic gyroscopes have already emerged for which even crude and unsophisticated fiber optic gyros have proven invaluable. Attitude reference systems, seeker heads, and oil drilling guidance are just some of the applications to which these gyros are presently being used. These early fiber optic gyros have demonstrated several advantages over conventional systems. Specifically, in the oil drilling case, these include an ability to withstand 1000 g shocks and 40 g vibrations while being constrained to fit within a small diameter pipe. This clearly illustrates the environmental ruggedness and packaging flexiblity of the fiber optic gyroscope. Also obvious is that a fiber optic gyro can be made to be quite small. One such gyro is shown on Figure 3.8. This drawing of the gyro is slightly larger than the actual gyro, which measures only 10 centimeters in diameter and 3.5 centimeters in depth. Future designs are likely to be smaller still. Furthermore, as more refined fiber optic gyroscopes are produced, and the advantages of mass production and economies of scale are applied, the fiber optic gyro is likely to become relatively cheap. [Ref. 34: pp. 90-95]

The bulk fiber optic gyroscope is constructed as shown in Figure 3.9. The light from a laser is incident on a beam splitter which divides the laser beam into two equal parts. The beams are coupled to the ends of a fiber coil and transverses the coil in opposite directions. Upon exiting the fiber ends, the beams are recombined to form a composite light beam that has an interference pattern that is exactly analogous to that described for the ring laser gyro. A photodetector set to detect the fringes will output a pulse whenever a fringe crosses the detector. The output will be a digital pulse code modulated signal. [Ref. 1: pp. 96-98]
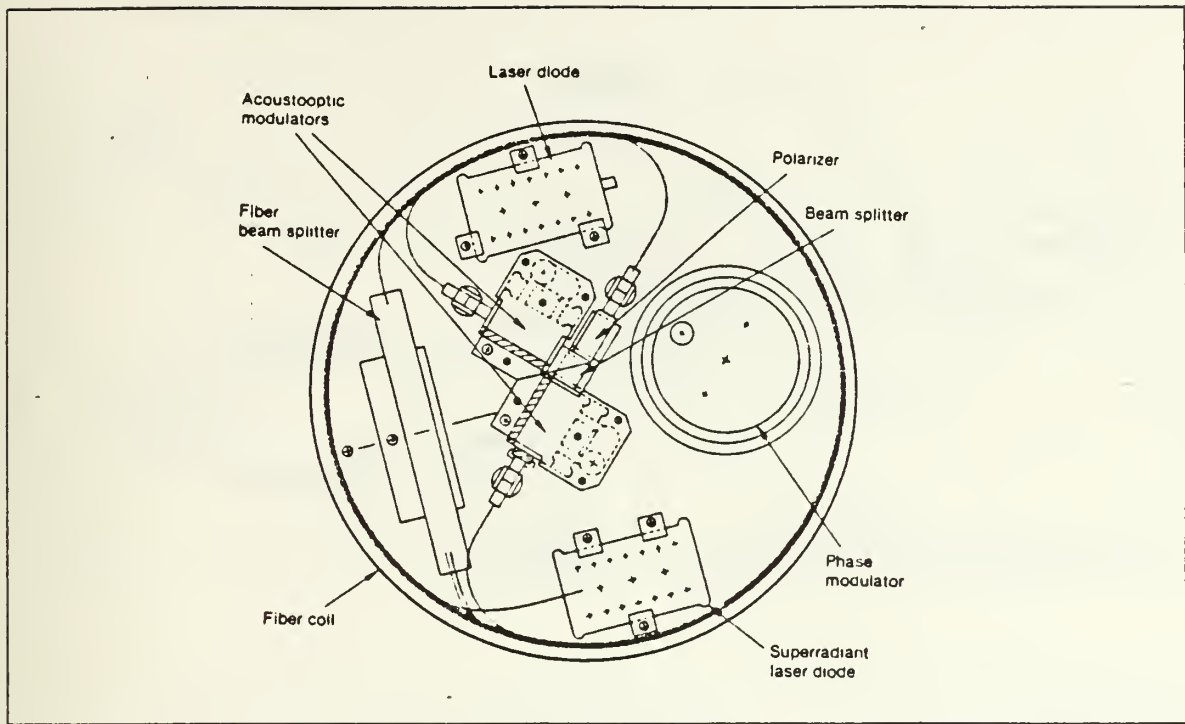
Figure 3.8   Thompson's Fiber Optic Gyro [Ref. 14: p. 59].

The heart of the fiber optic gyro is its fiber cable. Due to the huge investments being made in fiber optic communications systems worldwide, the quality and costs of fiber optic cables and devices have improved dramatically over the last few years. The performance of fiber optic components will most likely continue to improve substantially, and their costs drop rapidly, as the fiber industry continues to develop ever improving fiber products. Research and development in fiber cables and devices have continued to produce significant advances, and the fruition of these developments are being applied to a large variety of optical products. These include single polarization fibers, polarization maintaining fibers, coated and jacketed fibers, twin core fibers, birefringence fibers, coupler-based devices, polarizers, and beam splitters. [Ref. 22: pp. 102-103]

Efforts are now underway to place many of these devices in a single chip. The technology for making a low cost fiber optic gyro in the future depends largely on the ability to manufacture a fiber optic gyro that consists of an external bulk fiber coil, laser, and detector all attached to a single mass-reproducible integrated optical chip which can perform all of the optical functions required of the gyro system. These single optical integrated circuit chips are already being tested. Figure 3.10 shows a

63
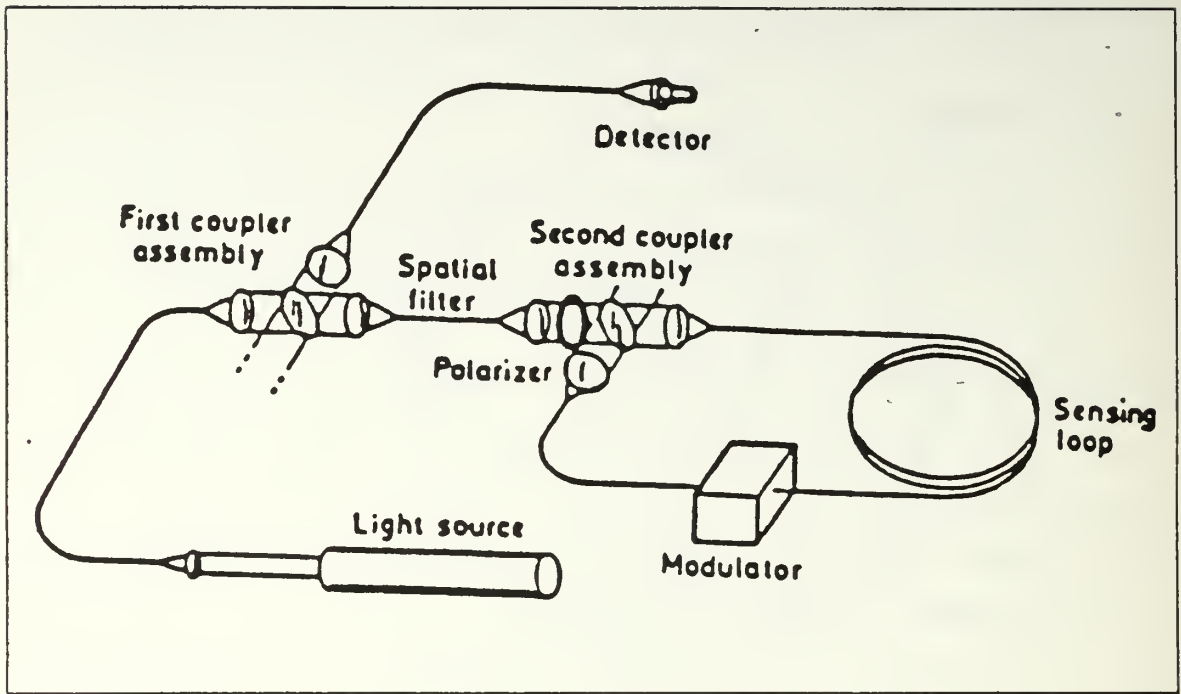
Figure 3.9   The Basic Fiber Optic Gyroscope [Ref. 8: p. 14].

typical fiber optic gyro constructed from a single optical integrated chip. These components when combined into a single integrated chip, will be used to reduce fiber optic gyro size, and complexity, and will improve the gyro system performance and reliability. Since many of these components are also used in many other fiber optic applications, costs are ultimately expected to be very low. Figure 3.11 shows some of these integrated optical circuit designs. [Ref. 13: pp. 96-98]

Additionally, laser sources are being developed which may be readily incorporated within the single chip design. Of these, the superluminescent diode devices are the most likely device for a laser source. It offers solid state reliability, low cost, and a short coherence length light which reduces Rayleigh backscatter noise. [Ref. 13: pp. 96-98]

The fiber in a fiber optic gyro acts like a light pipe, and confines the light within its walls. The fiber is wound in a coil about a spool, setting up a light rotating frame from which the Sagnac effect will occur. In this case the Sagnac effect that is observed is a function of the number of turns the fiber cable makes. The Sagnac frequency shift for a fiber optic gyro is given by Equation 3.5. [Ref. 6: p. 1]
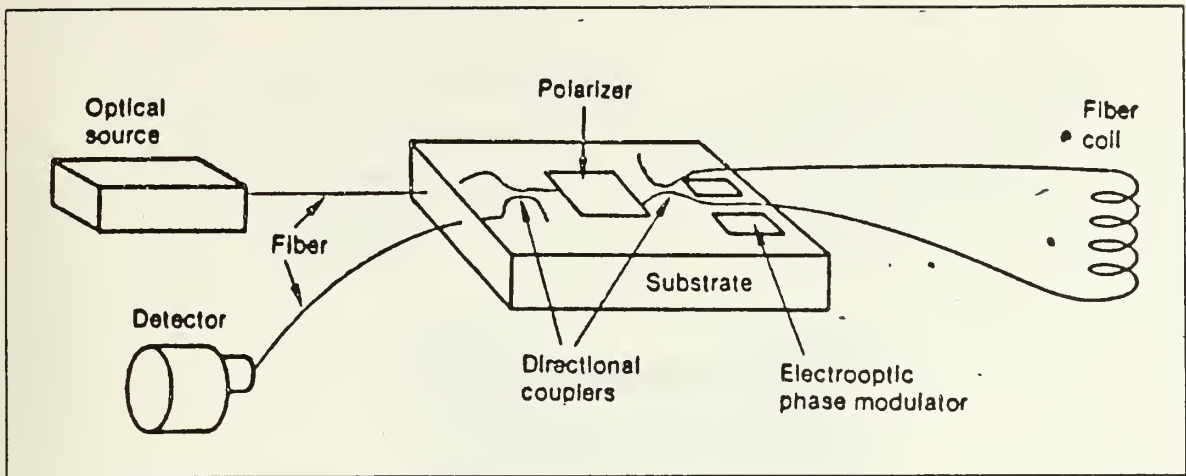
Figure 3.10   The Integrated Chip Fiber Optic Gyroscope Design [Ref. 14: p. 60].

$$\Phi = 4\pi R L \Omega / \lambda c \qquad \text{(eqn 3.5)}$$

where:

Φ = the Sagnac frequency shift

R   = the radius of the fiber coil

L   = the total length of the fiber coil

Ω = the angular velocity

λ = the optical wavelength through the medium

c   = the speed of light through the path medium

Despite the obvious differences between the ring laser gyro and the fiber optic gyro, the two operate on exactly the same physical principle. Quantum mechanics shows that the theoretical performance of the two devices to be similar. In fact, a fiber coil that has a given number of turns is fundamentally equivalent to a ring laser gyroscope whose photons undergo the same number of round trips, provided the instruments are of the same dimensions, optical powers, and frequencies. [Ref. 1: pp. 96-99]

The fiber optic gyroscope have no lock-in problem, no complicated base block fabrication, and no mirrors. Inertial grade gyro rate bias stability has already been demonstrated in laboratory conditions. Simple closed loop fiber optic gyroscopes have been built which have achieved a total rotation rate noise of 0.9 degrees per hour using
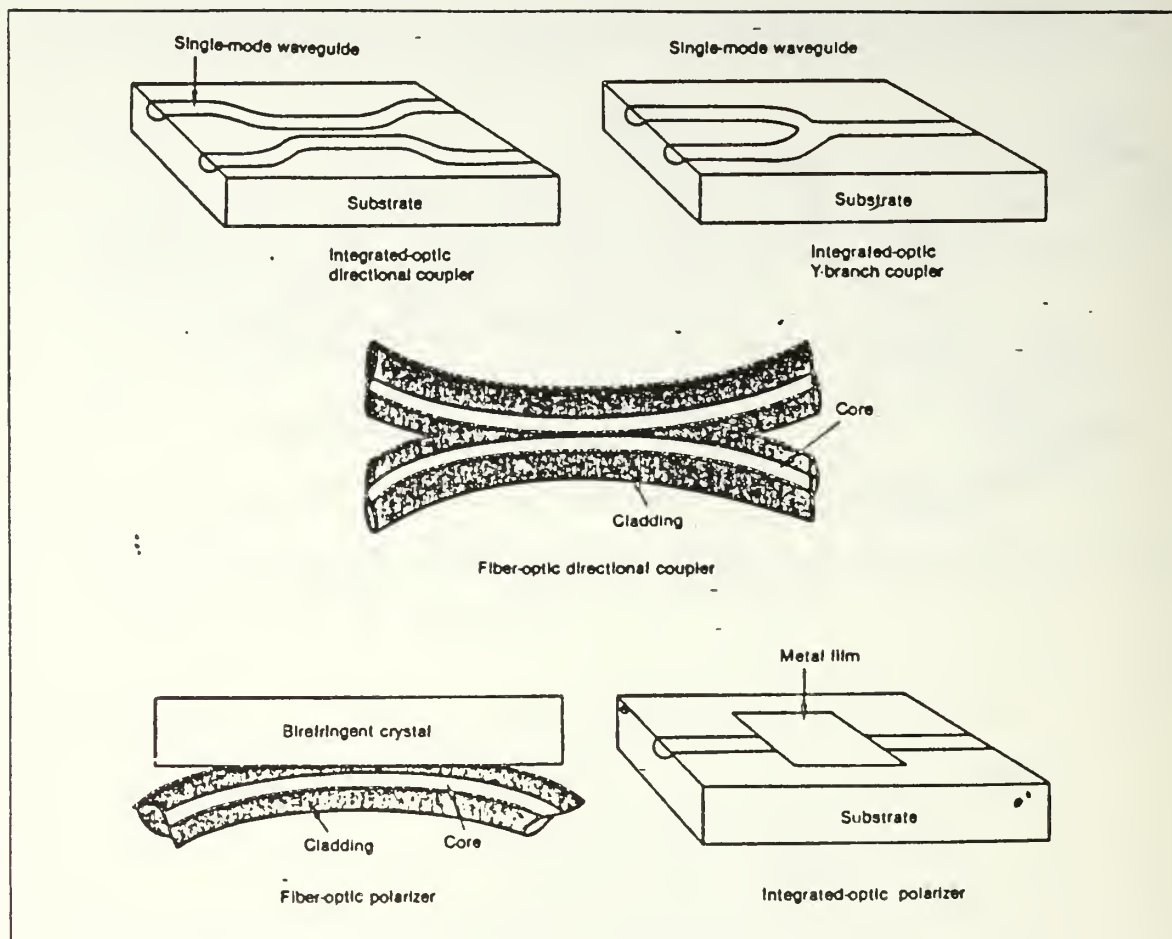
Figure 3.11   Basic Integrated Fiber Optic Devices [Ref. 14: p. 58].

a one second integration period, and 0.08 degrees per hour using a hundred second integration period. This gyro used the cheaper multimode laser diode and ordinary single mode fiber. A corresponding performance improvement would be expected using the more refined superluminescent laser diodes and polarization maintaining fibers. As constructed, the cheaper version fiber optic gyro's performance that was reported above was determined to be limited by the electronic noise in the amplifiers used. Thus, even better performing fiber optic gyros can be expected. Navigational quality gyros are expected to be attainable using current technologies. However, fiber optic gyros are largely still being tested and refined. The few fiber gyros that are being made are being constructed by hand, and until modern manufacturing techniques are applied, this is relatively expensive. The widespread industrial fabrication of fiber optic gyroscopes for commercial use is not expected to begin before 1990. [Ref. 7: pp. 68-73]

At this time the fiber optic gyro should firmly plant itself as the dominant gyro sold on the free market.

2. Error Sources in Fiber Optic Gyroscope

An accurate measurement of the motion of the gyro depends on the accurate measurement of the differential phase shift between two counterpropagating light beams independent from all sources other than rotation. The easiest solution is to ensure that the two counterpropagating light waves follow the exact same optical path. This leads to a single-mode fiber for the fiber coil. This reduces the effects of differences in the optical paths of the light beams on the resulting phase changes. The result is a more sensitive and accurate gyro. [Ref. 14: pp. 54-55]

Although both light waves travel in the same optical path, their effective optical paths can still differ. This difference can occur if the two light waves have different polarizations at any point, as the fiber conducts light of different polarizations at some slightly different speed. This property of a fiber is known as its birefringence. All presently manufactured fibers are somewhat birefringent, thus some effort must be taken to keep the counterpropagating light beams polarizations identical at all points. A polarizing filter is used at both the input and output of the fiber to reduce the effects of birefringence. [Ref. 27,14: pp. 74-75, pp. 54-55]

Another error source results because the rotation induced difference in path length is only a few wavelengths at most, even given very large rotation rates. Light propagating through a fiber is scattered at discrete joints, such as splices and couples. Additionally, some small amount of the photons traveling through the fiber cable will be backscattered when they strike the fiber atoms. This backscattering of light is known as Rayleigh scattering. The sum of the backscattered light will interfere with the main light beams. [Ref. 27: pp. 77-83] Because the light beams are at nearly the same frequency, the backscattered beam will tend to exhibit coherent interference with the main counterpropagating light beams. This is called coherent backscatter, and is a source of gyro drift in the fiber optic gyro. [Ref. 14: pp. 55-58]

Temperature fluctuations and vibrations can cause the optical path length of the light waves within the fiber to fluctuate, and this in turn causes the phase of the optical waves to vary in a random fashion about the theoretical output phase. The random phase variations are a noise source in the gyro, and the noise magnitude depends upon the demodulation technique used to determine the Sagnac phase shift. [Ref. 27: pp. 74-75]

Magnetic fields can directly affect optical waves in a fiber and cause rotation error rates of up to 10 degrees per hour, through Faraday's laws of electromagnetics. Thus the Earth's magnetic field becomes a potential error causing source. If the fiber is completely uniform, the errors caused by the Faraday effect would exactly cancel. However, since no fiber is exactly uniform, this error still exists. The solution takes two forms. First, the fiber coil is shielded from the magnetic fields. This has been shown to be quite effective. Secondly, polarization maintaining optical fibers are used. Such fibers are designed to keep a uniform polarization of light throughout the fiber's length, quenching the Faraday effect by the large birefringence built into the fibers. [Ref. 14: p. 56]

Finally, the speed of light through a fiber depends on its intensity, through a relationship known as the Kerr effect. As a result, two counterpropagating light beams that are slightly different in intensity will have slightly different velocities, even though they are traveling in the same fiber. The Kerr effect has been shown to be frequency dependent. The most popular solution is to use a light source whose intensity fluctuates with a 50 percent duty cycle. Modulating the output of a laser or using a source that has rapid intensity fluctuations also fulfills this condition. Superluminescent laser diodes and multimode laser diodes also tend to suppress the Kerr effect, by using very bright laser light source, even though such sources have a rather broad frequency spectrum. [Ref. 24,27: pp. 97-100, p. 55]

The net effect of these error sources is that the fiber optic gyro tends to exhibit a gyro random rate error. Current efforts have been directed at reducing this error, as it remains the dominant error source in the fiber optic gyro. Several complicated models have been proposed, although no favored model has appeared. [Ref. 15: pp. 1166-1172]

3. **The Future of the Fiber Optic Gyroscope**

Several unique fiber optic gyro designs have been proposed which offer interesting prospects. One of these designs has the fiber gyro close the fiber coil upon itself so that the optical beams can recirculate around the coil, much as they do in the ring laser gyro. This could enable a very small fiber coil, thus leading to a complete fiber optic gyro on a single chip. Other designs incorporate an optical amplifier to compensate for fiber propagation losses, and would use very large fiber coils. This could theoretically be made to be extremely sensitive, enough so that variations in the Earth's rotation rate and axis orientation could be monitored. Similar gyros could monitor continental drift and Earth plate tectonics. [Ref. 14: p. 59]

The ultimate future of the fiber optic gyro rests in its final cost. If the complete inertial grade navigation system is made and sold for the expected 7000 to 8000 dollars, then the fiber gyro is likely to be extremely successful with economies of scale reducing costs even further. Estimates as low as two thousand dollars for the entire inertial navigation system have been suggested as a likely possibility by the mid 1990's. With the reliability of present fiber optic gyros demonstrating mean time between failures in excess of 100,000 hours, life cycle costs are expected to be very low. Combined with its demonstrated environmental ruggedness and packaging flexibility, it is hard to imagine a large market for any other type gyro should these expectations of costs be met.

The fiber optic gyro and the ring laser gyro are actually different engineering implementations of the same physical phenomena, that of employing the Sagnac effect to measure rotation. The ring laser gyro has already emerged as a superior candidate over the mechanical gyro for virtually every inertial application. The fiber optic gyro offers all the advantages of the ring laser gyro and very few of its problems. [Ref. 6: p. 7] The many advantages unique to the fiber optic gyro make it ideally suited for use in a small submersible vehicle.

IV. SIMULATION OF THE INERTIAL NAVIGATION PROBLEM AND A KALMAN FILTER IMPLEMENTATION

A. THE INERTIAL NAVIGATION PROBLEM APPLIED TO OPTICAL GYROSCOPES

1. Optical Inertial Navigation Theory

The advantages of an optical gyroscope based inertial navigation system lead to a strapped down inertial navigation design. The strapped down inertial navigation system or analytic inertial navigation system does not physically maintain a reference frame, unlike the other inertial navigation systems. The strapped down gyro system uses the gyro outputs to calculate the relative orientation between the system's initial or stored state and its present state. Essentially, the reference frame is stored in memory instead of being physically maintained. Transformation theory must be used extensively in the strapped down inertial navigation system, and must be applied to both the gyro and the accelerometer outputs. The physical indications of north, south, east, or west would only be available after the computer transformations had been performed.

As determined in Chapter 2, the optical gyroscope based inertial navigation system must still establish and maintain a reference frame of coordinates, measure the specific forces applied to the vehicle, have knowledge of the local gravitational field, and time integrate the specific force data to obtain velocity and position information. These functions are common to all inertial navigation systems. However, the optical gyroscope based inertial navigation system uses an optical gyroscope to maintain the reference frame.

Since the inertially referred angular velocity results in a Sagnac frequency shift of the sensing light beams, and this frequency shift can be measured and compensated for, the optical gyroscopes can effectively maintain an established coordinate reference frame. Thus, the optical gyroscope can maintain a known spatial reference frame. An accelerometer system can be used to determine the inertial accelerations, with a double integration giving a change of position that can be referenced to the stored reference frame.

Obtaining the change in position requires measuring the specific forces or accelerations applied to the vehicle. The forces are measured using standard

accelerometers. Since Einstein's principle of equivalence states that it is impossible for an accelerometer to distinguish between inertial accelerations and gravitational accelerations, it is necessary to correct the accelerometer output for all accelerations that occur other than the inertial accelerations. Thus, in order for the measurements from the accelerometer to correlate to the inertial acceleration, detailed knowledge of the local gravitational field is necessary. The local gravitational field accelerations must be accounted for if an inertial position is to be found with sufficient accuracy. This is accomplished by using a Schuler tuned accelerometer system to locate the true vertical, enabling the local gravitational field to be uniquely determined and subtracted from the total sensed accelerations. The details are presented in Chapter 2.

A functional block diagram of a single axis position indication system based on an Earth frame of reference, is presented in Figure 2.1. In this figure, the output of the accelerometer is corrected such that only the inertial accelerations are evaluated. The acceleration components along the accelerometer axis that are due to gravity, Coriolis forces, and centripetal forces, are subtracted from the accelerometer output to give the inertial acceleration along the sensitive axis of the accelerometer.

Once the coordinate reference frame has been established, and the inertial accelerations determined, a double integration with respect to time produces the change in position with respect to the stored reference position, as per Equation 4.1.

$$\int \int a(t)\, dt \;=\; \Delta x \qquad\qquad \text{(eqn 4.1)}$$

Given the stored inertial reference frame, any arbitrarily moving frame can be expressed through a mathematical translation from the inertial frame of reference. Thus, the inertial navigation problem involves a translation of sensed motion to an equivalent in the reference frame. This involves acceleration vector and velocity vector transformations. These transformations have been solved for arbitrary rotations and translations, and solutions are readily available in published references. A mathematical development can be found in Chapter 2. A means of establishing initial velocity conditions and initial position conditions completes the inertial navigating solution. These initial conditions will be stored in an initialization matrix along with the coordinate reference frame. A simple example of a linear transformation is suggested by Equation 4.2.

$$r \;=\; r' \;+\; v * t \qquad\qquad \text{(eqn 4.2)}$$

Additional refinements include some means of resetting the navigational position periodically to correspond with externally derived or navigationally fixed position inputs. This essentially reduces to a recomputation of a portion of the initialization matrix terms. The problem of alignment in a strapped down inertial navigation system is basically that of determining the initial transformation matrix which relates the instrumented body frame to the reference computational frame. In an operational vehicle, the problem is even more difficult because a suitable determination of the initialization matrix must be made within a reasonably short period of time, without including effects from deleterious motions of the vehicle. A two-stage alignment scheme offers one solution to the problem. It is also important to note that only those terms in the initialization matrix that relate to the initial velocity and position conditions need be recomputed on a fix reset.

2. **Optical Inertial Navigation Errors**

The analysis of the inertial navigation system errors has been intensive and has led to several effective techniques to reduce the magnitude of the errors. The major sources of inertial navigation errors in optical gyros have been identified and measured. They include gyro drift rate errors, accelerometer measurement errors, accelerometer alignment errors, gyro system alignment errors, and errors due to gravity anomalies and deflections in the vertical. For the optical gyroscopes, the error of greatest concern is the error arising from the gyro random rate error as this error tends to result in a build up of position error with time that is much more significant than the other error sources. The contribution of the gyro random rate error in comparison to the other errors involved in a typical strapped down optical gyro based navigation system is portrayed in Figure 4.1. This figure portrays the individual error contributions for an aircraft based inertial navigation system with an average velocity of 840 feet per second and a flight duration of 2 hours 27 minutes. [Ref. 15: p. 1160]

The random behavior of the gyro disturbances can be modeled by an Auto Regressive Moving Average, ARMA, system that is driven by white noise. For example, a second order differential equation of the form given by Equation 4.3, can be employed to model the gyro disturbances. In this gyro random rate error model, c_i's are constants, "Z" refers to random rate error observations, and "a" refers to a discrete white noise sequence having a standard gaussian distribution with a zero mean and a specified variance. The various parameters in Equation 4.3 can be evaluated through several available techniques, as mentioned in Reference 26. [Ref. 26: pp. 455-457]

72
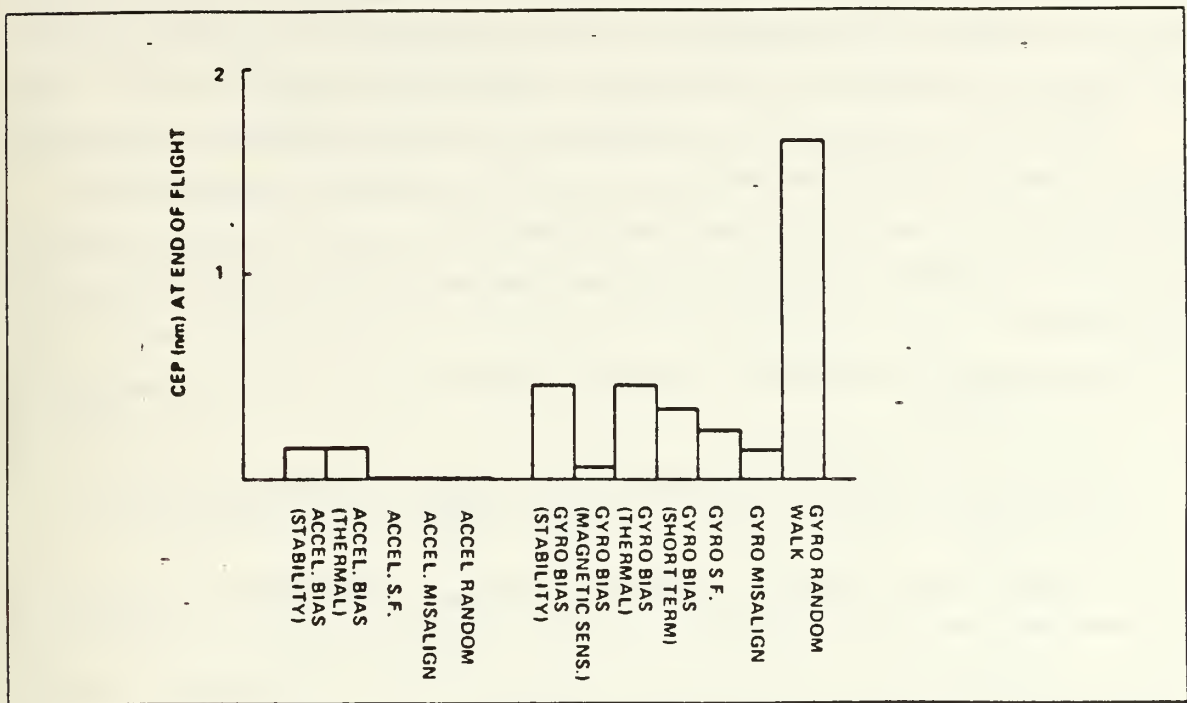
Figure 4.1   Individual Optical Gyro Error Source Contributions [Ref. 15: p.1160].

$$Z_k = c_1 Z_{k-1} + c_2 Z_{k-2} + c_3 a_k + c_4 a_{k-1} \qquad \text{(eqn 4.3)}$$

A Kalman filter was constructed that was based on the ARMA gyro random rate error model that was given in Reference 26. A Fortran program was written to test this Kalman filter and a computer simulation was conducted to examine the degree of improvement in performance that is potentially achievable. As the gyro random rate error has been shown to be the large majority of the gyro error actually encountered, a significant reduction of this error should result in a significantly more accurate optical gyroscope. The Fortran program used in the computer simulation is included in the appendix.

Efforts such as these are proving effective in reducing optical gyroscope based inertial navigation system errors, and are likely to provide the high accuracy inertial navigation systems more cheaply than other possible solutions. Indeed, a 24-state Kalman filter was used by SP Marine, Inc. and Honeywell, Inc. in a joint venture to develop a cost effective high performance optical gyroscope based inertial navigation system. In this case, a the Honeywell GG-1342 ring laser gyro was used. This gyro was taken directly off the high production line without any specification changes. Over

eight thousand of these gyros have been built to date, and the gyro has demonstrated an average of about 100,000 hours mean time between failures on deployed units. The gyro is being used primarily on large commercial aircraft. [Ref. 17: pp. 1-4]

The 24 state Kalman filter was designed specifically to provide an optimal position-fix reset and optimal velocity dampening. The Kalman filter also provided a self-calibration of the various gyro and accelerometer error sources so that they could be adequately monitored. This Kalman filter provided the following capabilities: [Ref. 17: pp. 1-4]

1. All major gyro error sources, except for the gyro random drift, were averaged out and calibrated.

2. Since the most significant gyro error source was gyro random drift, the root mean squared position error built up with the square root of elapsed time from the last reset.

3. The ship could perform any turning maneuvers whatsoever, including continuous turns, with a negligible effect on system performance.

4. The possibility of coning motion rectification due to synchronous boat oscillations on two-axes was essentially eliminated.

5. Special periodic dockside calibrations are not required.

6. The time required for dockside alignments was sharply reduced.

7. Individual inertial components could be replaced at sea without large concerns about the effects of component misalignments.

8. At sea tests aboard the USNS Vanguard showed that MARLIN demonstrated a significantly higher level of performance and accuracy than U.S. Navy (DINS) and NATO requirements call for.

These results showed that the gyro random rate error was still the error of major concern, despite an obvious improvement in error reduction in general. The gyro random rate error was not specifically modeled by the MARLIN 24-state Kalman filter. Thus, it becomes even more desirable to reduce this error if a continued performance improvement is wanted. The fiber optic gyro in particular should benefit from similar techniques. It is hoped that a significant gyro random rate error reduction will occur from a Kalman filter that is designed expressly to reduce this gyro random rate error. This may help make the less accurate but much cheaper fiber optic gyro based inertial navigation system viable for the autonomous submersible vehicle.

B.   AN INTRODUCTION TO THE KALMAN FILTER

The need to extract a signal from noisy observations is a standard signal estimation problem. This type of problem has been well documented and several

techniques exist to achieve the desired result. As applied to the optical gyro, the gyro's output is viewed as a degraded and noisy version of the exact gyro signal. Thus, the signal estimation problem is to extract a more nearly exact signal from the raw noisy gyro output. In this effort, a filter or optimal processor naturally comes to mind.

As an excessive amount of memory is not desired, which would be required if the estimate depended on past measurements, it is desirable to determine a time recursive expression that will determine the estimated signal. A recursive filter does not need to store all past measurements for the purpose of computing estimates. One manner of accomplishing this estimate is a powerful prediction-correction procedure known as the Kalman filter.

1. General Concepts in Kalman Filter Theory

In this section, the discrete Kalman filter will be introduced and some of the concepts involved explained. A thorough presentation of the academic material leading to the evolution and development of the discrete Kalman filter and the associated estimation theory will not be given. Excellent texts exist, such as Applied Optimal Estimation by A. Gelb, which explain in exhaustive detail the various aspects of estimation theory and Kalman filters. [Ref. 10: pp. 107-119] A prior knowledge of these subjects is therefore assumed and only a brief review, directed at the development of a Kalman filter to reduce gyro random rate error, will be attempted.

A discrete time system whose state at time t_k is denoted by the state vector $X(t_k)$, or simply X_k, where capital letters denote vectors, is modeled by Equation 4.4. The measurements actually observed are modeled by the observation vector, Y, as given in Equation 4.5.

$$X_{k+1} = H_k X_k + G_k U_k \qquad \text{(eqn 4.4)}$$

where:

X_k	= system state vector at time, t_k	(N by 1)
H_k	= state transition matrix at time, t_k	(N by N)
G_k	= noise distribution matrix at time, t_k	(N by L)
U_k	= noise vector at time, t_k	(L by 1)

$$Y_k = S_k X_k + V_k \qquad \text{(eqn 4.5)}$$

where:

Y_k	= observation vector at time, t_k	(M1 by 1)
S_k	= observable descriptive matrix at time, t_k	(M1 by N)

$$X_k \quad = \text{system state vector at time, } t_k \qquad \text{(N by 1)}$$
$$V_k \quad = \text{measurement noise vector at time, } t_k \qquad \text{(M1 by 1)}$$

The following assumptions are made.

1. H, G, Y, and S are known for all t_k's .

2. U and V are white noise, mutually uncorrelated sequences with zero means and with covariance matrices Q and R, respectively.

If the estimate for X_k is denoted E_k, and P_k is the error covariance matrix, then given an observation vector Y_{k+1}, the Kalman filter estimate of X_k for $k = 0,1,2,...$ is given by Equation 4.6. In Equation 4.6, $(\ )^t$ indicates a matrix transpose and $(\ )^{-1}$ indicates a matrix inverse.

$$E_{k+1} = X'_{k+1} - K_{k+1} (S_{k+1} X'_{k+1} - Y_{k+1}) \qquad \text{(eqn 4.6)}$$

where:

$$X'_{k+1} = H_k E_k$$
$$K_{k+1} = P'_{k+1} S^t_{k+1} (S_{k+1} P'_{k+1} S^t_{k+1} + R_{k+1})^{-1}$$

and:

$$P'_{k+1} = H_k P_k H^t_k + G_k Q_k G^t_k$$
$$P_{k+1} = P'_{k+1} - K_{k+1} S_{k+1} P'_{k+1}$$

This algorithm successfully estimates X_{k+1} and the estimate's variance P_{k+1}. The development of discrete Kalman filter theory is presented in Reference 10, and the equations presented above strictly follow the Kalman filter equations summary in Reference 10. [Ref. 10: pp. 107-119] The notation was modified to be in accordance with the IMSL, Inc. Fortran subroutine FTKALM, which was used in the Kalman filter implementation.

2. The Optical Gyroscope Kalman Filter

In the simpliest simulation, the optical gyro would have as its main output component that portion of gyro output that is due to the gyro random rate error. This would correspond to a ship that is pierside in calm waters. There would be no motion due to sea state effects. In this simple ship model, it is expected that the Kalman filter should prove very effective in filtering out the gyro random rate error. Thus, this first simulation can be used to calibrate the Kalman model and to validate the system state and measurement equations.

A more complex simulation would involve adding states to the Kalman filter to correspond to motion resulting from wave action and sea state effects while limiting the motion resulting from ship propulsion. This is analogous to a ship that is anchored, but is in fairly rough water. The second simulation details this scenario.

Another situation would involve adding states to the Kalman filter to correspond to motion resulting from the ship steering a steady course along with the motions due to wave action and sea state effects. This is analogous to a ship that is navigating an open ocean transit in fairly rough water. The third simulation details this scenario.

Finally, a situation could be included which would allow a ship to maneuver and change course. Additional states could be added to the Kalman filter, system state, and measurement equations to model this new situation. Or alternately, the noise variances could be relaxed to allow a larger deviation from the existing model to enable tracking the ship's maneuver. This would involve detecting when a ship course change is ordered and then relaxing the noise variance parameters accordingly. Upon reaching the new ordered course, the original noise variance parameters could be reinstated.

It is the latter method that was investigated in the final simulation. This was chosen because of concerns involving the growing computational requirements associated with increasing the number of states in the Kalman filter. It was desired to determine how well this simpler computational method would perform. The fourth simulation details this analysis.

C. SIMULATION RESULTS AND CONCLUSIONS

1. The Stationary Vehicle in Calm Water

Figure 4.2 shows a pictorial representation of the optical gyro signal generation. It is this representation that forms the basis for the simpliest Kalman filter used in these simulations. Essentially the gyro signal is viewed as having chiefly two components, a random rate error term and a propulsive ship motion term . The propulsive ship motion term has a zero value with some specified variance, to allow for minor ship motions that can still occur to a ship that is tied to a pier. The random rate error term is given as per the model for the random rate error presented below.

The model for the gyro random rate error that was used is of the form of Equation 4.3, and was taken from Reference 26. The constant's numerical values were taken from the same reference. Optimal constant values may change subject to many
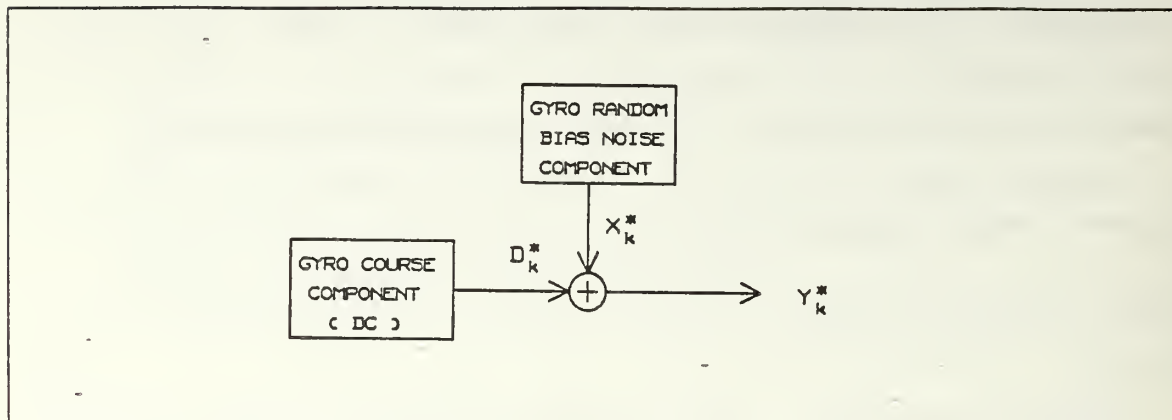
Figure 4.2   The Gyro Random Bias Noise Mathematical Model.

factors including sampling period, age of the gyro, type of gyro, operating environment, and etcetera. However, since the model has to show a random walk characteristic, it must exhibit at least one pole close to the point $Z = 1$. The model for the gyro random rate error used is given by Equation 4.7, which uses a four minute sampling period and has a zero at $Z = 0.909$ and poles at $Z = 0.9902$ and $Z = 0.3908$. [Ref. 26: p. 456]

$$Z_k = 1.381 \, Z_{k-1} - 0.387 \, Z_{k-2} + a_k - 0.909 \, a_{k-1} \qquad \text{(eqn 4.7)}$$

For this simulation, the system state model and the measurement model are given by Equations 4.8 through 4.12. Y^*_k represents the actual signal observed at the output of the optical gyroscope. D^*_k represents that part of the gyro output that is due to the ship's propulsion. X^*_k represents that part of the gyro output that is due to the gyro random rate error. The gyro random rate error model requires two state variables since a second order ARMA model was used.

$$Y^*_k \;=\; \begin{vmatrix} D^*_k \\ X^*_k \end{vmatrix} \;=\; \begin{vmatrix} D_k \\ X_k \\ X_{k-1} \end{vmatrix} \qquad \vdots \qquad \text{(eqn 4.8)}$$

$$\begin{vmatrix} D_{k+1} \\ X_{k+1} \\ X_k \end{vmatrix} = \begin{vmatrix} 1.0 & 0.0 & 0.0 \\ 0.0 & 1.381 & -0.387 \\ 0.0 & 1.0 & 0.0 \end{vmatrix} \begin{vmatrix} D_k \\ X_k \\ X_{k-1} \end{vmatrix} + G_k U_k \qquad \text{(eqn 4.9)}$$

$$G_k U_k = \begin{vmatrix} 1.0 & 0.0 \\ 0.0 & 1.0 \\ 0.0 & 0.0 \end{vmatrix} \begin{vmatrix} a_k \\ b_k \end{vmatrix} \qquad \text{(eqn 4.10)}$$

$$Y_k = \begin{vmatrix} 1.0 & 1.0 & -0.909 \end{vmatrix} \begin{vmatrix} D_k \\ X_k \\ X_{k-1} \end{vmatrix} + V_{k+1} \qquad \text{(eqn 4.11)}$$

$$V_{k+1} = 0.0 \qquad \text{(eqn 4.12)}$$

In Equation 4.10, the covariance of the noise sequences a_k and b_k are given by σ_d and σ_x, respectively. In this simpliest simulation, the gyro signal is viewed as having chiefly two components, a random rate error term and a propulsive ship motion term. This first simulation models a ship that is pierside in calm waters. The propulsive ship motion term has a zero mean value with some specified variance, to allow for minor ship motions that can still occur to a ship tied to a pier. The random rate error term is given as per the model for the random rate error presented earlier. In this simple ship model, it is expected that the Kalman filter should prove very effective in filtering out the gyro random rate error. Thus, this simulation can be used to calibrate the Kalman filter model, and to validate the system state and the measurement equations.

Figure 4.3 shows the error contribution due to the gyro random rate error before any filtering is performed. As the gyro random rate error model will remain unchanged throughout the four simulations, Figure 4.3 will be compared to the resulting error contribution due to the remaining gyro random rate error after Kalman filtering is performed for each simulation.

Figures 4.4 to 4.8 detail the results of this first simulation. Figure 4.4 shows the actual gyro signal which should be estimated by the Kalman filter if it was a perfect filter, i.e. if it could remove all noise. In this case, the exact gyro signal is a constant DC signal with a value of zero. Figure 4.5 shows the observed gyro signal that enters

the the Kalman filter. In this case, the signal is all gyro random rate error. Figure 4.6 shows the signal that is outputed from the Kalman filter. This is the estimated gyro signal that will be used by the inertial navigation system to maintain the gyroscopic frame of reference. If the filter was perfect, the output of the 3-state Kalman filter would be exactly zero. Figure 4.7 shows the error between the exact gyro signal and the estimated gyro signal that is at the output of the Kalman filter. The small amount of error generated in this simple case shows that the random rate error was nearly eliminated. Figure 4.8 shows the integrated error with respect to time, and is the inertial navigation system error due to any remaining gyro random rate error. Although Figure 4.7 shows that the random rate error is effectively reduced, Figure 4.8 is required to show that the angular position error resulting from the random rate error is also reduced. This angular position error is obtained by integrating the total angular rate error with respect to time.

A comparison of Figure 4.3 with Figure 4.8 shows that the angular position error associated with the random rate error has been virtually eliminated. This is as expected for this simple ship model.

2. **The Five State Kalman Filter Implementation**

Figure 4.9 shows a pictorial representation of the optical gyro signal generation. It is this representation that forms the basis for the Kalman filter used in more complex simulations. Essentially the gyro signal is viewed as having three components: a term due to the random rate error, a term due to the movement of the ship through the water, and a term due to the motion of the ship resulting from the sea state.

For the more complicated simulations, the system state and measurement models are given by Equations 4.13 through 4.17. Y^*_k represents the actual signal observed at the output of the optical gyroscope. D^*_k represents that part of the gyro output that is due to the ship's propulsive motion. S^*_k represents that part of the gyro output that is due to the motion of the ship that is due to the sea state. X^*_k represents that part of the gyro output that is due to the gyro random rate error. The random rate error model still requires two state variables to accurately implement the model. The sea state also requires two state variables to be accurately modeled, as the sea state effects are time varying.
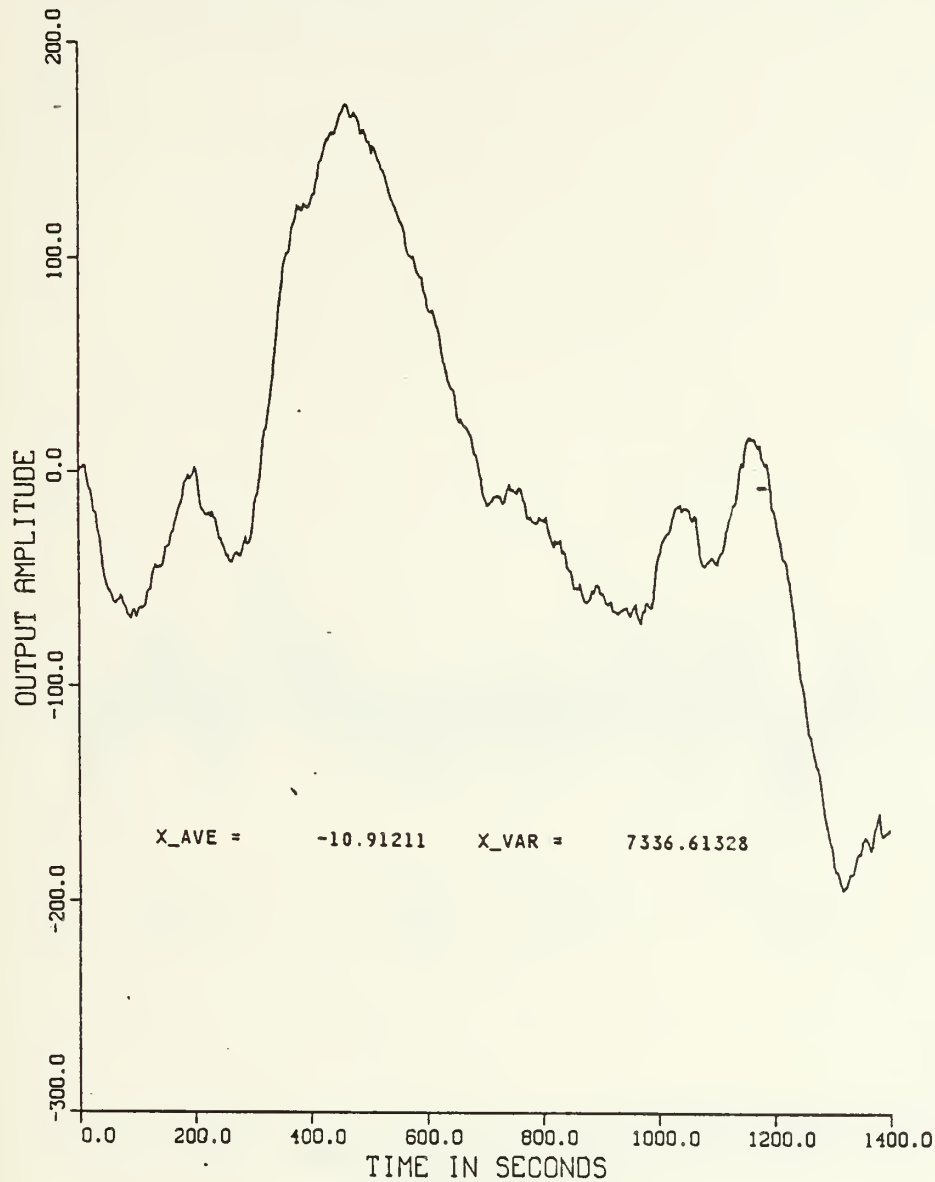
Figure 4.3   The Random Bias Drift Rate Noise Integrated over Time.

Figure 4.4   The Actual "Clean" Gyro Signal for Simulation #1.

82
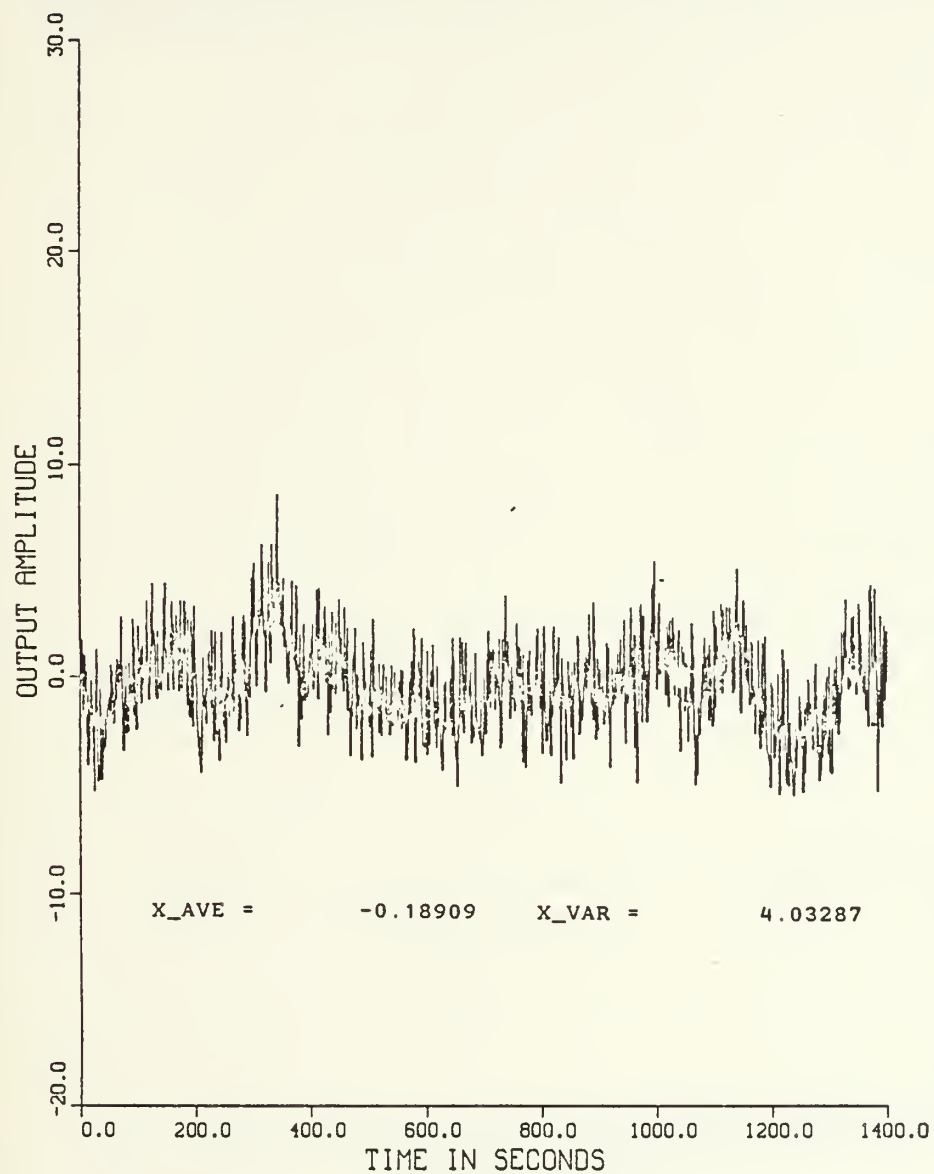
Figure 4.5   The Actual "Noisy" Gyro Signal for Simulation #1.
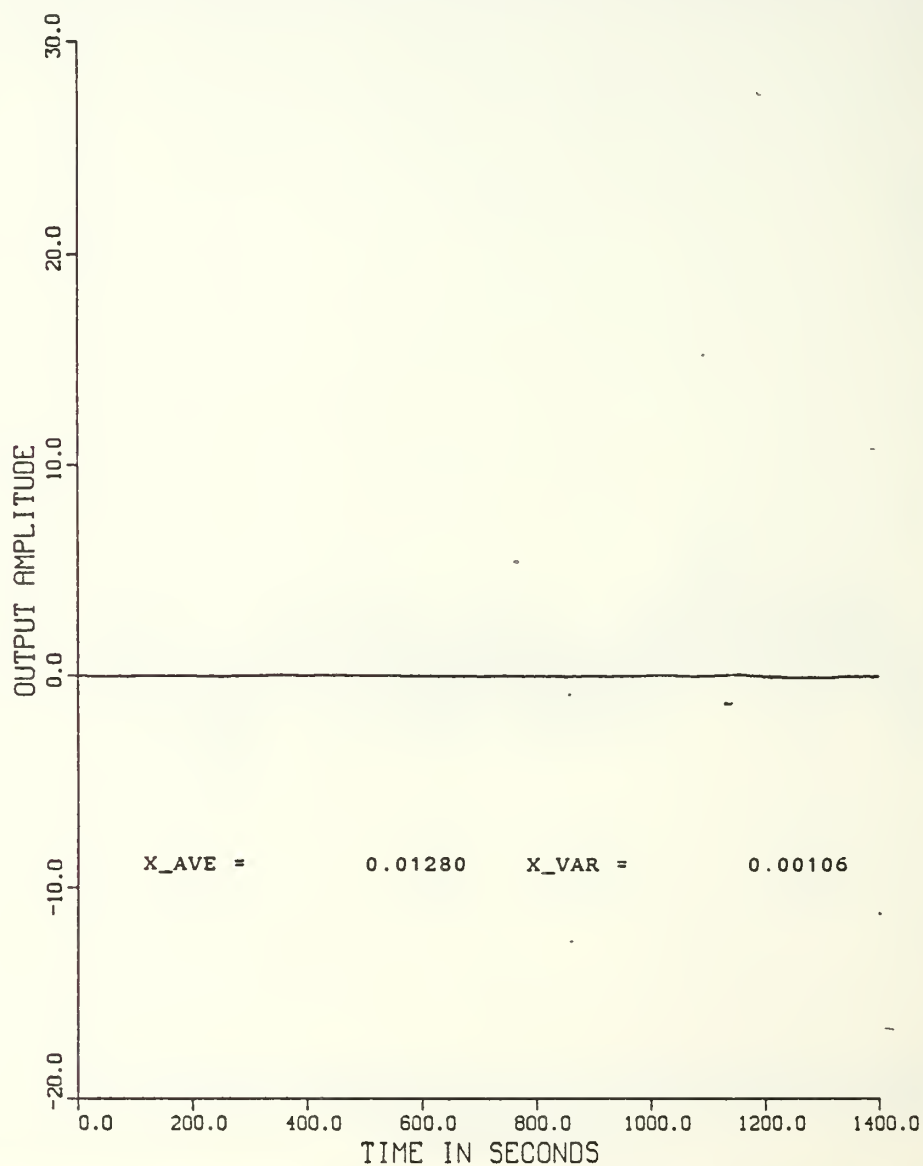
Figure 4.6   The Best Estimated Gyro Signal for Simulation #1.
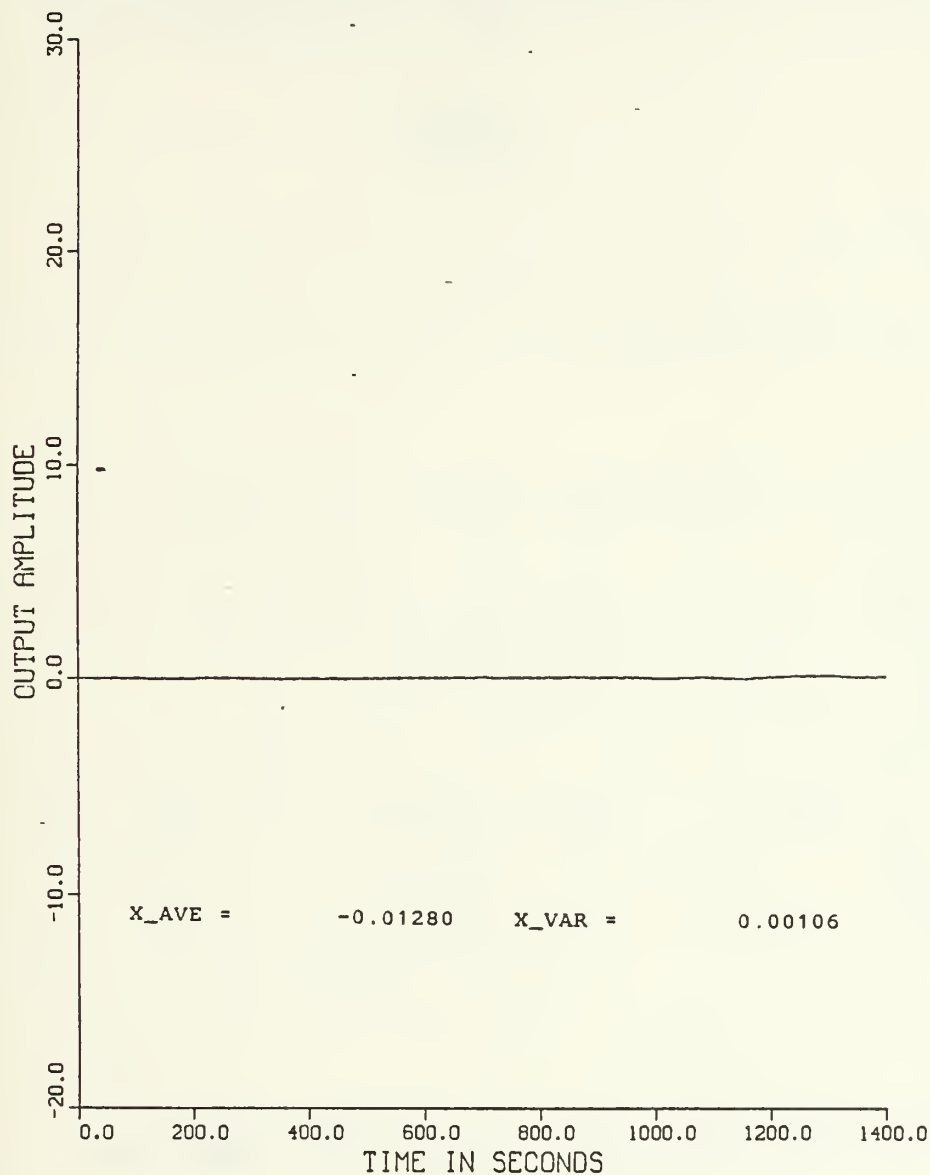
Figure 4.7   The Error in the Best Estimate for Simulation #1.
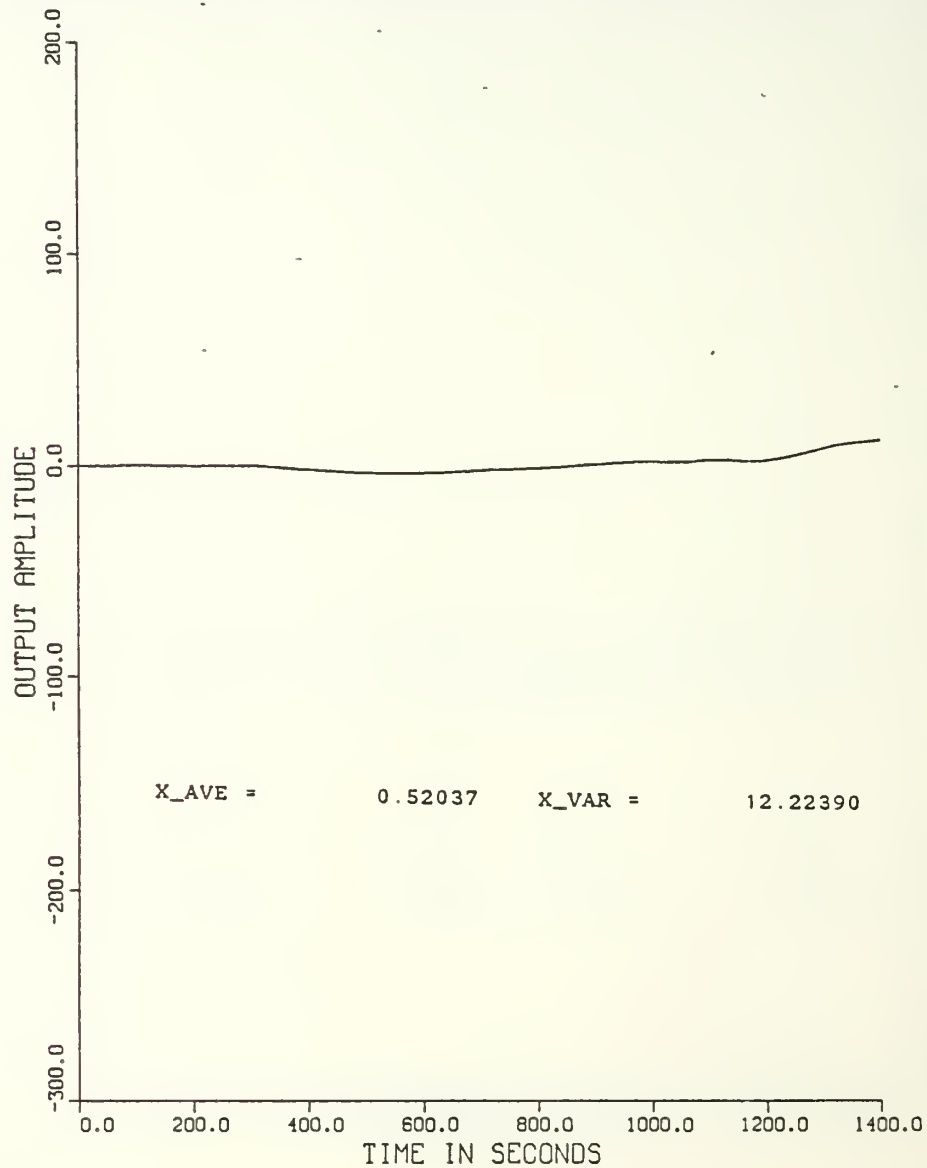
Figure 4.8   The Integrated Error with Respect to Time for Simulation #1.
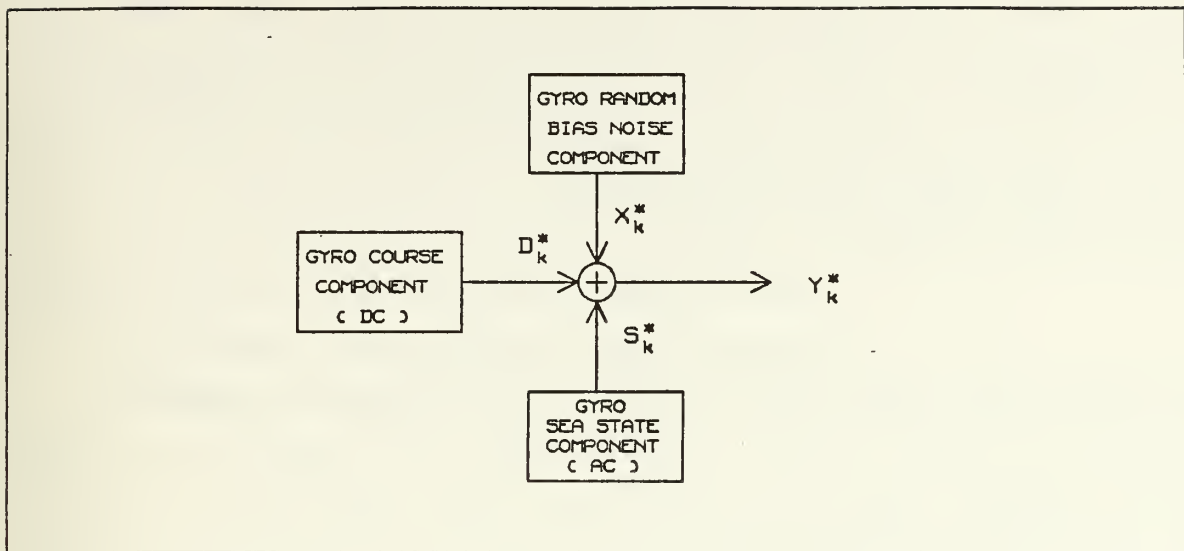
Figure 4.9   The Random Gyro Noise Plus Sea State Mathematical Model.

$$Y^*_k = \begin{vmatrix} D^*_k \\ S^*_k \\ X^*_k \end{vmatrix} = \begin{vmatrix} D_k \\ S_k \\ S_{k-1} \\ X_k \\ X_{k-1} \end{vmatrix} \qquad \text{(eqn 4.13)}$$

$$\begin{vmatrix} D_{k+1} \\ S_{k+1} \\ S_k \\ X_{k+1} \\ X_k \end{vmatrix} = \begin{vmatrix} 1 & 0 & 0 & 0 & 0 \\ 0 & c & -1 & 0 & 0 \\ 0 & 1 & 0 & 0 & 0 \\ 0 & 0 & 0 & a & b \\ 0 & 0 & 0 & 1 & 0 \end{vmatrix} \begin{vmatrix} D_k \\ S_k \\ S_{k-1} \\ X_k \\ X_{k-1} \end{vmatrix} + G_k \dot{U}_k \qquad \text{(eqn 4.14)}$$

where:

$a = 1.381$

$b = -0.387$

$c = 2\cos(\omega_0)$, $\omega_0 =$ ship natural frequency

$$G_k \, U_k \;\; = \;\; \begin{vmatrix} 1 & 0 & 0 \\ 0 & 1 & 0 \\ 0 & 0 & 0 \\ 0 & 0 & 1 \\ 0 & 0 & 0 \end{vmatrix} \begin{vmatrix} a_k \\ b_k \\ c_k \end{vmatrix} \qquad \text{(eqn 4.15)}$$

$$Y_k \;\; = \;\; \begin{vmatrix} 1 & 1 & 0 & 1 & d \cdot \end{vmatrix} \begin{vmatrix} D_k \\ S_k \\ S_{k-1} \\ X_k \\ X_{k-1} \end{vmatrix} \; + \; V_{k+1} \qquad \text{(eqn 4.16)}$$

where:

$$d = -0.909$$

$$V_{k+1} \;\; = \;\; 0.0 \qquad \text{(eqn 4.17)}$$

In Equation 4.15, the covariance of the noise sequences a_k, b_k, and c_k are given by σ_d, σ_s, and σ_x, respectively.

3. The Stationary Vehicle in a Moderate Sea State

This simulation involves adding states to the 3-state Kalman filter to correspond to motion resulting from wave action and sea state effects while still neglecting motion resulting from ship propulsion. The result is the 5-state Kalman filter presented in the previous section. This simple simulation is analogous to a ship that is anchored, but is in fairly rough water. The second simulation details this scenario.

Figures 4.10 to 4.14 detail the results of the second simulation. Figure 4.10 shows the actual gyro signal, and is the gyro signal that would be outputed from the 5-state Kalman filter if it was a perfect filter, i.e. if it could remove all noise. In this case, the exact gyro signal is the sum of a constant DC signal with a constant zero value and an approximately sinusoidal signal that occurs as a response to the sea state. Figure 4.11 shows the observed gyro signal that enters the the Kalman filter. Figure 4.12 shows the signal that is outputed from the Kalman filter. This is the estimated gyro signal that will be used by the inertial navigation system to maintain the gyroscopic frame of reference. It appears to be an accurate estimation of the exact

88

gyro signal. Figure 4.13 shows the error between the exact gyro signal and the estimated gyro signal that is at the output of the Kalman filter. It shows that the gyro random rate error was again nearly eliminated, but not quite as well as in the first simulation. Figure 4.14 shows the integrated total angular rate error with respect to time, and is a dynamic representation of the inertial navigation system angular position error with respect to time. A comparison of this figure with Figure 4.3 shows that the buildup of gyro error with time has been markedly reduced.

4. The Steady Course Vehicle in a Moderate Sea State

Another situation would involve the ship steering a steady course. Additional states are not needed in the 5-state Kalman filter that was designed in the earlier section, as a ship steering a steady course outputs a DC signal component that has already been taken into account in the 5-state Kalman filter model. Also taken into account within the 5-state Kalman filter model are any motion due to wave action and sea state effects. This is analogous to a ship that is navigating an open ocean transit in fairly rough water. The third simulation details this scenario.

Figures 4.15 to 4.19 detail the results of this third simulation. Figure 4.15 shows the actual gyro signal, and is the gyro signal that would be outputed from the Kalman filter if it was a perfect filter. In this case, the exact gyro signal is the sum of a constant non-zero propulsion signal, a gyro random bias signal, and a sea state signal. Figure 4.16 shows the observed gyro signal that enters the the Kalman filter. As was the case before, the gyro random rate error has sufficiently degraded the exact signal such that it is unacceptable for inertial guidance. Figure 4.17 shows the signal that is outputed from the Kalman filter. This is the estimated gyro signal that will be used by the inertial navigation system to maintain the gyroscopic frame of reference. Figure 4.18 shows the error between the exact gyro signal and the estimated gyro signal that is at the output of the Kalman filter. It shows that the gyro random rate error was again nearly eliminated, but not as well as in the first two simulations. The resulting signal error is very small. Figure 4.19 shows the integrated gyro angular rate error with respect to time, and is a dynamic representation of the inertial navigation system total angular position error. A comparison with Figure 4.3 shows that the buildup of error with time has again been markedly reduced.

Figure 4.10 The Actual "Clean" Gyro Signal for Simulation #2.

Figure 4.11   The Actual "Noisy" Gyro Signal for Simulation #2.

91
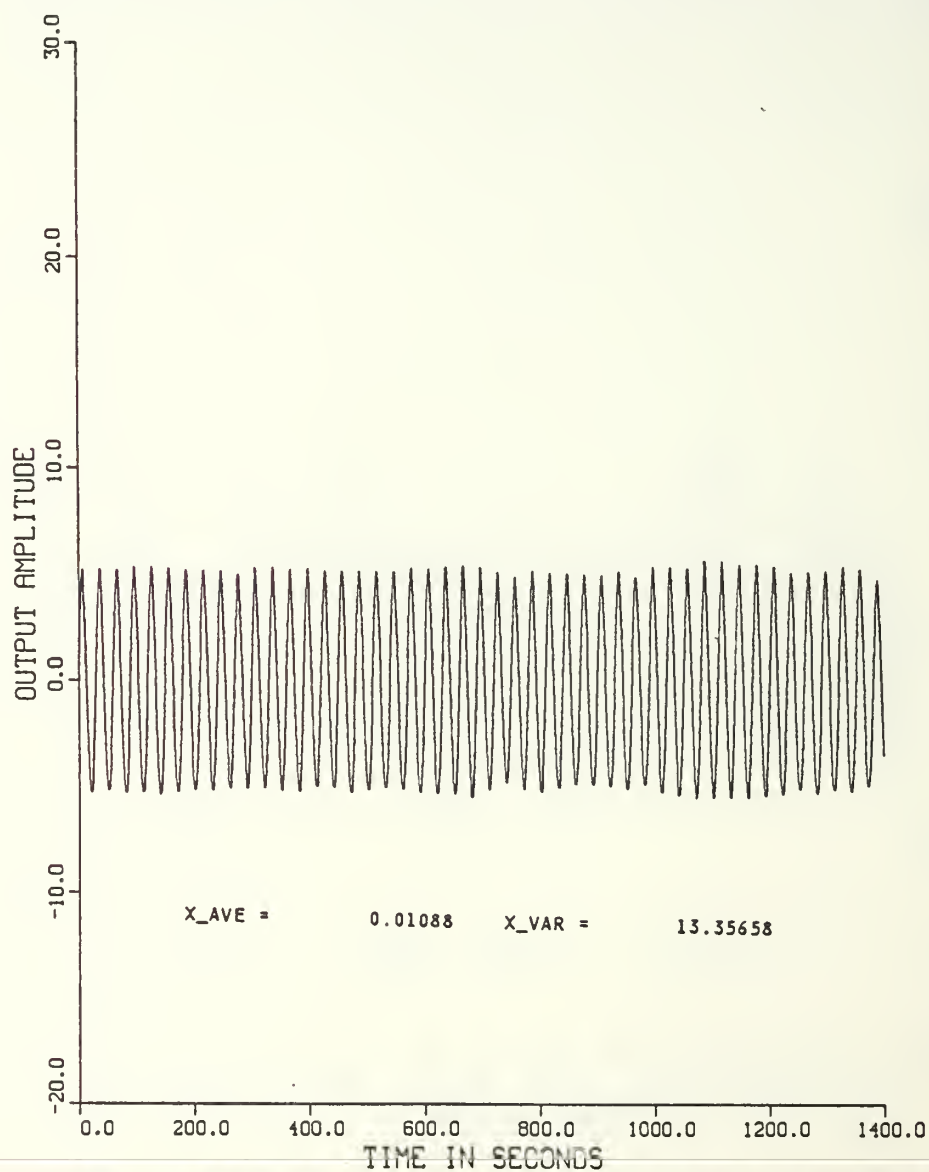
Figure 4.12   The Best Estimated Gyro Signal for Simulation #2.

92
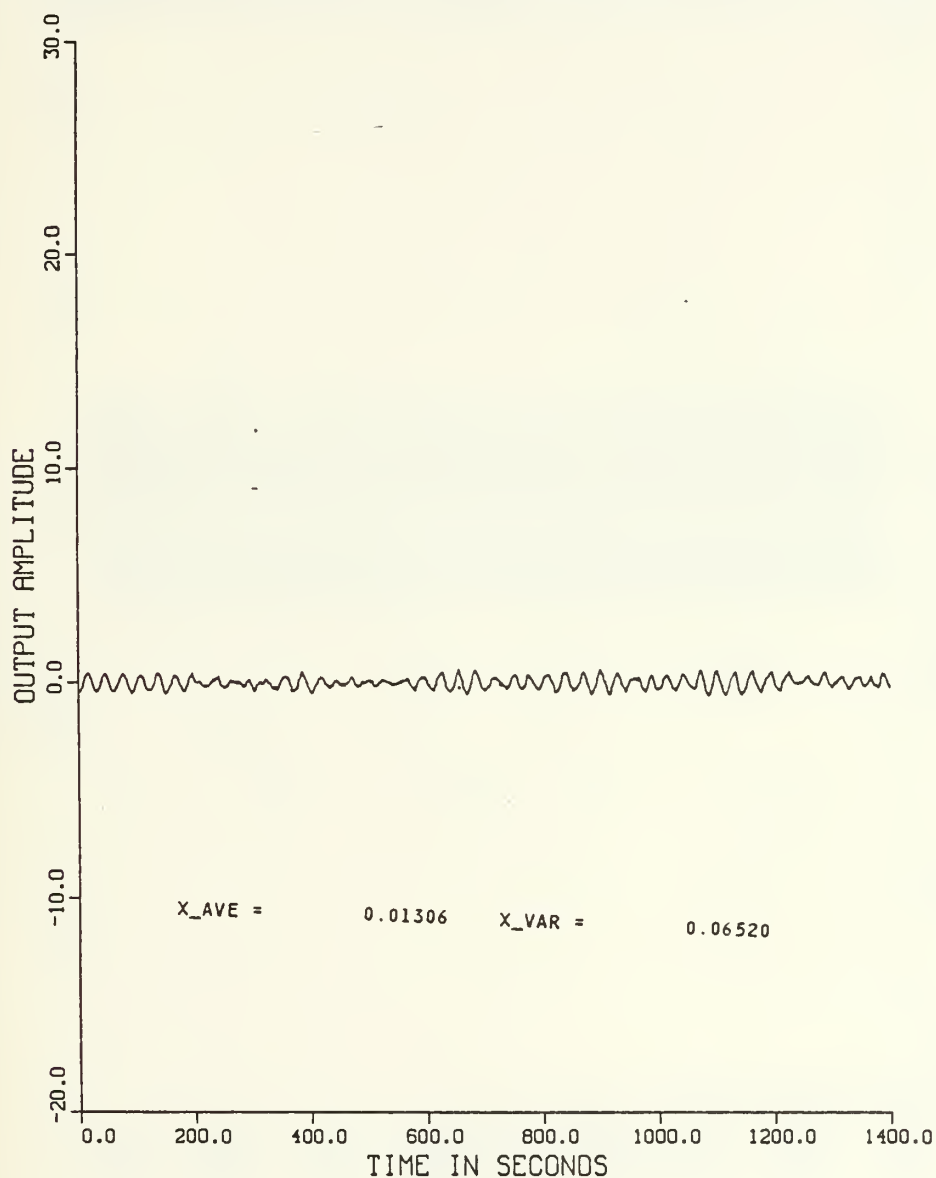
Figure 4.13   The Error in the Best Estimate for Simulation #2.
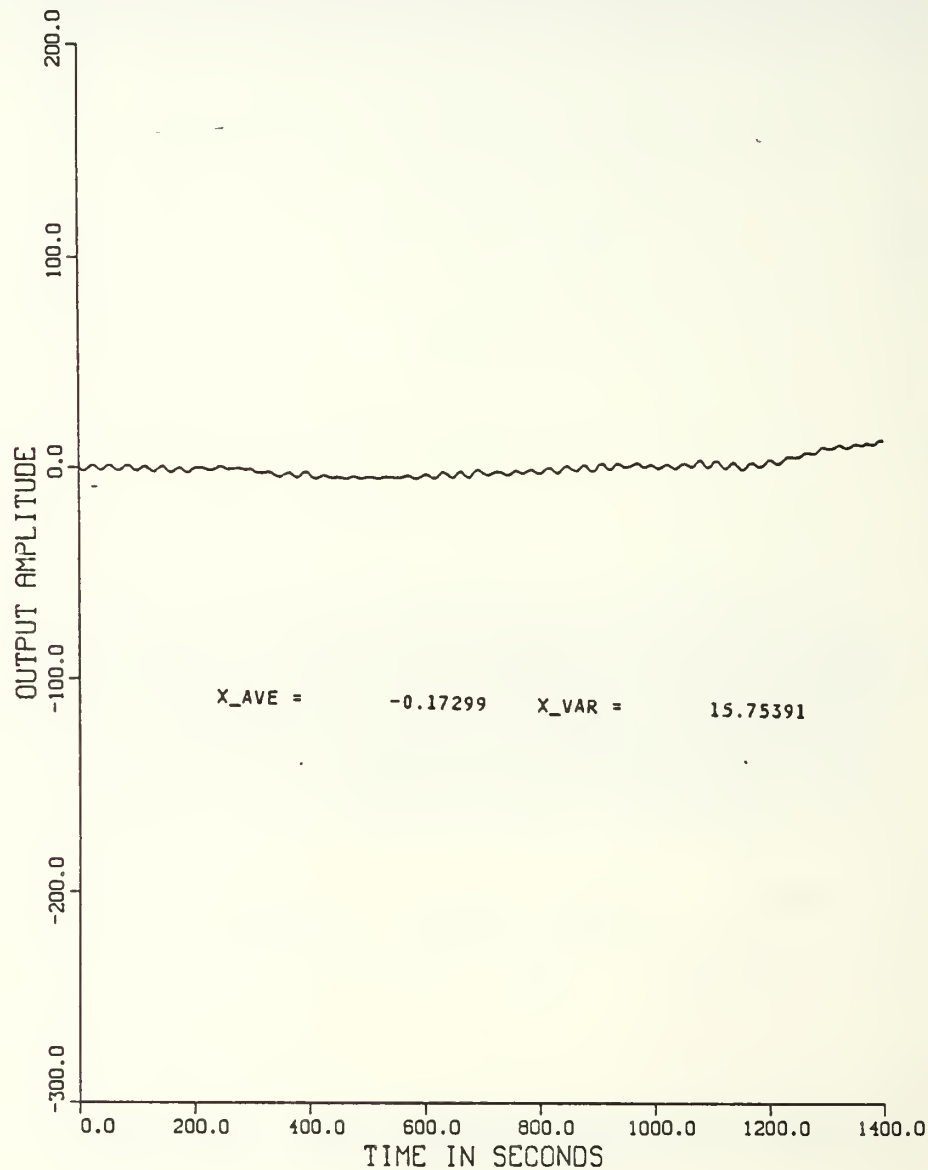
Figure 4.14   The Integrated Error with Respect to Time for Simulation #2.

Figure 4.15   The Actual "Clean" Gyro Signal for Simulation #3.

95

Figure 4.16   The Actual "Noisy" Gyro Signal for Simulation #3.

96
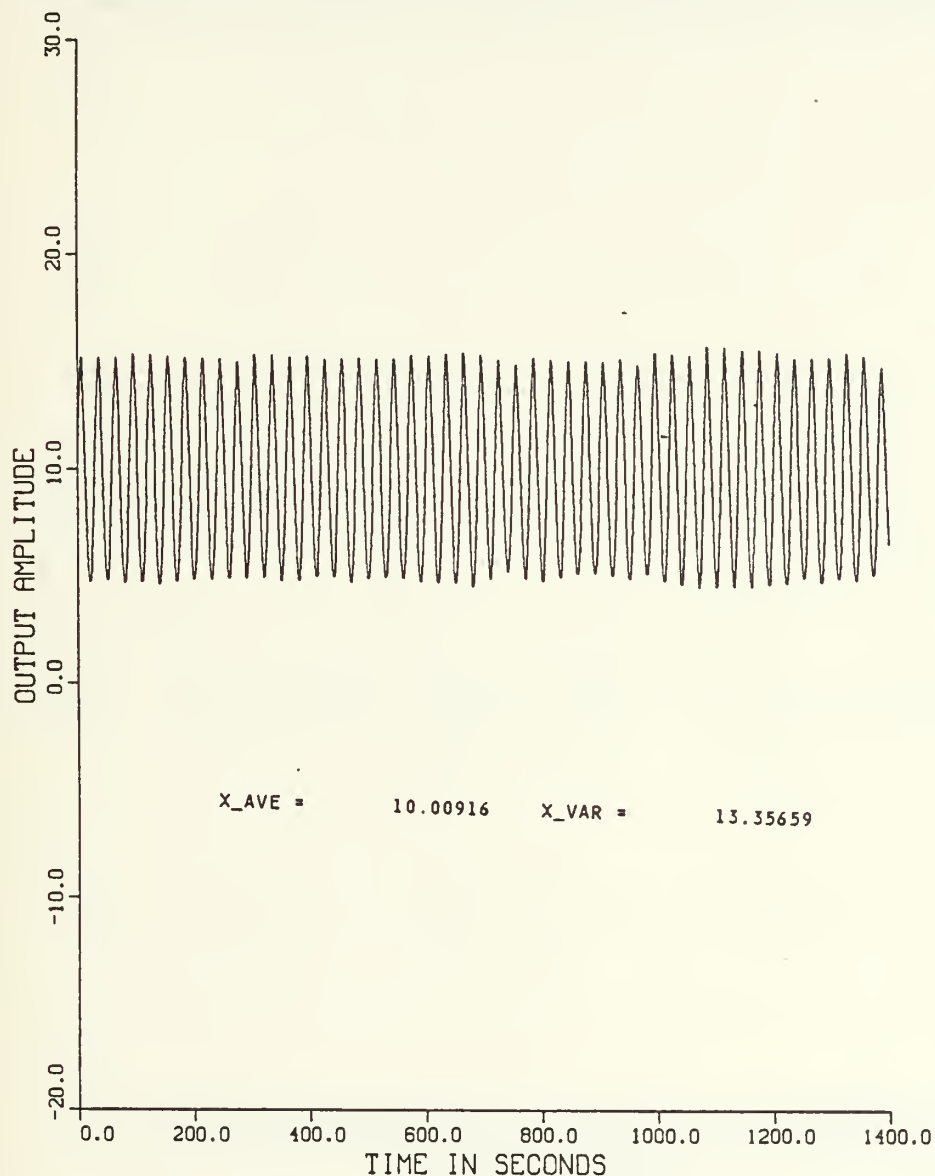
Figure 4.17   The Best Estimated Gyro Signal for Simulation #3.
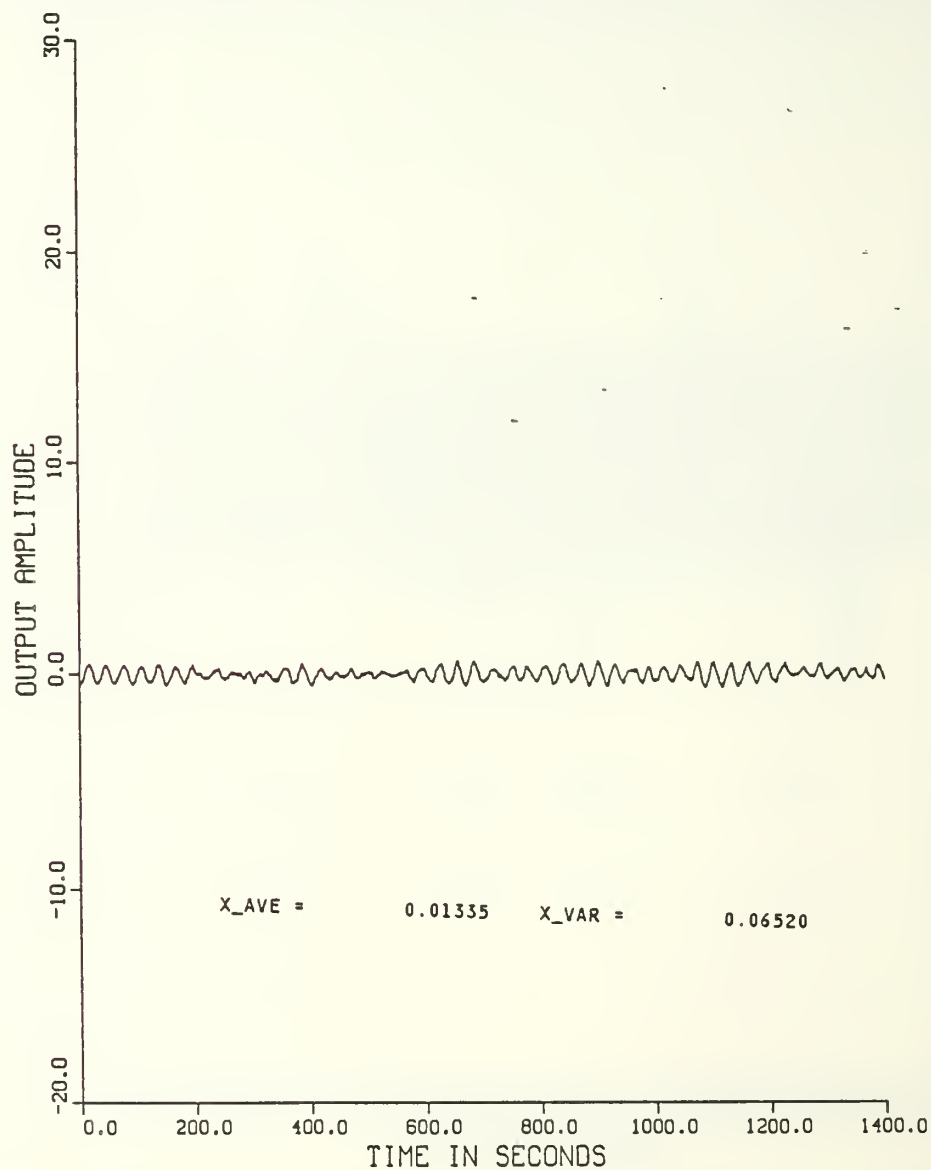
Figure 4.18   The Error in the Best Estimate for Simulation #3.
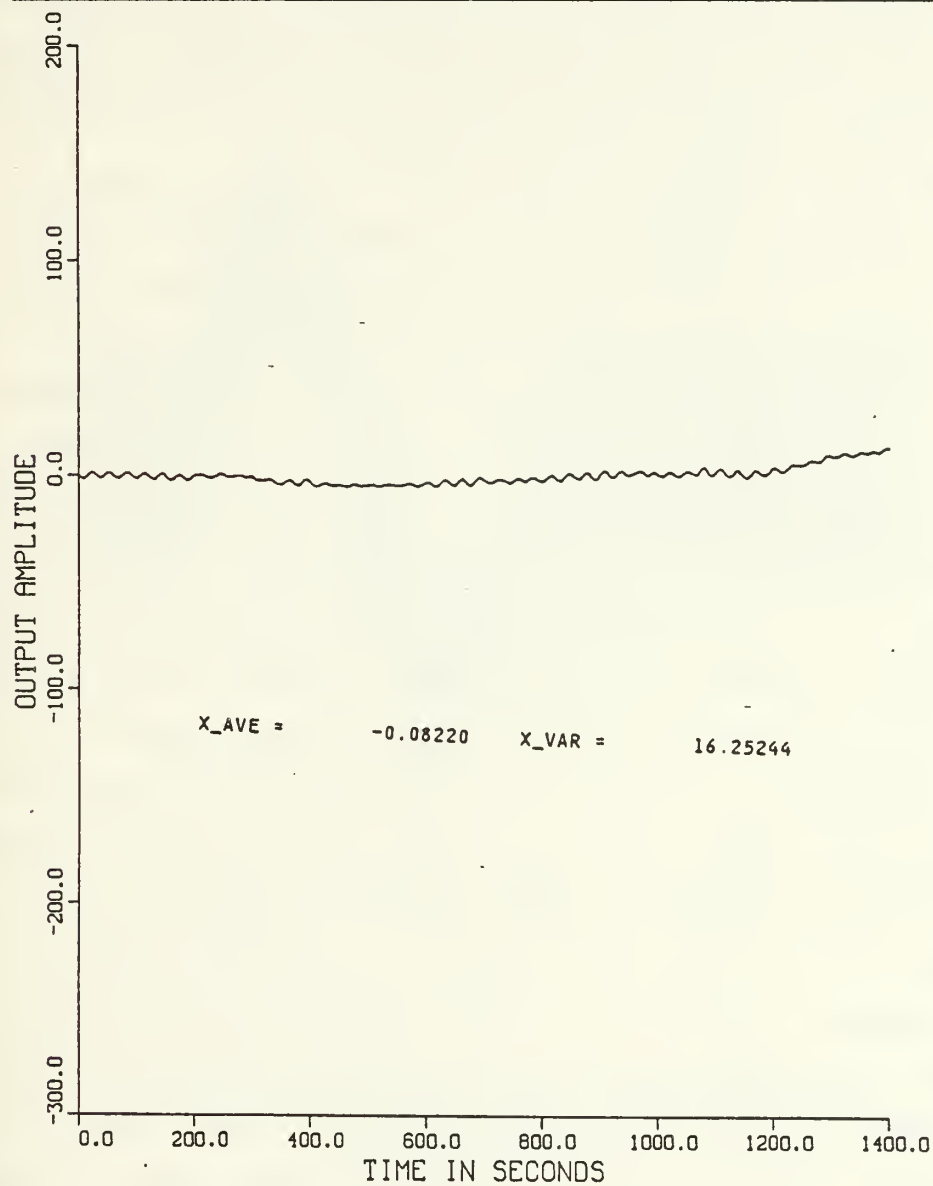
Figure 4.19 The Integrated Error with Respect to Time for Simulation #3.

5. The Maneuvering Course Vehicle in a Moderate Sea State

Finally, the last situation included allows a ship to maneuver and change course. Two possible methods for modifying the previous 5-state Kalman filter exist. The first method would be to add an additional state to model the ship's course change. The second method would be to change the noise variance parameters to such an extent that the Kalman filter could continue to track the ship's changing course through the maneuver. This would involve detecting when a ship course change is ordered and then relaxing the noise variance parameters accordingly. Upon reaching the new ordered course, the original noise variance parameters could be reinstated. It was this latter method that was chosen for this simulation.

Figures 4.20 to 4.24 detail the results of the fourth and last simulation. Figure 4.20 shows the actual gyro signal, and is the gyro signal that would be outputed from the Kalman filter if it was a perfect filter, i.e. if the filter could remove all the noise. Note that the majority of the time being examined in this simulation is involved in the ship's course change. The estimated gyro signal has been obtained by increasing the variance of the noise input to the stochastic model. The effect of this is the appearance of larger variations in the estimated signal, which allows more gyro random rate error through the Kalman filter. Figure 4.21 shows the observed gyro signal that enters the the Kalman filter. Figure 4.22 shows the signal that is outputed from the Kalman filter. This is the estimated gyro signal that will be used by the inertial navigation system to maintain the gyroscopic frame of reference. Figure 4.23 shows the error between the exact gyro signal and the estimated gyro signal that is at the output of the Kalman filter. It is obvious from looking at the figure exactly where the noise parameters were changed. Even with the relaxed noise parameters, the estimated signal is much improved. Figure 4.24 shows the integrated gyro angular rate error with respect to time, and is a dynamic representation of the inertial navigation system angular position error. A comparison with Figure 4.3 shows that the buildup of error with time has still been markedly reduced. Despite allowing some of the gyro random error through the Kalman filter, the integrated error shows a variance that is about a sixth of the value given in Figure 4.3. The Kalman filter was still reasonably effective in removing the gyro random rate error. This method provides a means of adapting the Kalman filter to unknown and unmodeled changes that can actually occur in operating inertial navigating systems.
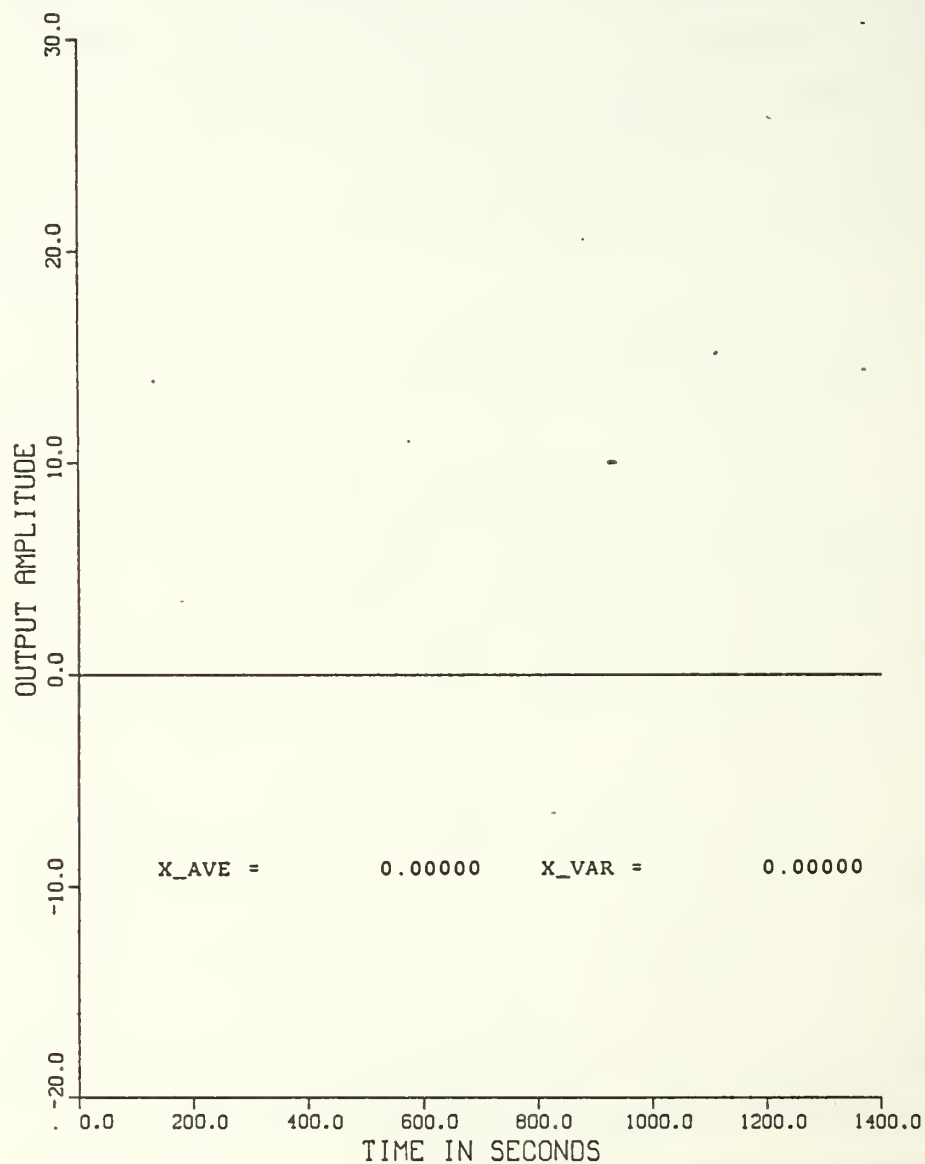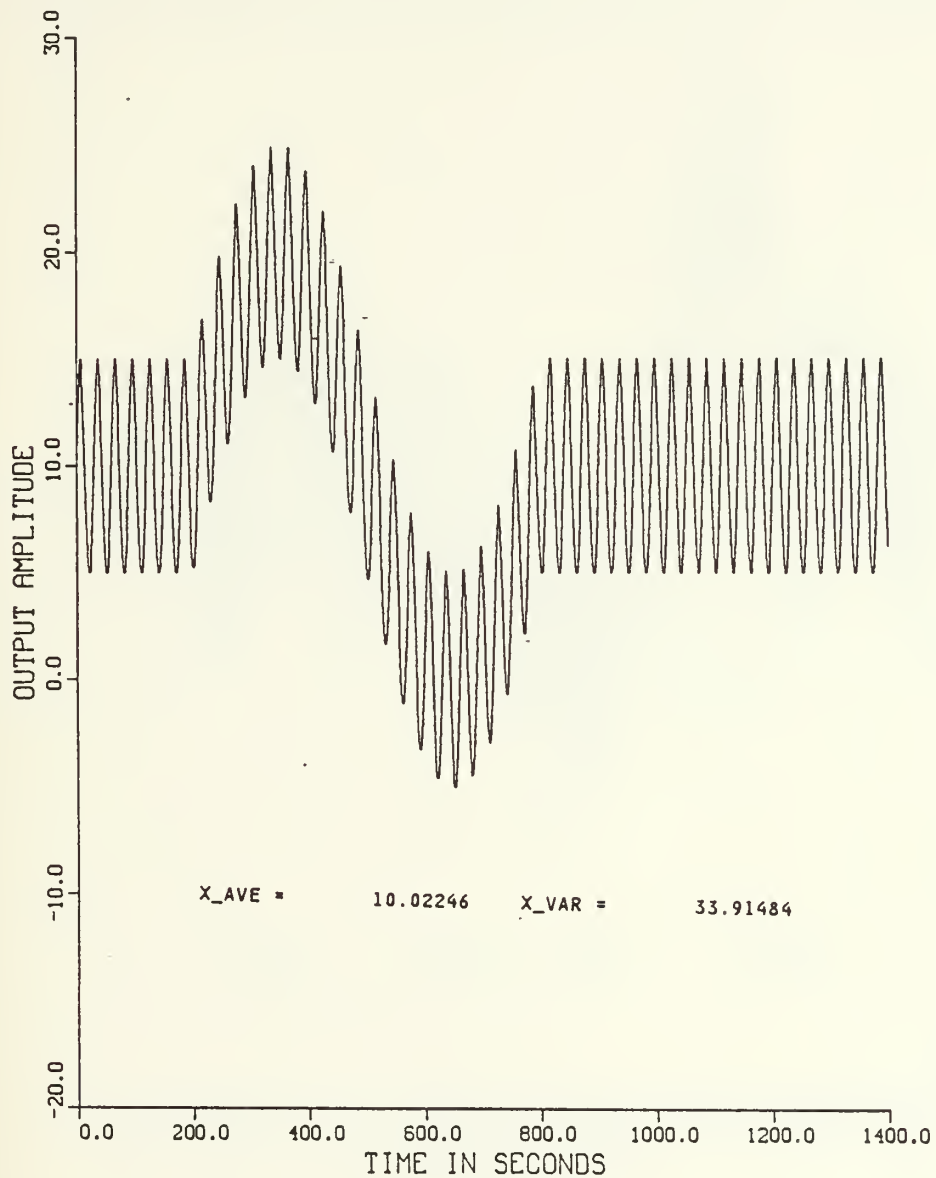
Figure 4.20   The Actual "Clean" Gyro Signal for Simulation #4.

101
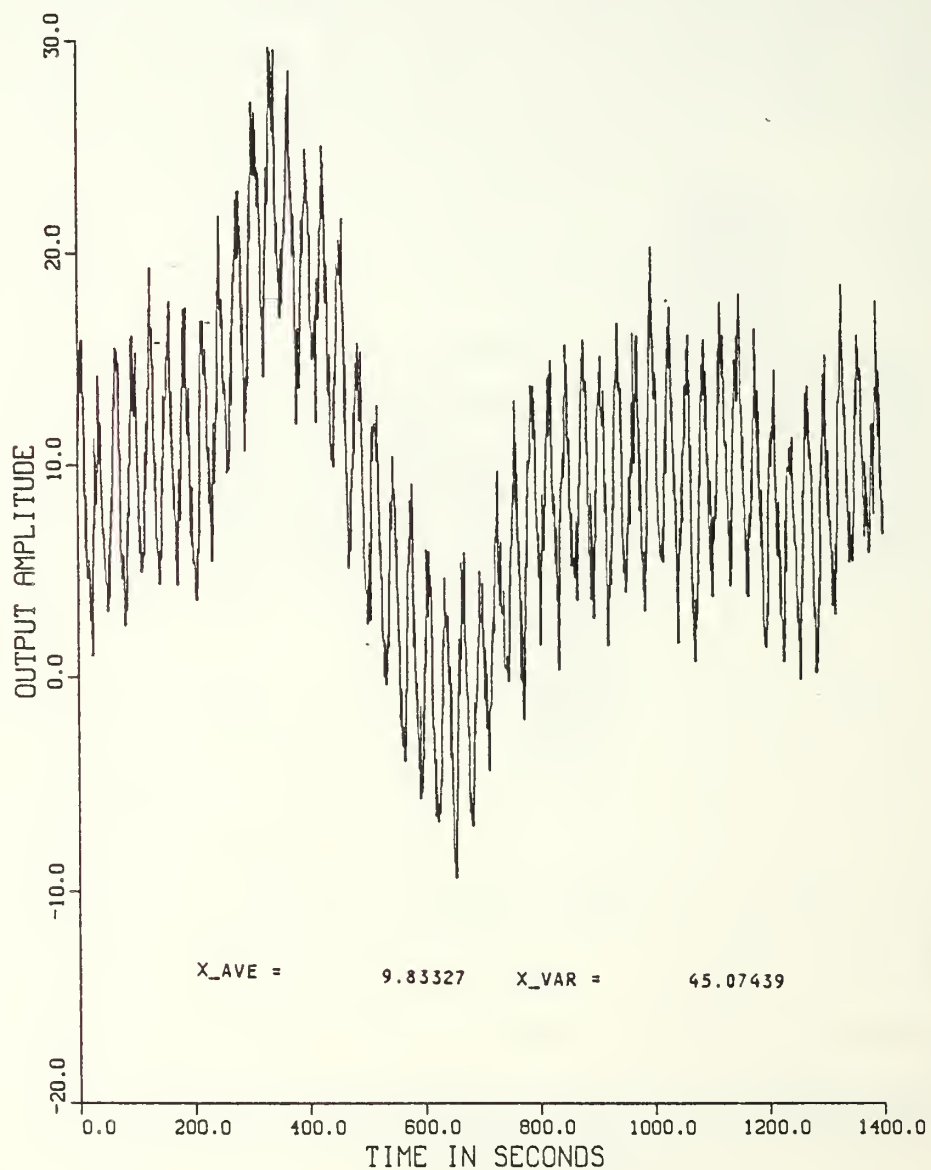
Figure 4.21   The Actual "Noisy" Gyro Signal for Simulation #4.
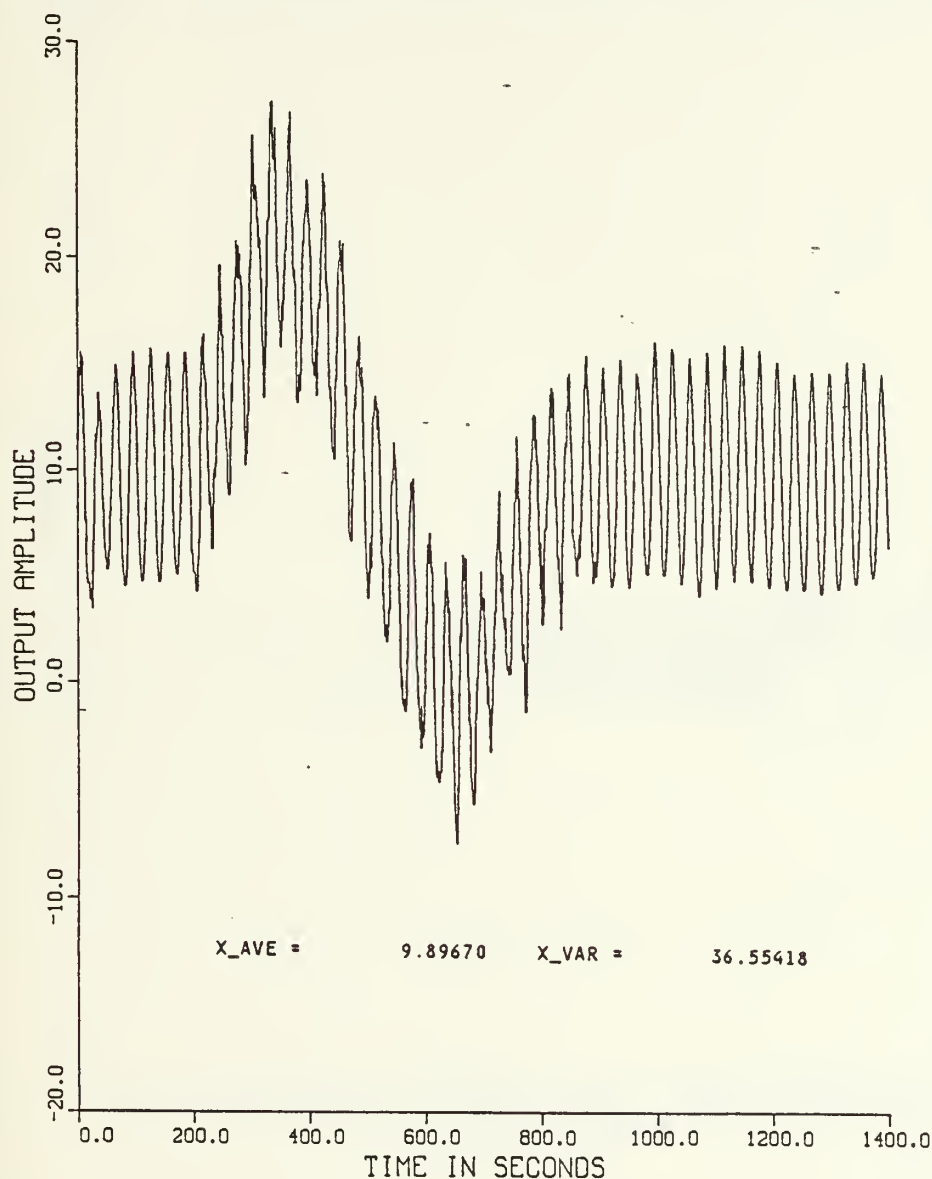
Figure 4.22   The Best Estimated Gyro Signal for Simulation #4.
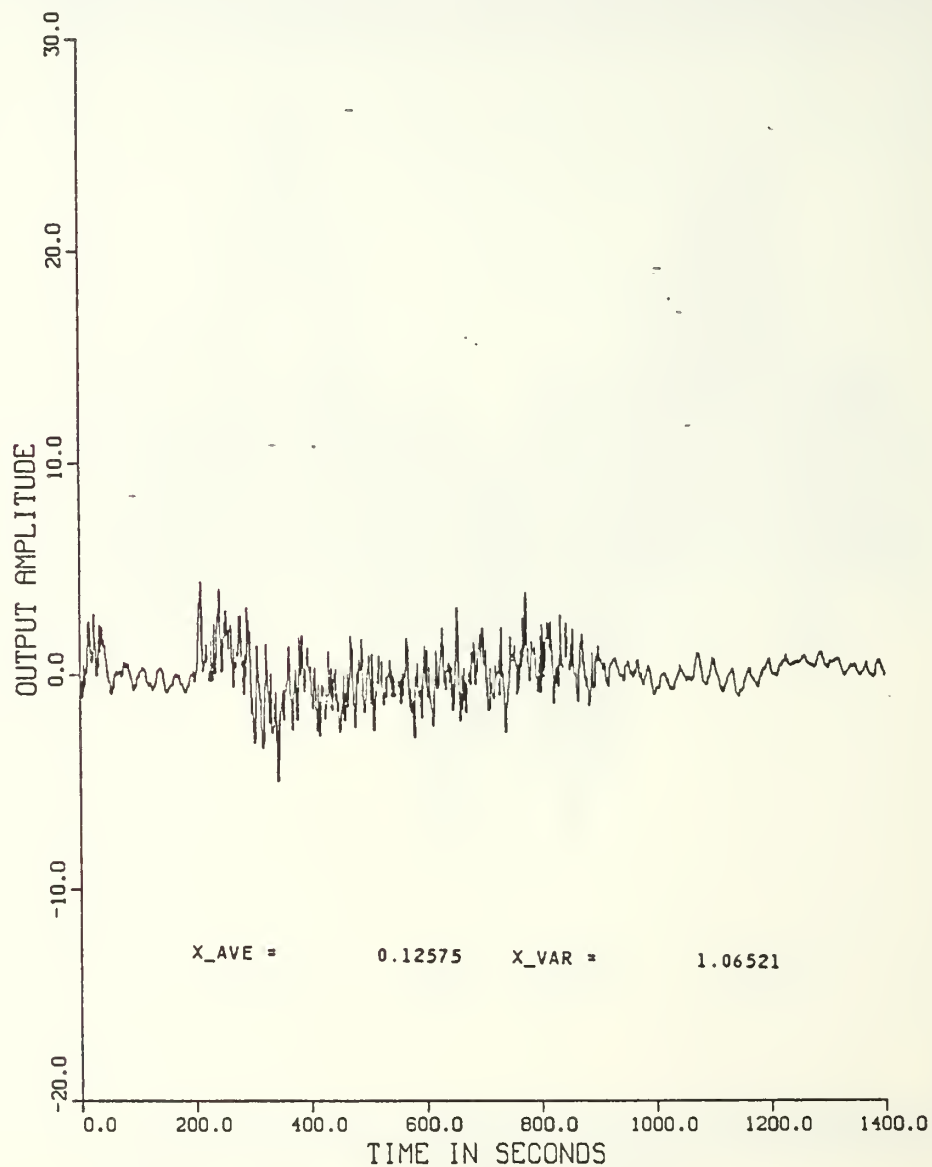
Figure 4.23   The Error in the Best Estimate for Simulation #4.

Figure 4.24   The Integrated Error with Respect to Time for Simulation #4.

105

6. Summary of Kalman Filter Implementation

The Kalman filter has been shown to be an extremely effective tool in filtering out noise for which an adequate known model exists. The major known noise of concern for optical gyroscopes is the gyroscope random rate noise, for which several models have been proposed. Using one such model, which has been shown to be accurate to within third order terms, the Kalman filter proved very adept at removing most of the random rate error in an optical gyro based inertial navigation system. Table 3 summarizes the performance of the Kalman filter implementation for each simulation run.

Any Kalman filter implementation which can be used must allow the inertial navigation system to operate in real time. That requires the calculations of this simulation to be well within the computational capacity of a dedicated microprocessor. The simulation programming was run on a 80286 based microprocessor to determine the length of time required to execute a thousand iterations of the simulation program, which corresponds to a thousand seconds of the gyro output. This dedicated microprocessor executed the thousand iterations in 110 seconds, giving a computational duty cycle of eleven percent. It is worthwhile to note that although this performance is clearly acceptable, the programming was written without regard to its optimal real time execution, and it is expected that much better performance with regards to execution time could be achieved.

The Kalman filter used in the simulation runs presented above, demonstrated a high degree of adaptability when incorporating the changing parameter technique. If it is desirable to remove as much of the random rate error as possible, then an additional state to model the ship's maneuver would prove the best answer. However, the unique flexibility suggested by the varying parameter approach shows great opportunity for an operational optical gyro based inertial navigation system.

TABLE 3

KALMAN FILTER PERFORMANCE SUMMARY

Simulation Run No.	Sea State	Steady Course	Maneuver Course	Percent Noise Removed	Integrated Error Variance
1	No	No	No	99.83	12.22
2	Yes	No	No	99.79	15.75
3	Yes	Yes	No	99.78	16.25
4	Yes	Yes	Yes	80.97	1395.9

V. CONCLUSIONS AND RECOMMENDATIONS ON THE DESIGN OF AN INERTIAL NAVIGATION SYSTEM FOR THE AUTONOMOUS SUBMERSIBLE

The autonomous submersible testbed vehicle will provide a testing platform from which state of the art techniques and equipment can be safely evaluated without unnecessarily risking the lives of submariners. Additionally, since the vehicle is dedicated to the testbed function, a capable and reliable test vehicle is possible. The advantages to the fighting submarine will include: a shorter lag time for technology to go from the laboratory to the fleet, less risk involved in the new equipment placed in the fleet, and a better understanding of the new equipment when it is used.

The design of an autonomous submarine requires an inertial navigation system to control it. As the test vehicle would ideally be fairly small, a small inertial navigation system is called for. This leads to the examination of new gyroscope technologies to determine the different possible types of inertial systems available for this use. In particular, the small optical gyroscopes present intriguing possibilities.

A. RECOMMENDATIONS FOR INERTIAL NAVIGATION SYSTEM

1. Overall System Design

The modern mechanical gyroscope is relatively cheap, accurate, and well understood. Small miniature gyroscopes are widely available which could well be used in a small inertial navigation system. However, these mechanical gyro systems suffer several major disadvantages. A fairly large gimbal support structure is required for these mechanical gyroscopes. Gimbals are complex, expensive, and take up a good deal of space. Mechanical gyroscopes are not very reliable, with an average mechanical gyroscope offering a mere 275 hours mean time between failures. [Ref. 12: p. 4] Finally, the mechanical gyroscope requires precise alignment to be sufficiently accurate, and demands periodic special calibrations and tuning procedures.

The optical gyroscopes are proving a better solution than their mechanical counterparts. They offer high degrees of reliability that have not been matched by the mechanical gyroscopes. Optical gyroscopes operating in Boeing 757 and 767 aircraft have measured reliability performance of more than 10,000 hours mean time between failures. That is a five times better reliability performance than the most reliable

mechanical gyroscope system. [Ref. 12: p. 4] Optical gyroscopes need no special calibrations and the normal calibrations that are performed are greatly simplified. Finally, there are no critical alignment problems when installing the optical gyro, enabling the gyro to be easily replaced at sea.

The ring laser gyroscope is the more developed optical gyro. Although extremely sensitive and accurate, the real advantage that the ring laser gyroscope has over the mechanical gyroscope is that the mechanical gyro has many complicated moving parts while the ring laser gyro has virtually none. Thus the ring laser gyro is far easier to maintain, and therefore less costly over the service life, than the mechanical gyro. Ring laser gyroscopes also feature instant turn on, whereas mechanical gyroscopes require significant periods of time to attain rated speed and accuracy. However, the ring laser gyro requires extremely fine mirrors which must be mounted within very small tolerances. Accordingly, a three axis ring laser gyro is normally manufactured within a single monolithic block. Because of these fine manufacturing tolerances and refined mirrors, the ring laser gyroscope is still a moderately expensive product.

The fiber optic gyroscope is the more promising of the two optical gyroscopes in terms of cost. The fiber optic gyroscope does not require any mirrors and does not demand exact positioning of its components. The expectation of a very low cost continues to be anticipated. The fiber optic gyroscope also has the advantage of a smaller size and a more variable package shape. However, the fiber optic gyroscope is still being developed. The research and development effort continues to be very strong, and it is likely that full production of fiber optic gyroscopes will begin by 1990.

The end result is that an optical gyroscope is likely to be used in the inertial navigation system for the autonomous submersible testbed vehicle. A conceptual design of such an inertial navigation and guidance system is presented in Figure 5.1. Of note is that a NAVSTAR Global Positioning System receiver is used to provide a high accuracy fix position reset. A depth sensor is also incorporated to reduce errors about the depth dimension, as it is the most accurate indication available. Ship control is effected by control signals sent from the inertial navigation and guidance computer to the propulsion, rudder, diving planes, and buoyancy controllers. A means to enter a programmed track and task assignment, through stored programming, is required. Finally, an obstacle avoidance scheme is included to handle potential problems with any unknown obstacles that may occur. These may include sonar contacts, the ocean bottom, shoal water, or a variety of navigation hazards.

```
        NAVIGATION  AND  GUIDANCE  SYSTEM

  ┌─────────────┐    ┌─────────────┐    ┌─────────────┐
  │ PROPULSION  │    │   RUDDER    │    │DIVING PLANES│
  │ CONTROLLER  │    │ CONTROLLER  │    │ CONTROLLER  │
  └─────────────┘    └─────────────┘    └─────────────┘

  ┌─────────────┐  ┌───────────────────────┐  ┌──────────────────┐
  │GPS RECEIVER │  │  INERTIAL NAVIGATION  │  │ ADVANCED OPTICAL │
  └─────────────┘  │  AND GUIDANCE COMPUTER │  │    GYROSCOPE     │
  ┌─────────────┐  │                        │  └──────────────────┘
  │DEPTH SENSOR │  └───────────────────────┘
  └─────────────┘

       ┌──────────────────┐   ┌──────────────────┐
       │OBSTACLE AVOIDANCE│   │   PROGRAMMED      │
       │    ALGORITHM     │   │ NAVIGATIONAL TRACK│
       └──────────────────┘   └──────────────────┘

    ┌──────────┐  ┌──────────────┐
    │COLLISION │  │CHART TERRAIN │
    │AVOIDANCE │  │ PROGRAMMED   │
    │  SONAR   │  │ INFORMATION  │
    └──────────┘  └──────────────┘
```
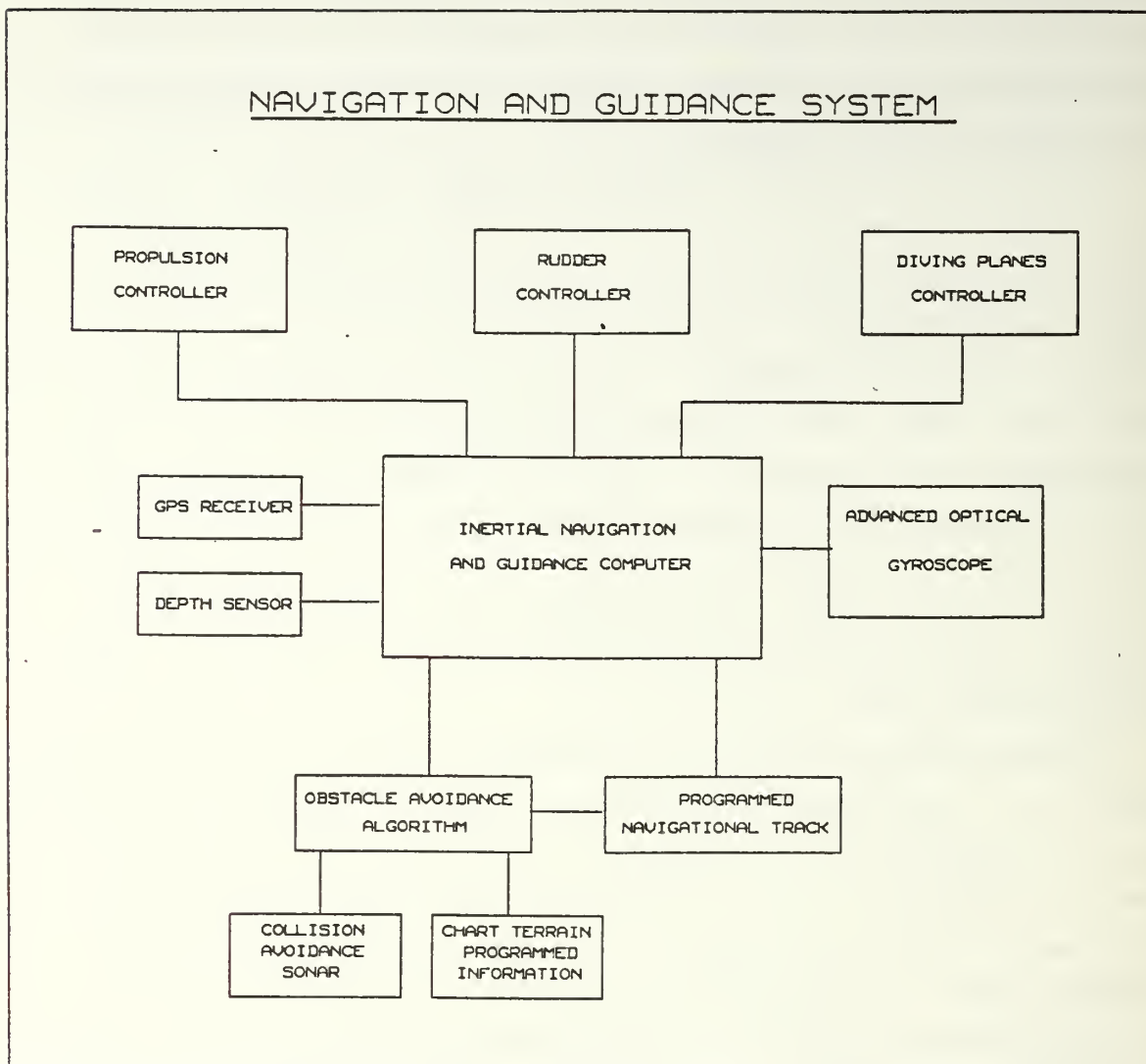
Figure 5.1   An Overview of the Inertial Navigation System Design.

The NAVSTAR Global Positioning System was chosen as the only fix source for the inertial navigation system, as it has several advantages which make it the optimal fix source choice for the autonomous submersible vehicle. NAVSTAR GPS uses 18 satellites in six orbital planes to provide a very high accuracy fix with nearly worldwide continuous coverage. The GPS fix process is not a long process, as all the processing is done internal to the receiver in a very rapid manner. There are four basic types of GPS receivers produced by the Department of Defense. The so called low cost receiver, for which optimal receiver performance was sacrificed for lower costs, greatly exceeded performance specifications and consistently demonstrated accuracies

in the 20-30 meter range. [Ref. 3: pp. 1177-1186] The benefits of low cost, small size, continuous rapid navigation availability, and high accuracy, makes NAVSTAR GPS an excellent fix source for the autonomous submersible vehicle.

The advantages of an optical gyroscope based inertial navigation system lead to a strapped down inertial navigation design. The strapped down inertial navigation system or analytic inertial navigation system does not physically maintain a reference frame. Unlike the other inertial navigation systems, the strapped down gyro system uses the gyro outputs to calculate the relative orientation between the system's initial or stored state and its present state. Essentially, the reference frame is stored in memory instead of being physically maintained. Transformation theory must be used extensively in the strapped down inertial navigation system, and must be applied to both the gyro and the accelerometer outputs.

2. A Conceptual Design of the Inertial Subsystems

Figures 5.2 and 5.3 shows a conceptual design for a strapped down inertial navigation system. Figure 5.2 shows the reference frame maintenance subsystem. It involves the use of an optical gyroscope to determine any changes in angular velocities that may occur. These angular velocity changes, once detected, are compensated for, such that the initial reference frame is maintained computationally. An additional aspect of this subsystem is the maintenance and generation of the initialization matrix. The problem of alignment in a strapped down inertial navigation system is basically that of determining the initial transformation matrix which relates the instrumented body frame to the reference computational frame. In an operational vehicle, the problem is even more difficult because a suitable determination of the initialization matrix must be made within a reasonably short period of time, without including effects from deleterious motions of the vehicle. A two-stage alignment scheme is recommended, which would allow the position to be reset without adversely effecting the other initialization matrix terms.

Figure 5.3 shows the inertial acceleration subsystem, and is concerned with sensing the inertial accelerations, measuring time, and double integrating the inertial accelerations to determine the resulting change in position. The accelerometer section outputs only the inertial accelerations as described in Chapter 2. Figure 2.1 shows one possible acceleration section implementation. The first integrator outputs the vehicle's velocity with respect to time. The second integrator outputs the vehicle's change in position with respect to time. The transformer is used to convert the change in

REFERENCE FRAME STORAGE SYSTEM

OPTICAL GYRO

The optical gyro outputs angular velocity, with a lot of gyro random bias noise.

GPS RECEIVER

The GPS receiver is used to reset the INS system when a fix is determined.

RESET TIME

KALMAN FILTER

The Kalman filter is used to reduce the gyro noise and minimize system errors.

INTEGRATOR

The integrator integrates the best estimated angular velocity from the filter.

RESET FRAME

REFERENCE FRAME

The reference frame is updated by the change in angular position, such that the stored reference frame is maintained.

INITIALIZATION MATRIX

The initialization matrix embodies the stored frame and alignment data.

Figure 5.2   The Inertial Reference Frame Subsystem Design.

position determined above into an absolute position output. This conversion requires inputs from the reference frame storage subsystem for reference coordinate data. Initialization matrix information is also required in order to relate the instrumented body frame calculations to the reference computational frame.

INERTIAL ACCELERATIONS SUBSYSTEM

ACCELEROMETER SUBSYSTEM

The accelerometer subsystem is designed such that it outputs only inertial accelerations, as described in Chapter 2.

GPS RECEIVER SUBSYSTEM

The GPS receiver is used to provide a fix reset, whenever a navigation fix is available.

RESET TIME

INTEGRATOR

This first integrator outputs the linear velocity components.

RESET TIME

INTEGRATOR

The second integrator outputs the linear change in position over time, from the stored initial position.

REFERENCE FRAME STORAGE SUBSYSTEM

The reference frame storage subsystem inputs the stored initialization matrix into the transformer.

TRANSFORMER SUBSYSTEM

The transformer transforms the change in position given above, into the vehicle's position with respect to the stored reference frame.

Figure 5.3   The Inertial Acceleration Subsystem Design.

B.   GYROSCOPE SELECTION RECOMMENDATIONS

1. Brief Overview of the Gyroscope Commercial Market

Several ring laser gyroscopes are widely available which offer substantial design flexibility. Complete 3-axis ring laser gyro systems are being constructed from a single monolithic block. Sizes ranging from hand held to basketball size units can be obtained. Competition within the laser gyro industry is intense, and prices are dropping rapidly. Current ring laser prices start at around 60,000 dollars for large

volume purchases and 120,000 dollars for small volume purchases.

The Honeywell H-770 ring laser inertial navigation system, for example, provides a complete inertial navigation system within a frame that is 15.0"L x 8.4"H x 13.0" W, for a cost of 90,000 dollars. It also provides several operational and supportability benefits which are summarized below.

1. Delivers reliability that is five times greater than conventional systems.
2. Uses less than half the power of comparable gimbaled systems.
3. Needs no scheduled maintenance.
4. Needs no scheduled recalibrations.
5. Requires no special shore support.
6. Offers full rated performance within 30 seconds from startup.
7. 2000 hours mean time between failures guaranteed.
8. Delivers 50% lower life cycle costs than conventional systems.

Despite being designed for use in fighter aircraft, and thus using larger scale factors that result in a less accurate navigation performance, the system still maintains less than an average 0.8 nautical miles per hour position error rate. Velocity error rates are less than 2.5 feet per second, for an aircraft designed maximum speed over 2.0 mach. It would be a very simple matter to change the scale factors involved in this existing system to be more applicable to submersible operating constraints, and this should result in significant improvements in the overall navigation performance.

Despite the obvious differences between the ring laser gyro and the fiber optic gyro, the two operate on exactly the same physical principle. However, the fiber optic gyroscope has no lock-in problem, no complicated base block fabrication, and no mirrors. The fiber optic gyro and the ring laser gyro are actually different engineering implementations of the same physical phenomena, that of employing the Sagnac effect to measure rotation. The ring laser gyro has already emerged as a superior candidate over the mechanical gyro for virtually every inertial application. The fiber optic gyro offers all the advantages of the ring laser gyro and very few of its problems. The many advantages unique to the fiber optic gyro make it ideally suited for use in a small submersible vehicle.

However, the fiber optic gyros are not currently widely available. Several companies are preparing to mass produce these gyros, however, and should be selling these gyros for about 25,000 dollars initially, and about 8,000 dollars after a short time. The widespread availability of these gyros should occur within the next five years.

2. Gyroscope Recommendations

The choice of which gyroscope to use depends largely on exactly when the gyroscope is to be constructed. If the fiber optic gyroscopes are widely available, then they probably are the best choice. At the present, however, these gyroscopes are not available. For now, the gyroscope of choice is the ring laser gyro. It has better accuracy, size, reliability, and over the life of the gyro is much cheaper than the mechanical counterpart. About the only reason to choose the mechanical gyro would be if initial cost were the prime consideration. The initial cost of a mechanical miniature gyro is much less than that of the ring laser gyro.

C. THE FUTURE IN INERTIAL NAVIGATION

Fiber optic gyros offer several advantages over other gyro systems, which include the following: an all solid state design which lends itself to extended operational high reliability, low maintenance, and low life cycle costs; a high degree of environmental ruggedness; instant turn on; small packaging with significant geometric flexibility; insensitivity to accelerations; low power requirements; no critical alignments; potential low cost given continuing developments being driven by the telecommunications industry; and the potential for greater sensitivity than current gyro systems.

Applications of fiber optic gyroscopes have already emerged for which even crude and unsophisticated fiber optic gyros have proven invaluable. Attitude reference systems, seeker heads, and oil drilling guidance are just some of the applications to which these gyros are presently being used. These early fiber optic gyros have demonstrated several advantages over conventional systems. Specifically, in the oil drilling case, these include an ability to withstand 1000 g shocks and 40 g vibrations while being constrained to fit within a small diameter pipe. This clearly illustrates the environmental ruggedness and packaging flexiblity of the fiber optic gyroscope.

Also obvious is that a fiber optic gyro can be made to be quite small. Fiber optic gyros have been made which measures only 10 centimeters in diameter and 3.5 centimeters in depth. Future designs are likely to be considerably smaller still. Furthermore, as more refined fiber optic gyroscopes are produced, and the advantages of mass production and economies of scale are applied, the fiber optic gyro is likely to become relatively cheap, and the most common inertial navigation system of choice.

Efforts are now underway to place many of these devices in a single chip. These components when combined into a single integrated chip, will be used to reduce fiber

optic gyro size, and complexity, and will improve the gyro system performance and reliability. Since many of these components are also used in many other fiber optic applications, costs are ultimately expected to be very low.

The analysis of the inertial navigation system errors has been intensive and has led to several effective techniques to reduce the magnitude of the errors. For the optical gyroscopes, the error of greatest concern is the error arising from the gyro random bias drift rate as this error tends to result in a build up of position error with time that is much more significant than the other error sources.

In this regard, a Kalman filter was constructed that was based on a gyro random bias rate noise model to reduce this major error source. A Fortran program was written to test this Kalman filter and a computer simulation conducted to examine the degree of improvement in performance that is potentially achievable. The Kalman filter was shown to be an extremely effective tool in filtering out noise for which an adequate known model exists. The Kalman filter used in these simulation runs also demonstrated a high degree of adaptability when incorporating the changing parameter technique. It is likely that Kalman filter designs will enable better accuracy fiber optic gyro systems to be marketed in the very near future.

Ultimately, the fiber optic gyro will replace all other gyro types in nearly all applications. The extended reliability, extremely low costs, small size, and packaging flexibility, will make consideration of any other gyro nearly impracticable. The possibility of obtaining a complete inertial navigation system for under 10 thousand dollars, potentially offers a complete gyro system for less than 10 percent of today's cost. As this should occur within the next decade, the gyro of choice for any autonomous vehicles following this testbed vehicle will probably be the fiber optic gyro.

D.   RESEARCH EXTENSIONS

There are several useful research extensions to this conceptual design of an inertial navigation system. Some of these possible extensions are listed below.

1. Continue the Kalman filter design to include additional states to model a continuously maneuvering ship.
2. Develop the changing parameter concept for the Kalman filter for various ship operating conditions, possibly having one set of parameters for normal submerged operations and another for periscope depth operations.
3. Analyze actual strapped down gyro output data and determine better models for the major errors encountered, and use an iterative Kalman filter design to further reduce system error.

4. Design a subsystem which would incorporate the depth indication information into the inertial navigation system to reduce overall system error.

5. Design a subsystem which will perform the initialization matrix calculations and navigation fix reset using the GPS information.

6. Design a subsystem which will perform the collision avoidance calculations and still maintain an optimal navigation track.

The design of the inertial navigation and guidance system will necessarily need to be broken up into several critical parts. The block diagrams included in this chapter are intended to suggest an initial task division assignment. To expedite the design process, a preliminary design effort followed by a critical design review for the proposed inertial navigation system, would, in the author's judgement, be the next logical step within the design process. This could be followed by the design and implementation of each subsystem leading to a working prototype inertial navigation and guidance system. A modular design is recommended, both to simplify subsequent system and subsystem design, and to better enable future system and subsystem design refinements and iterations.

APPENDIX
KALMAN FILTER AND SIMULATION IMPLEMENTATION

```
****************************************************************************
****************************************************************************
***              THSPGM   (SIGMA SIGNAL/DC = 0.0001/0.100)             ***
***                                                                    ***
***         THIS PROGRAM MODELS THE GYRO RANDOM BIAS DRIFT RATE        ***
***      OF A FIBER OPTIC GYROSCOPE, WHICH IS THE MAIN SOURCE OF       ***
***      ERROR OF CONCERN FOR THIS GYRO.  THE GYRO MODEL USED TAKES    ***
***      THIS GYRO RANDOM BIAS DRIFT RATE NOISE AND ADDS IT TO A       ***
***      DETERMINISTIC AND KNOWN "EXACT" GYRO SIGNAL, TO FORM THE      ***
***      "NOISY" GYRO SIGNAL.   THE PROGRAM THEN USES A KALMAN FILTER  ***
***      IMPLEMENTATION TO OPERATE ON THIS "NOISY" GYRO SIGNAL IN      ***
***      ORDER TO PRODUCE A GYRO SIGNAL WHICH INCLUDES MUCH LESS       ***
***      GYRO RANDOM BIAS NOISE EFFECTS, AND THUS PROVIDING A MORE     ***
***      ACCURATE INERTIAL NAVIGATION SYSTEM WITH THE CHEAPER FIBER    ***
***      OPTIC GYRO.  A 5-STATE DYNAMIC KALMAN FILTER IS USED, THUS    ***
***      SINCE A 3-DIMENSIONAL ENVIRONMENT REQUIRES AT LEAST 3 GYROS,  ***
***      THIS WOULD CORRESPOND TO A 15 STATE 3 KALMAN FILTER FOR       ***
***      THE 3 AXIS CASE.  THIS PROGRAM ONLY ADDRESSES THE SINGLE      ***
***      DIMENSION CASE.                                               ***
***         THE PROGRAM THEN COMPARES THE KALMAN FILTERED ESTIMATE     ***
***      OF THE GYRO SIGNAL TO THE ACTUAL KNOWN "EXACT" GYRO SIGNAL.   ***
***      THE ERROR BETWEEN THE TWO SIGNALS IS CALCULATED AND STORED    ***
***      IN AN ERROR ARRAY, E.                                         ***
***         AS WE ARE REALLY CONCERNED WITH THE GENERATED INERTIAL     ***
***      NAVIGATION POSITION, THE PROGRAM INTEGRATES THE ERROR ARRAY   ***
***      WITH RESPECT TO TIME, THUS FORMING THE DYNAMIC RESPONSE OF    ***
***      THE POSITION RELATED ERROR OF OUR KALMAN FILTERED INERTIAL    ***
***      NAVIGATION SYSTEM.   INTEGRATION IS DONE VIA THE TRAPEZOIDAL  ***
***      INTEGRATION APPROXIMATION.                                    ***
***         AS A GENERAL NOTE, THE PROGRAM ONLY WORKS CORRECTLY        ***
***      WHEN THE NUMBER OF POINTS,N , AS GIVEN BY THE FOLLOWING       ***
***      FORMULA, IS AN EXACT INTEGER.                                 ***
***                      (N - 2)/3                                     ***
***      THIS IS BECAUSE OF THE MANNER IN WHICH THE SUBROUTINE TRAP    ***
***      PERFORMS THE INTEGRATION.  THIS CAN BE CHANGED QUITE EASILY.  ***
***                                                                    ***
***          INPUT  PARAMETERS: NONE                                   ***
***          OUTPUT PARAMETERS: NONE                                   ***
***                                                                    ***
****************************************************************************
*                                                                          *
*       THIS SUBROUTINE PRODUCES 1 OF 5 GRAPHS, WHICH ARE  APPROPRIATELY  *
*   LABELED.  THE GRAPH BEING PRODUCED IS CONTROLLED BY THE INPUT          *
*   PARAMETER I.  THE OUTPUT PRODUCED IS AS FOLLOWS.                       *
*                                                                          *
*          I                  GRAPH                                        *
*                                                                          *
*          1         ACTUAL "CLEAN" GYRO SIGNAL                            *
*          2         ACTUAL "NOISY" GYRO SIGNAL (WHAT ENTERS FILTER)       *
*          3         BEST ESTIMATED GYRO SIGNAL (WHAT EXITS FILTER)        *
*          4         ERROR IN BEST ESTIMATED GYRO SIGNAL                   *
*          5         INTEGRATED ERROR WITH RESPECT TO TIME                 *
*                                                                          *
****************************************************************************
****************************************************************************
*                                                                          *
          SUBROUTINE THSPGM
          REAL X(1400),Y(1400)
          INTEGER I
*   I IS A FLOW CONTROL PARAMETER, WHICH EFFECTS WHAT OUTPUT AMPLITUDE    *
*        IS ACTUALLY OUTPUTED IN THE ARRAY X, WHICH IS GRAPHED.           *
```

```
          DO 45 I=1,5
          IF (I.EQ.1) THEN
             CALL RESET ('ALL')
             CALL AREA2D (6.0,8.0)
             CALL XNAME ('TIME IN SECONDS$',100)
             CALL YNAME ('OUTPUT AMPLITUDE$',100)
             CALL HEADIN ('ACTUAL "CLEAN" GYRO SIGNAL$',100,-2.0,1)
             CALL GRAF (0.0,200.0,1400.0,-20.0,10.0,30.0)
             CALL TMAIN(X,Y,I)
             CALL CURVE (X,Y,1399,0)
*   NOTE THAT THE CALL TO CURVE HAS ONE LESS THAN THE DIMENSION OF X      *
             CALL COMPLX
             CALL HEIGHT (0.2)
             CALL RESET ('COMPLX')
             CALL RESET ('HEIGHT')
             CALL ENDPL(0)
          ELSEIF (I.EQ.2) THEN
             CALL RESET ('ALL')
             CALL AREA2D (6.0,8.0)
             CALL XNAME ('TIME IN SECONDS$',100)
             CALL YNAME ('OUTPUT AMPLITUDE$',100)
             CALL HEADIN ('ACTUAL "NOISY" GYRO SIGNAL$',100,-2.0,1)
             CALL GRAF (0.0,200.0,1400.0,-20.0,10.0,30.0)
             CALL TMAIN(X,Y,I)
             CALL CURVE (X,Y,1399,0)
             CALL COMPLX
             CALL HEIGHT (0.2)
             CALL RESET ('COMPLX')
             CALL RESET ('HEIGHT')
             CALL ENDPL(0)
          ELSEIF (I.EQ.3) THEN
             CALL RESET ('ALL')
             CALL AREA2D (6.0,8.0)
             CALL XNAME ('TIME IN SECONDS$',100)
             CALL YNAME ('OUTPUT AMPLITUDE$',100)
             CALL HEADIN ('BEST ESTIMATED GYRO SIGNAL$',100,-2.0,3)
             CALL HEADIN ('SIGMA SIGN = 0.0001, DC = 0.0001$',100,-2.0,3)
             CALL HEADIN ('SIGMA DISTURBANCE EQUALS 2.25$',100,-2.0,3)
             CALL GRAF (0.0,200.0,1400.0,-20.0,10.0,30.0)
             CALL TMAIN(X,Y,I)
             CALL CURVE (X,Y,1399,0)
             CALL COMPLX
             CALL HEIGHT (0.2)
             CALL RESET ('COMPLX')
             CALL RESET ('HEIGHT')
             CALL ENDPL(0)
          ELSEIF (I.EQ.4) THEN
             CALL RESET ('ALL')
             CALL AREA2D (6.0,8.0)
             CALL XNAME ('TIME IN SECONDS$',100)
             CALL YNAME ('OUTPUT AMPLITUDE$',100)
             CALL HEADIN ('ERROR BETWEEN THE ACTUAL GYRO$',100,-2.0,3)
             CALL HEADIN ('SIGMA SIGN = 0.0001, DC = 0.0001$',100,-2.0,3)
             CALL HEADIN ('SIGMA DISTURBANCE EQUALS 2.25$',100,-2.0,3)
             CALL GRAF (0.0,200.0,1400.0,-20.0,10.0,30.0)
             CALL TMAIN(X,Y,I)
             CALL CURVE (X,Y,1399,0)
             CALL COMPLX
             CALL HEIGHT (0.2)
             CALL RESET ('COMPLX')
             CALL RESET ('HEIGHT')
             CALL ENDPL(0)
          ELSEIF (I.EQ.5) THEN
             CALL RESET ('ALL')
             CALL AREA2D (6.0,8.0)
             CALL XNAME ('TIME IN SECONDS$',100)
             CALL YNAME ('OUTPUT AMPLITUDE$',100)
             CALL HEADIN ('INTEGRATED ERROR OVER TIME$',100,-2.0,3)
             CALL HEADIN ('SIGMA SIGN = 0.0001, DC = 0.0001$',100,-2.0,3)
             CALL HEADIN ('SIGMA DISTURBANCE EQUALS 2.25$',100,-2.0,3)
```

119

```
          CALL GRAF (0.0,200.0,1400.0,-300.0,100.0,200.0)
          CALL TMAIN(X,Y,I)
          CALL CURVE (X,Y,1399,0)
          CALL COMPLX
          CALL HEIGHT (0.2)
          CALL RESET ('COMPLX')
          CALL RESET ('HEIGHT')
          CALL ENDPL(0)
       END IF
45     CONTINUE
       RETURN
       END
***********************************************************************
***********************************************************************
***                SUBROUTINE TMAIN     .                          ***
***                                                                 ***
***       THIS PROGRAM DEFINES THE X & Y ARRAYS TO BE PLOTTED       ***
***    IN THE GRAPHICS CODE GIVEN IN THE SUBROUTINE THSPGM.         ***
***    IT FUNCTIONS SIMILARLY TO A "MAIN" PROGRAM IN THAT IT IS     ***
***    LARGELY MADE UP OF SUBROUTINE CALLS AND HAS AS ITS PURPOSE   ***
***    TO CONTROL THE FLOW OF EXECUTION THROUGH THE REST OF THE     ***
***    PROGRAMMING CODE.  AFTER DEFINING THE POINTS TO BE PLOTTED,  ***
***    THE PROGRAM WRITES THE DATA TO DEVICE 08.                    ***
***                                                                 ***
***       INPUT  PARAMETERS: I - FLOW CONTROL PARAMETER FROM THSPGM ***
***       OUTPUT PARAMETERS: T,X                                    ***
***       T  =  AN ARRAY REPRESENTING THE ELAPSED TIME              ***
***       X  =  AN ARRAY REPRESENTING OUTPUT ARRAY AMPLITUDE        ***
***             FOR THE GRAPH OUTPUT FOR THE I-TH GRAPH             ***
***                                                                 . ***
***********************************************************************
*                                                                   *
*      THIS SUBROUTINE DEFINES THE GYRO RANDOM BIAS DRIFT RATE NOISE *
* AS A FUNCTION OF TIME, DEFINES THE TIME ARRAY IN ARRAY T, DEFINES  *
* THE "EXACT" GYRO SIGNAL IN THE ARRAY S, AND DEFINES THE "NOISY" GYRO *
* SIGNAL IN THE ARRAY X.  DEPENDING ON THE VALUE OF THE INPUT        *
* PARAMETER I, THE SUBROUTINE DIRECTS THE SUBSEQUENT CALL STRUCTURE  *
* TO OUTPUT THE PURE EXACT GYRO SIGNAL, THE NOISY GYRO SIGNAL, THE   *
* ERROR IN THE GYRO SIGNAL, AND THE ERROR IN THE GYRO SIGNAL         *
* INTEGRATED WITH RESPECT TO TIME.  THIS INTEGRATED ERROR IS         *
* PROPORTIONAL TO THE POSITION ERROR THAT WOULD RESULT IN AN INERTIAL *
* NAVIGATION SYSTEM WHICH USES A GYRO WITH A COMPARABLE GYRO RANDOM  *
* DRIFT RATE AND THIS KALMAN FILTER IMPLEMENTATION.  THE RESULTS FOR *
* THE SIMULATION RUN FOR WHICH I=5 IS SOMEWHAT ANALOGOUS TO THE      *
* POSITION ERROR THAT WOULD RESULT FROM AN OPTICAL GYROSCOPE WITH    *
* SIMILAR GYRO RANDOM BIAS DRIFT RATES.                              *
*      ON EACH CALL THE SUBROUTINE DETERMINES SOME BASIC STATISTICS  *
* ON THE OUTPUT AMPLITUDE ARRAY, X, AND PRINTS THE RESULTS OF THESE  *
* STATISTICS CALCULATIONS INTO DEVICE UNIT 08.                      *
*      ARRDIM DEFINES THE ARRAY DIMENSION DESIRED, OR THE NUMBER OF  *
* POINTS (X,Y) TO BE RETURNED.                                      *
*      SIGMA IS A CONSTANT USED TO MULTIPLY THE INPUT GAUSSIAN       *
* WHITE NOISE      N(0,1)   , FROM THE SUBROUTINE DSTRB, TO GENERATE *
* A  N(0,SIGMA) DISTRIBUTION.  THIS IS USED TO GENERATE THE GYRO     *
* RANDOM BIAS DRIFT RATE.                                            *
*                                                                   *
***********************************************************************
***********************************************************************
*                                                                   *
       SUBROUTINE TMAIN(T,X,I)
       DIMENSION T(1400),X(1400),S(1400),E(1400)
       REAL*4   T,X,S,E,XAVE,XVAR,SIGMA
       INTEGER  ARRDIM
       ARRDIM = 1400
       SIGMA = 1.5
       IF (I.EQ.1) THEN
            CALL DSTRB (T,X,SIGMA,ARRDIM)
            CALL SIGNL (X,S,ARRDIM)
            CALL SWAP(X,S,ARRDIM)
            CALL STATS(X,XAVE,XVAR,ARRDIM)
```

120

```
                    CALL WRTD(SIGMA,XAVE,XVAR,ARRDIM)
          ELSEIF (I.EQ.2) THEN
                    CALL DSTRB (T,X,SIGMA,ARRDIM)
                    CALL SIGNL (X,S,ARRDIM)
                    CALL STATS(X,XAVE,XVAR,ARRDIM)
                    CALL WRTD(SIGMA,XAVE,XVAR,ARRDIM)
          ELSEIF (I.EQ.3) THEN
                    CALL DSTRB (T,X,SIGMA,ARRDIM)
                    CALL SIGNL (X,S,ARRDIM)
                    CALL KALMAN(X,ARRDIM)
                    CALL STATS(X,XAVE,XVAR,ARRDIM)
                    CALL WRTD(SIGMA,XAVE,XVAR,ARRDIM)
          ELSEIF (I.EQ.4) THEN
                    CALL DSTRB (T,X,SIGMA,ARRDIM)
                    CALL SIGNL (X,S,ARRDIM)
                    CALL KALMAN(X,ARRDIM)
                    CALL ERROR(X,S,E,ARRDIM)
        .           CALL SWAP(X,E,ARRDIM)
                    CALL STATS(X,XAVE,XVAR,ARRDIM)
                    CALL WRTD(SIGMA,XAVE,XVAR,ARRDIM)
          ELSEIF (I.EQ.5) THEN
                    CALL DSTRB (T,X,SIGMA,ARRDIM)
                    CALL SIGNL (X,S,ARRDIM)
                    CALL KALMAN(X,ARRDIM)
                    CALL ERROR(X,S,E,ARRDIM)
                    CALL SWAP(X,E,ARRDIM)
                    CALL TRAP(X,ARRDIM)
                    CALL STATS(X,XAVE,XVAR,ARRDIM)
                    CALL WRTD(SIGMA,XAVE,XVAR,ARRDIM)
          END IF
          RETURN
          END
***********************************************************************
***********************************************************************
***               SUBROUTINE WRTD                                  ***
***                                                                ***
***       THIS SUBROUTINE WRITES THE DATA GIVEN IN THE VARIABLES   ***
***   SIGMA, XAVE, AND XVAR INTO THE DEVICE UNIT 08.               ***
***   NO CHANGES TO THE INPUT PARAMETERS ARE MADE.                 ***
***                                                                ***
***       INPUT  PARAMETERS: SIGMA,XAVE,XVAR,ARRDIM                ***
***       OUTPUT PARAMETERS: NONE                                  ***
***                                                                ***
***********************************************************************
***********************************************************************
*                                                                   *
          SUBROUTINE WRTD (SIGMA,XAVE,XVAR,ARRDIM)
          REAL*4    SIGMA,XAVE,XVAR
          INTEGER   ARRDIM
          WRITE (UNIT=8,FMT=111) SIGMA,XAVE,XVAR
111       FORMAT ('SIGMA = ',F6.3,4X,'X_AVE = ',F14.5,4X,'X_VAR = ',F14.5)
          RETURN
          END
***********************************************************************
***********************************************************************
***               SUBROUTINE DSTRB                                 ***
***                                                                ***
***       THIS SUBROUTINE DEFINES THE GYRO RANDOM BIAS DRIFT RATE  ***
***   ARRAY (NOISE) AND THE TIME ARRAY, INTO X(I) & T(I).          ***
***   USE OF THE IMSL ROUTINE GGNQF IS MADE TO GENERATE A          ***
***   NORMAL GAUSSIAN DISTRIBUTED FUNCTION  N   (O,1).             ***
***                                                                ***
***       INPUT  PARAMETERS: ARRDIM                                ***
***       OUTPUT PARAMETERS: T,X,SIGMA                             ***
***          T  =  AN ARRAY REPRESENTING THE ELAPSED TIME          ***
***          X  =  AN ARRAY REPRESENTING THE GYRO RANDOM BIAS      ***
***                DRIFT RATE AS A FUNCTION OF TIME                ***
***       SIGMA =  CONSTANT USED TO MULTIPLY THE NORMAL GAUSSIAN   ***
***                DISTRIBUTION VALUES GIVEN BY GGNQF TO INCREASE  ***
***                THE SCALE OF THE NOISE EFFECT.                  ***
```

```
***                                                                    ***
************************************************************************
************************************************************************
*                                                                      *
      SUBROUTINE DSTRB (T,X,SIGMA,ARRDIM)
      DIMENSION T(1400),X(1400)
      REAL*4   X,T,XAVE,XVAR,A,AD,SIGMA
      REAL*8   DSEED
      INTEGER I,J,ARRDIM
      DSEED = 27812356.0 D0
      A = 0.0
      T(1) = 0.0
      T(2) = 1.0
      X(1) = 0.0
      X(2) = 0.1
      DO 100 I=3,ARRDIM
          AD = A
          A = GGNQF(DSEED)
          A = SIGMA * A
          X(I) = 1.381*X(I-1)-0.387*X(I-2)+A-0.909*AD
          T(I) = T(I-1)+1.0
100   CONTINUE
      RETURN
      END
************************************************************************
************************************************************************
***           SUBROUTINE STATS                                         ***
***                                                                    ***
***      THIS SUBROUTINE TAKES THE INPUTED ARRAY X(I) AND              ***
***   DETERMINES ITS AVERAGE VALUE AND VARIANCE, WHICH ARE             ***
***   RETURNED TO THE CALLING PROGRAM AS XAVE & XVAR.                  ***
***                                                                    ***
***      INPUT  PARAMETERS: X,ARRDIM                                   ***
***      OUTPUT PARAMETERS: XAVE,XVAR                                  ***
***      XAVE =   THE MEAN VALUE OF THE INPUTED ARRAY X                ***
***      XVAR =   THE VARIANCE VALUE OF THE INPUTED ARRAY X          - ***
************************************************************************
************************************************************************
*                                                                      *
      SUBROUTINE STATS(X,XAVE,XVAR,ARRDIM)
      DIMENSION X(1400)
      REAL*4     X,SUMAVE,XAVE,SUMVAR,XVAR
      INTEGER    ARRDIM,I,J
      SUMAVE = 0.0
      SUMVAR = 0.0
      DO 101 I=1,ARRDIM
          SUMAVE = SUMAVE + X(I)
101   CONTINUE
      XAVE = SUMAVE / ARRDIM
      DO 103 I=1,ARRDIM
          SUMVAR = SUMVAR + (X(I)-XAVE)**2
103   CONTINUE
      XVAR = SUMVAR / ARRDIM
      RETURN
      END
************************************************************************
************************************************************************
***           SUBROUTINE KALMAN                                        ***
***                                                                    ***
***      THIS SUBROUTINE PERFORMS THE 5-STATE KALMAN FILTER            ***
***   IMPLEMENTATION.  THE INPUT "NOISY" GYRO SIGNAL IS DEFINED        ***
***   IN THE INPUT ARRAY OBS.  THESE ARE THE OBSERVATIONS TO BE        ***
***   FILTERED.  ON OUTPUT THE OBS ARRAY WILL CONTAIN THE FILTERED     ***
***   OR BEST ESTIMATED VALUES.                                        ***
***      THE IMSL SUBROUTINE "FTKALM" IS USED TO IMPLEMENT A           ***
***   TIME VARYING OR OPTIMAL 5-STATE KALMAN FILTER.                   ***
***                                                                    ***
***      INPUT  PARAMETERS: OBS,ARRDIM                                 ***
***         OBS =   THE INPUT "NOISY" GYRO SIGNAL TO BE FILTERED       ***
```

122

```
***          OUTPUT PARAMETERS: OBS                              ***
***            OBS =   THE FILTERED BEST ESTIMATED VALUES OF THE  ***
***                    INPUTED ARRAY                              ***
***                                                              ***
****************************************************************
****************************************************************
*                                                                *
      SUBROUTINE KALMAN(OBS,ARRDIM)
      DIMENSION  OBS(1400),X(5,1),H(5,5),G(5,3),Y(1,1),S(1,5),V(1,1)
      DIMENSION  Q(3,3),R(1,1),P(5,5),T1(5,5),T2(5,5),T3(5,5)
      REAL*4     OBS,X,H,G,Y,S,Q,R,P,T1,T2,T3,PI
      INTEGER    ARRDIM,K,IN,IS,IL,N,M1,L,IT,IER
      PI = 2.0 * ASIN (1.0)
      N = 5
      M1 = 1
      L = 3
      IN = 5
      IS = 1
      IL = 3
      IT = 5
C     SET UP PARAMETERS FOR THE FIRST CALL TO FTKALM
      K = 0
* THE NEXT LINE ESTABLISHES THE INITIAL CONDITION FOR THE GYRO VELOCITY*
      X(1,1) = 10.0
* THE NEXT TWO LINES ESTABLISH THE INITIAL CONDITIONS FOR THE SEA STATE*
      X(2,1) = 0.382
      X(3,1) = -0.707
* THE NEXT TWO LINES ESTABLISH THE INITIAL CONDITIONS FOR THE NOISE    *
      X(4,1) = 0.0
      X(5,1) = 0.0
      H(1,1) = 1.0
      H(1,2) = 0.0
      H(1,3) = 0.0
      H(1,4) = 0.0
      H(1,5) = 0.0
      H(2,1) = 0.0
* THE NEXT LINE ESTABLISHES THE SEASTATE STATE VARIABLES               *
      H(2,2) = 2.0 * COS ( 2.0 * PI/30.0 )
      H(2,3) = -1.0
      H(2,4) = 0.0
      H(2,5) = 0.0
      H(3,1) = 0.0
      H(3,2) = 1.0
      H(3,3) = 0.0
      H(3,4) = 0.0
      H(3,5) = 0.0
      H(4,1) = 0.0
      H(4,2) = 0.0
      H(4,3) = 0.0
* THE NEXT TWO LINES ESTABLISH THE NOISE STATE VARIABLES               *
      H(4,4) = 1.381
      H(4,5) = -0.387
      H(5,1) = 0.0
      H(5,2) = 0.0
      H(5,3) = 0.0
      H(5,4) = 1.0
      H(5,5) = 0.0
      G(1,1) = 1.0
      G(1,2) = 0.0
      G(1,3) = 0.0
      G(2,1) = 0.0
      G(2,2) = 1.0
      G(2,3) = 0.0
      G(3,1) = 0.0
      G(3,2) = 0.0
      G(3,3) = 0.0
      G(4,1) = 0.0
      G(4,2) = 0.0
      G(4,3) = 1.0
      G(5,1) = 0.0
```

```
                G(5,2) = 0.0
                G(5,3) = 0.0
                S(1,1) = 1.0
                S(1,2) = 1.0
                S(1,3) = 0.0
                S(1,4) = 1.0
                S(1,5) = -0.909
                Q(1,1) = 0.0001
                Q(1,2) = 0.0
                Q(1,3) = 0.0
                Q(2,1) = 0.0
                Q(2,2) = 0.0001
                Q(2,3) = 0.0
                Q(3,1) = 0.0
                Q(3,2) = 0.0
                Q(3,3) = 2.25
                R(1,1) = 0.0
*   Y MATRIX  -- THE ACTUAL OBSERVED VALUES (SIGNAL & NOISE)              *
          WRITE (UNIT=9,FMT=110)
          DO 300 I=1,ARRDIM
                Y(1,1) = OBS(I)
                K = I-1
                CALL FTKALM (K,X,H,G,Y,S,Q,R,P,IN,IS,IL,N,M1,L,T1,T2,IT,T3,IER)
                WRITE (UNIT=9,FMT=111) I,X(1,1),X(2,1),X(3,1),X(4,1),X(5,1),IER
*   WE WANT THE OBS MATRIX TO CONTAIN THE BEST ESTIMATE OF SIGNAL        *
*       BEST EST = DC COMPONENT + SINUSOIDAL COMPONENT                   *
                OBS(I)  =    X(1,1)    +    X(2,1)
300       CONTINUE
110       FORMAT (5X,'I',5X,'X(1,1)',4X,'X(2,1)',4X,'X(3,1)',4X,
          *'X(4,1)',4X,'X(5,1)',6X,'IER')
111       FORMAT (I6,3X,5(F7.3,3X),I6)
          RETURN
          END
****************************************************************************
****************************************************************************
***                  SUBROUTINE TRAP                                   ***
***                                                                    ***
***           THIS SUBROUTINE PERFORMS THE TRAPEZOIDAL RULE            ***
***     INTEGRATION APPROXIMATION ON THE INPUT ARRAY X.  ON OUTPUT     ***
***     THE ARRAY X CONTAINS THE INTEGRAL VALUES OF THE INPUT ARRAY    ***
***     WITH RESPECT TO TIME.                                          ***
***           AS A GENERAL NOTE, THIS ROUTINE ONLY WORKS CORRECTLY     ***
***     WHEN THE NUMBER OF POINTS,N , AS GIVEN BY THE FOLLOWING        ***
***     FORMULA, IS AN EXACT INTEGER.                                  ***
***                         (N - 2)/3                                  ***
***     THIS IS BECAUSE OF THE MANNER IN WHICH THE SUBROUTINE TRAP     ***
***     PERFORMS THE INTEGRATION.  THIS CAN BE CHANGED QUITE EASILY.   ***
***                                                                    ***
***           INPUT  PARAMETERS: X,ARRDIM                              ***
***              X  =   THE INPUT ARRAY TO BE INTEGRATED               ***
***           OUTPUT PARAMETERS: X                                     ***
***              X  =   THE INTEGRAL OF THE INPUT ARRAY WITH RESPECT   ***
***                     TO TIME                                        ***
***                                                                    ***
****************************************************************************
****************************************************************************
*                                                                        *
          SUBROUTINE TRAP(X,ARRDIM)
          DIMENSION  X(1400),C(1400)
          REAL*4    X,C,DELTA
          INTEGER   ARRDIM,I,J
          C(1) = 0.0
          DO 200 I=4,ARRDIM,3
              C(I) = C(I-3) + 0.5 * ( X(I-2) + 2.0 * X(I-1) + X(I) )
200       CONTINUE
          DO 201 I=4,ARRDIM,3
              DELTA = (C(I) - C(I-3))/3.0
              C(I-2) = C(I-3) + DELTA
              C(I-1) = C(I-3) + 2.0 * DELTA
201       CONTINUE
```

124

```
          DO 202 I=1,ARRDIM
             X(I) = C(I)
202   CONTINUE
      RETURN
      END
*****************************************************************
*****************************************************************
***              SUBROUTINE SIGNL                           ***
***                                                         ***
***       THIS SUBROUTINE DEFINES THE SIGNAL PORTION OF THE ***
***   GYRO OUTPUT, S, AND ADDS IT TO THE INPUTED NOISE PORTION ***
***   OF THE GYRO OUTPUT (THE GYRO RANDOM BIAS) TO FORM THE  ***
***   "NOISY" GYRO OUTPUT TO BE OBSERVED.                    ***
***                                                         ***
***       INPUT  PARAMETERS: X,ARRDIM                       ***
***          X   =   THE INPUT GYRO RANDOM BIAS DRIFT RATE (NOISE) ***
***       OUTPUT PARAMETERS: S,X                            ***
***          S   =   THE "EXACT" GYRO OUTPUT (NO NOISE)      ***
***          X   =   THE "NOISY" GYRO OUTPUT (OBSERVATION)   ***
***                                                         ***
*****************************************************************
*****************************************************************
*                                                               *
      SUBROUTINE SIGNL (X,S,ARRDIM)
      DIMENSION  X(1400),S(1400)
      REAL*4     X,S,PI
      INTEGER  ARRDIM,I,J
      PI = 2.0 * ASIN (1.0)
      DO 100 I=1,ARRDIM
*     SIGNAL = COURSE COMPONENT +  SEA STATE COMPONENT          *
         CRSE =  10.0
         SEAST  =  5.0 * SIN (PI * I/15.0)
         S(I)   =     CRSE        +     SEAST
         X(I) = X(I) + S(I)
100   CONTINUE
      RETURN
      END
*****************************************************************
*****************************************************************
***              SUBROUTINE ERROR                           ***
***                                                         ***
***       THIS SUBROUTINE DETERMINES THE AMOUNT OF ERROR BETWEEN ***
***   THE BEST ESTIMATED GYRO SIGNAL THAT IS OUTPUTED FROM THE ***
***   KALMAN FILTER, AND THE "EXACT" GYRO SIGNAL DEFINED IN THE ***
***   SUBROUTINE SIGNL.                                      ***
***                                                         ***
***       INPUT  PARAMETERS: X,S,ARRDIM                     ***
***          X   =   THE INPUTED BEST ESTIMATED GYRO SIGNAL  ***
***          S   =   THE "EXACT" GYRO OUTPUT (NO NOISE)      ***
***       OUTPUT PARAMETERS: S,X                            ***
***          E   =   THE DIFFERENCE BETWEEN THE S & X ARRAYS ***
***                                                         ***
*****************************************************************
*****************************************************************
*                                                               *
      SUBROUTINE ERROR(X,S,E,ARRDIM)
      DIMENSION  X(1400),S(1400),E(1400)
      REAL*4     X,S,E
      INTEGER  ARRDIM,I,J
      DO 100 I=1,ARRDIM
*     ERROR = TRUE SIGNAL - BEST ESTIMATE OF SIGNAL            *
         E(I)  =      S(I)    -      X(I)
100   CONTINUE
      RETURN
      END
*****************************************************************
*****************************************************************
***              SUBROUTINE SWAP                            ***
***                                                         ***
***       THIS SUBROUTINE EXCHANGES THE VALUES IN ARRAY A(I) WITH ***
```

125

```
***       THE VALUES IN ARRAY B(I), OF THE SAME DIMENSION.             ***
***                                                                    ***
***          INPUT  PARAMETERS: A,B,ARRDIM                             ***
***              A  =   THE FIRST INPUTTED ARRAY TO BE SWAPPED.        ***
***              B  =   THE SECOND INPUTTED ARRAY TO BE SWAPPED WITH   ***
***          OUTPUT PARAMETERS: A,B                                    ***
***              A  =   THE SWAPPED VALUES THAT WERE IN B ON INPUT     ***
***              B  =   THE SWAPPED VALUES THAT WERE IN A ON INPUT     ***
***                                                                    ***
************************************************************************
************************************************************************
*                                                                      *
      SUBROUTINE SWAP(A,B,ARRDIM)
      DIMENSION  A(1400),B(1400),C(1400)
      REAL*4    A,B,C
      INTEGER   ARRDIM,I
      DO 100 I=1,ARRDIM
          C(I) = A(I)
          A(I) = B(I)
          B(I) = C(I)
100   CONTINUE
      RETURN
      END
```

LIST OF REFERENCES

1. Anderson, D. A., "Optical Gyroscopes", *Scientific American*, v. 254, pp. 94-99, April 1986.

2. Blidberg D. R., *Time- Ordered Architecture for Knowledge-Based Guidance of an Unmanned Untethered Submersible*, paper presented at the Oceans Engineering Conference, Washington, DC., 10-12 September 1984.

3. Bradford, P., and Gilbert, S., "NAVSTAR: Global Positioning System - Ten Years Later", *Proceedings of the Institute of Electrical and Electronics Engineers*, v. 71, pp. 1156-1176., October 1983.

4. Britting, K., *Inertial Navigation Systems Analysis*, John Wiley and Sons, Inc., 1971.

5. Broxmeyer C., *Inertial Navigation Systems*, McGraw-Hill Book Company, 1964.

6. Burns, W., "Fiber Optic Gyroscopes", *Computer Design*, pp. 12-23, February 1984.

7. Dankowych, J., and others, *Closed Loop Fiber Optic Gyroscope*, paper presented at the International Society for Optical Engineering Meeting, v. 566, San Diego, California, 20-23 August 1985.

8. Ezekiel S., *Recent Developments in Solid State Optical Gyroscopes: An Overview*, paper presented at the International Society for Optical Engineering Meeting, v. 566, San Diego, California, 20-23 August 1985.

9. Friedman, N., *Submarine Design and Development*, Naval Institute Press,1984.

10. Gelb, A., and others, *Applied Optimal Estimation*, The Massachusetts Institute of Technology Press, 1974.

11. Honeywell, Aerospace Division, *Inertial Guidance Primer*, July 1972.

12. Honeywell, Military Avionics Division, *A Quantum Leap Towards Perfection*, July 1986.

13. Johnson, L., *Integrated-Optical Components for Fiber Gyroscopes*, paper presented at the International Society for Optical Engineering Meeting, v. 566, San Diego, California, 20-23 August 1985.

14. Kim, B., and Shaw, H., "Fiber Optic Gyroscopes", *The Institute of Electrical and Electronics Engineers Spectrum*, pp. 54-60, March 1986.

15. Kuritsky, M., and Goldstein, M., "Inertial Navigation", *Proceedings of the Institute of Electrical and Electronics Engineers*, v. 71, pp. 1156-1176, October 1983.

16. Levinson, E., *Accuracy Enhancement Techniques Applied to the Marine Ring Laser Inertial Navigator*, paper presented at the Avionics Maintenance Conference, Seattle, Washington, 2-5 April 1984.

17. Litton Guidance and Control Systems, *Fiber Optic Gyroscopes: Advances and Future Developments*, by G. Pavlath and M. Suman, August 1986.

18. Markey, W., and Hovorka, J., *The Mechanics of Inertial Position and Heading Indication*, John Wiley and Sons, Inc., 1961.

19. Martin, G. J., "Gyroscopes May Cease Spinning", *The Institute of Electrical and Electronics Engineers Spectrum*, pp. 48-53, February 1986.

20. McClure, C., *The Theory of Inertial Guidance*, Prentice-Hall, Inc, 1960.

21. Merrill, G., *Principles of Guided Missile Design*, D. Van Nostrand Company, Inc., 1962.

22. Montgomery, J., Glasco J., and Dixon F., *Precision Fiber Optic Sensor Market Forecast*, paper presented at the International Society for Optical Engineering Meeting, v. 566, San Diego, California, 20-23 August 1985.

23. Motyka P., and Bergmann E., *The Design of a Control-System for the Ballast and Trim of an Unmanned Submersible*, paper presented at the American Control Conference, San Diego, California, 6-8 June 1984.

24. Naval Research Laboratory Code 6570, *A Constant Accuracy, High Dynamic Range Fiber Optic Gyroscope*, by N. Frigo, August 1986.

25. Otaguro, W., and Udd, E., *Fiber Optic Gyro for Space Applications*, paper presented at the International Society for Optical Engineering Meeting, v. 616, Los Angeles, California, 21-22 January 1986.

26. Pandit, S., and Weibang, Z., "Modeling Random Gyro Drift Rate by Data Dependent Systems", *The Institute of Electrical and Electronics Engineers Transactions on Aerospace and Electronic Systems*, Vol. AES-22, No. 4, pp. 455-460, July 1986.

27. Phillips, R., *Noise Problems in Rotation Sensors*, paper presented at the International Society for Optical Engineering Meeting, v. 566, San Diego, California, 20-23 August 1985.

28. *Principles of Naval Engineering*, 3rd ed., Bureau of Naval Personnel, 1970.

29. *Principles of Naval Weapons Systems*, 5th ed., U. S. Naval Academy, June 1980.

30. Ravula R., and Rattan K., *Robust-Control Law Design of an Unmanned Research Vehicle*, paper presented at the Annual National Aerospace and Electronics Conference, 38th, Dayton, Ohio, 19-23 May 1986.

31. Savage P., *Laser Gyros in Strapdown Inertial Navigation Systems*, paper presented at the Institute of Electrical and Electronics Engineers Position Location and Navigation Symposium, San Diego, California, 1-3 November 1976.

32. Stensland, R., *Principles of Strapdown Laser Inertial Navigation*, paper presented at the Avionics Maintenance Conference, Seattle, Washington, 2-5 April 1984.

33. Summary Technical Report of Division 6, Naval Defense Research Committee, *Methods of Submarine Buoyancy Control*, by J. B. Conant, 1946.

34. Udd, E., and Wagoner, R., *The Transition of Fiber Optic Gyro Technology into Products*, paper presented at the International Society for Optical Engineering Meeting, v. 566, San Diego, California, 20-23 August 1985.

35. Watkins L., *Syntactic Foam Buoyancy Systems for Manned and Unmanned Submersibles*, paper presented at the Conference on Ocean Engineering and the Environment, San Diego, California, 12-14 November 1985.

36. Wrigley, W., Woodbury, R., and Hovorka, J., *Inertial Guidance*, paper presented at the Institute of the Aeronautical Sciences Annual Meeting, 25th, New York, New York, 28-31 January 1957.

INITIAL DISTRIBUTION LIST